Stochastic Partial Differential Equations Applied to Hydrocarbon Reservoir Modelling

Mohammed Aziz
St Anne's College
University of Oxford

A thesis submitted for the degree of
Master of Science by Research
Trinity Term 2010

Acknowledgements

I would like to thank my supervisors Dr Ben Hambly and Dr Chris Farmer for their advice, guidance and help throughout this endeavour. Without their encouragement from the very beginning, this work would not be possible. I appreciate their patience and constructive suggestions in many discussions.

This research was generously supported by a grant from EPRSC and Schlumberger, and I would like to thank both of them for making this available to me.

Last but not the least; I would like to thank my parents for their continuous love and encouragement. The tiredness, the depression, and the pressure I brought home from long working day would evaporate in their smiling.

Stochastic Partial Differential Equations Applied to Hydrocarbon Reservoir Modelling

Mohammed Aziz

St Anne's College
University of Oxford

A thesis submitted for the degree of
Master of Science by Research

Trinity Term 2010

This thesis describe the generation of random fields using elliptic stochastic partial differential equations driven by Gaussian white noise. The intended application is that of sampling from a prior probability density in the solution of an inverse problem.

In the first part of thesis, we will study two specific examples of isotropic models, namely the stochastic Helmholtz equation and stochastic biharmonic equation. We will address the analytical properties of a particular solution and the conditions required for the uniqueness of the Green's function. A useful formula is also derived linking the computation of the covariance function of the solution to that of the Green's function. Moreover, in each example the correlation function and approximate realizations are computed and simulated.

In the second part of the thesis, we will investigate the possibility of using vector fields to guide the random fields. The vector fields will be used to build tensor coefficients for an elliptic stochastic partial differential equation. The model considered is capable of producing non-stationary random fields on curved layers. Approximate realizations of this model will be drawn by using the finite element method, which is applied using the MATLAB PDE toolbox.

Contents

List of Figures

Chapter 1

Introduction

A hydrocarbon reservoir is a porous and permeable subsurface rock formation which contains oil, water and gas under pressure. These formations have been made by a combination sedimentary and diagenetic processes and transformed by a history of tectonic changes and therefore they are heterogeneous structures on many scales. When a reservoir containing hydrocarbons is discovered, the knowledge of the spatial distribution of the petrophysical properties (porosity and permeability) is of primary importance for optimizing its development, and engineers are required to understand the geological structure of the earth so that this information can be added into numerical simulators.
The objectives of reservoir modelling are to build models which incorporate the geological environment of the deposition, allowing updates of new data, and to represent a sufficiently wide range of possible scenarios of the reservoir.

1.1 Reservoir Modelling

The workflow involved in reservoir modelling can be summarized in the following three stages:

1.1.1 Defining the reservoir's large-scale structure

The aim of this process is to obtain as detailed an understanding of the geological formations of the reservoir as the measurements will allow. There are many tools of investigation to quantify the petrophysical properties of the reservoir, and the nature of the information obtained from these tools is very different. For example:

- **Seismic acquisition**: Seismic acquisition consists of transmitting acoustic energy into the subsurface and analysing the echoes. This provides useful information regarding the large scale geometry of the reservoir (on a scale of 10-20 metres) and sometimes detailed information regarding the acoustic properties of the reservoir.

- **Well data**: Well data consists of gathering core samples from wells. These samples are then taken to laboratories for microscopic examination to learn about the rock's origin and the diagenetic processes that have taken place.

- **Outcrop data**: Although every individual reservoir is unique, nevertheless repeated depositional environments create groups of reservoirs that are broadly similar. Using observations from outcrop studies, it is possible to learn about large scale geometric features and their associated length scales. In addition they assist geologists to distinguish between various reservoir architectures and to define geological rules for building reservoir models.

- **Well logging**: The purpose of well logging is to identify the properties of the fluids in the rocks and the geometric and physical properties of the rock. By interpreting the well log measurements, we can indentify the boundaries between rock layers and the occurrence of fracturing.

- **Well testing**: The aim of well testing is to investigate the dynamic behaviour of the reservoir around wells. A well test involves imposing some flow rate impulse in the reservoir and measuring the pressure responses. These measurements are then used to deduce the permeability in the vicinity of the well.

Once the large-scale structure of the reservoir is established, the next stage concentrates on specifying the heterogeneity within each depositional unit.

1.1.2 Defining the small-scale structure using geostatistical techniques

Large-scale reservoir models consist of thousands of grid blocks. Each grid block is about 100 metres square horizontally and about 1 metre thick. However in order to learn about small-scale heterogeneity, we need to consider smaller grid blocks. This

requires more measurements than are currently available. For example, seismic data typically cannot measure fluid flow properties such as permeability. Although it can reach everywhere, there is not enough knowledge relating seismic data to physical rock properties. The geostatistical method for modelling heterogeneous reservoirs allows integrating various kinds of data, and helps to evaluate uncertainties by simulating multiple possible scenarios of the reservoir's heterogeneity. One of the key geostatistical tools used is stochastic simulation. Stochastic simulation allows the reproduction of a given geological pattern constrained to various type of data. For detailed discussions on geostatistics see [22,34,28].

1.1.3 Upscaling the geological model for fluid flow simulation

Upscaling is the process of transforming a fine grid to a coarse grid while preserving the reservoir's geological properties. Geostatistical methods provide fine grid data to describe the geological media and upscaling is needed because these fine grids which contains millions of cells need huge amounts of computational time to a generate a reservoir simulation. For detailed discussions on upscaling see [22,34].

1.2 Inverse Problems

The most advanced technology available today for producing reservoir performance prediction is reservoir simulation. However, in practice we cannot have the density of data required by simulators. This is because in order to accurately simulate field performance, we need to know the geological properties throughout the reservoir and in reality there is never enough data to completely describe the subsurface. The combination of significant spatial heterogeneity with sparse numbers of observations leads to uncertainty about the values of the geological properties and therefore to uncertainty in predicting flow behavior in the reservoir. This is an example of an inverse problem. Notice that forward problems consists of finding the output given the model and the input, whereas inverse problems consists of determining a model for a given output. That is, given a limited number of observations e.g. from well logging, seismic data and so on, we need to infer geological properties such as reservoir permeability. The main characteristic of an inverse problem, in comparison to a well-posed forward problem, is that in most cases inverse problem produces solutions

which are not unique or stable to small changes in the given observation data, and this situation is usually known as ill-posedness. In the literature, inverse problems are either studied in a deterministic framework using Tikhonov regularization, or in a probabilistic framework using Bayesian theory. Tikhonov regularization restates the problem as a least squares minimization problem and provides point estimates of the unknowns without taking into account the statistics of the uncertainties. The Bayesian approach on the other hand has a number of advantages. It regularizes the ill-posed inverse problem through prior probability density, and instead of only calculating deterministic point estimates, it calculates the probability density of the geological properties conditioned on the observation data.

For a geological property ϕ (random field) and family of observations $\mathcal{O}$, Bayes' rule is given by

$$\pi(\phi \mid \mathcal{O}) = \frac{\pi(\mathcal{O} \mid \phi)\pi(\phi)}{\pi(\mathcal{O})}, \tag{1.1}$$

where $\pi(\phi)$, termed the prior density, describes the uncertainty of the geological property before any observations, $\pi(\mathcal{O} \mid \phi)$ denotes the likelihood function, $\pi(\mathcal{O})$ describes the probability density of the observations $\mathcal{O}$ and $\pi(\phi \mid \mathcal{O})$ is the posterior density.

Formally, solving the inverse problem is closely related to drawing samples from the posterior distribution. Although this calculation might seem straightforward, the technique used to draw the samples is not and most of current research concentrates on building samplers that are both representative and efficient in taking samples from $\pi(\phi \mid \mathcal{O})$.

Selecting a suitable prior density is usually a critical part in solving the inverse problem. The major problem with computing a suitable prior model lies in the nature of the prior information. The prior information is usually qualitative in nature and so one needs to convert the qualitative information into a quantitative form so that it can then be incorporated in the prior model. More specifically, the prior model can be represented by a collection of possible realizations ϕ which follows a particular spatial continuity model. If the prior model is inadequate then either the inverse problem has no solution because the chosen prior model does not agree with the observation data or, the inverse problem have many solutions but are all inconsistent with the spatial variability of the rock property. For instance, if a prior puts zero measure on

regions of the parameter space then no observation can change that value. This is known as a "dogmatic" prior and such priors can be dangerous.

1.3 Permeability Fields

The focus of this thesis will be on building prior models for the logarithm of rock permeability. Permeability, measuring the ease with which fluids passes through rocks, is considered to be one of the most critical parameters responsible for controlling reservoir performance, but at the same time it is one of the most difficult parameters to quantify. The permeability tensor, κ, occurs in Darcy's law which is given by

$$\mathbf{v}(\mathbf{x}) = \frac{-\kappa(\mathbf{x})}{\mu} \cdot \nabla p(\mathbf{x}), \qquad \mathbf{x} \in \mathbb{R}^d \tag{1.2}$$

where $\mathbf{v}(\mathbf{x})$ is the fluid velocity, μ is viscosity and $p(\mathbf{x})$ is pressure. Although $\kappa(\mathbf{x})$ is a tensor, in this thesis we shall assume the permeability tensor to be a diagonal tensor with the same value in each component direction, and so a single scalar governs the permeability fields.

Permeability can be quantified by collecting core samples and measuring flow rates in a laboratory, but the disadvantages with this approach are that it is expensive and there can be significant problems with measurement error when collecting the samples. Moreover, the value of the permeability field is only computed at a point in the sample, and so despite using many core samples, we still has a problem determining the rest of the spatial variations. This has led to the development of stochastic methods which represent permeability as a random field. Random field models provide a description of rock heterogeneities when the geological knowledge of the rock is not enough to predict flow properties deterministically. In theory, a random field model needs to be selected with spatial correlation structure that matches that of the actual reservoir. In practice, not enough information is known about this distribution and only for a few highly studied reservoirs has the permeability been measured densely. Therefore the decision to select a prior model is made on the basis of practicality, efficiency and to give answers that are reasonably realistic. In addition the selected model also requires some assumptions about the smoothness of the permeability field. The realism of any random field model can be assessed by sampling the prior and checking that the samples accord with the intuitions of engineers and geologists. In

fact in many practical situations, geologists have a reasonably good understanding about the geological formation of the reservoir, and this information can be included in the mathematical modelling of the reservoir.

To simulate flow through porous media, we need to provide realizations of the permeability fields. A widely used model of the permeability field $\kappa(\mathbf{x})$ is the lognormal random field,

$$\kappa(\mathbf{x}) = \kappa_0 e^{\phi(\mathbf{x})}, \qquad \mathbf{x} \in \mathbb{R}^d, \tag{1.3}$$

where $\phi(\mathbf{x})$ is a zero mean second order Gaussian random field with a prescribed covariance function and κ_0 is some representative value such that,

$$\mathbb{E}(\log(\frac{\kappa(\mathbf{x})}{\kappa_0})) = 0. \tag{1.4}$$

This model is known to be practically reasonable, as indicated by experiments in [8], and preserves the positivity of the permeability field. However, (1.3) cannot be used to model a reservoir with a fully general system of faults and layers. In addition, it typically leads to realizations that show no significant correlation of extreme values, so that both low and high permeability areas have little structure and connectivity. To model realistic features of geological layers, non-Gaussian random fields need to be considered. Therefore, in the following we shall study Gaussian and non-Gaussian random fields.

1.4 Stochastic Partial Differential Equations

There are various stochastic simulation techniques for generating Gaussian random fields and in chapter 2 we shall briefly explain some of the widely used methods. These methods however, can only be applied when the principal directions of correlation align with Cartesian coordinate directions. In general, rock layers are not flat and most geological boundaries do not conform to the simple coordinate lines of rectangular mesh systems. Therefore in order to use random field generators which rely on rectangular coordinates, a transformation to "stratigraphic" coordinates is usually required to map the actual geological layers into flat rectangular layers. But as the geological complexity increases, constructing such transformations becomes extremely difficult and tedious to achieve.

Therefore, a random field generator which does not require stratigraphic coordinates and can be applied to arbitrary shapes is of interest to software developers in the oil industry. Farmer in [4,33], reviewed and developed further an approach for generating random fields on arbitrary shapes, which can be conditioned on observation data, using Partial Differential Equations. One of the many attractive features of this method of simulation is that it does not require any particular assumption of a coordinate system until one has to actually perform a computation and then only locally for each cell of a grid. Hence one can generate random fields directly on the physical domain without the need for a transformation to rectangular coordinates.

Generating random fields using PDEs was first motivated by the pioneering work of Whittle [7], where agricultural yields were analyzed using a two dimensional elliptic stochastic differential equation. Whittle [11] extended the model outlined in Whittle [7] to higher dimensions and to include elliptic operators with fractional orders. He also demonstrated that the correlation function of the model considered is given by the *Matérn* correlation function. However a limitation with *Matérn* correlation functions is that it does not contain any correlation function with negative values, such as oscillating correlation function. For detailed explanations on *Matérn* correlation function see [61]. Heine [14] studied various examples of two dimensional elliptic, parabolic and hyperbolic stochastic PDE and computed the corresponding Green's function and correlation functions in each case. Numerical procedures to simulate realizations for elliptic stochastic partial differential equations were then developed in [36,37]. More recently Lindgren et al [12] have used the model introduced in Whittle [11] to sample from a prior density to solve various inverse problem.

In chapters 3 and 4 of this thesis, we shall consider isotropic elliptic PDEs driven by Gaussian white noise. We will study two specific examples of such models, namely the stochastic Helmholtz equation and the stochastic biharmonic equation. In each example the correlation function and approximate realizations are computed and simulated, and the regularity properties are investigated. A useful formula linking the computation of the covariance function to that of the Green's function is also derived. The stochastic Helmholtz equation is almost identical to the model considered in Whittle [7,11] and has exponentially decaying correlation functions. On the other hand, a variety of spatial correlations including damped oscillatory ones are observed

for the stochastic biharmonic equation.

Since geological features and their associated petrophysical properties are generally not distributed isotropically within a depositional environment, we shall investigate in chapter 5 of this thesis, the possibility of using vector fields to guide the random fields. The vector fields will be used to build tensor coefficients for an elliptic stochastic boundary value problem. The model considered is capable of producing non-stationary random fields with curvilinear features. Approximate realizations of this model will be drawn by using the finite element method, which is applied by using the MATLAB PDE toolbox.

Chapter 2

Gaussian Random Fields

One of the critical tasks in reservoir modelling is the simulation of a representative permeability field. Since it is unreasonable to describe reservoir heterogeneity in a deterministic manner, stochastic methods are applied to generate random fields.
In this chapter, we will give a brief account of some of the widely used methods to generate Gaussian random fields. These methods represent statistical characteristics of reservoir heterogeneity and they require at least the specification of the covariance function before generating realizations. Specifically, we shall emphasise using Fast Fourier Transform based techniques for generating realizations. But first we present a few properties of Gaussian random fields.

2.1 Random Fields

Let $(\Omega, \mathcal{F}, \mathbb{P})$ be a probability space, where Ω is the space of all events, $\mathcal{F}$ is a σ-algebra of subsets of Ω, and $\mathbb{P}$ is a probability measure defined on $\mathcal{F}$. Let $\xi : \Omega \to \mathbb{R}$ be a real valued random variable.

Definition 1 *$\xi(\omega)$ is said to be Gaussian (or normally distributed) if it has the density function*

$$\pi(x) = \frac{1}{\sqrt{2\pi}\sigma} e^{\frac{-(x-m)^2}{2\sigma^2}} \qquad x \in \mathbb{R}, \tag{2.1}$$

where m and σ^2 respectively denote the mean and the variance of $\xi(\omega)$. When $m = 0$ and $\sigma = 1$ we say that $\xi(\omega)$ is a standard Gaussian random variable.

An $\mathbb{R}^d$ valued random variable $\xi = (\xi_1, ..., \xi_d)$ is said to be multivariate Gaussian if, for every $\mathbf{a} = (a_1, ..., a_d) \in \mathbb{R}^d$, $\Sigma_{j=1}^d a_j \xi_j$ is Gaussian. In this case there exists a mean

vector $\mathbf{m} \in \mathbb{R}^d$ and a positive definite covariance matrix C, such that the probability density function of ξ is given by

$$\pi(\mathbf{x}) = \frac{1}{(2\pi)^{\frac{d}{2}} \mid C \mid^{\frac{1}{2}}} e^{-\frac{1}{2}(\mathbf{x}-\mathbf{m})^T C^{-1}(\mathbf{x}-\mathbf{m})}, \tag{2.2}$$

where $\mid C \mid$ is the determinant of C.

Definition 2 *An $\mathcal{L}^q(\Omega, \mathcal{F}, \mathbb{P})$ space, $q \geq 1$, is the linear normed space of random variables ξ that satisfy the condition*

$$\mathbb{E} \mid \xi \mid^q = \int_\Omega \mid \xi(\omega) \mid^q \mathbb{P}(d\omega) < \infty, \tag{2.3}$$

and the corresponding norm is defined by

$$\| \xi \|_{\mathcal{L}^q} = (\mathbb{E} \mid \xi \mid^q)^{\frac{1}{q}}. \tag{2.4}$$

In this thesis we shall primarily study random variables which satisfy (2.3) for $q = 2$. Such random variables are called second order random variables and they are equipped with the scalar product

$$\mathbb{E}[\xi_1 \xi_2] = \int_\Omega \xi_1(\omega)\xi_2(\omega)\mathbb{P}(d\omega), \tag{2.5}$$

where ξ_1 and ξ_2 are random variables.

Definition 3 *Let $(\Omega, \mathcal{F}, \mathbb{P})$ and a parameter set X be given. A random field is then a real valued function $\phi(\mathbf{x}, \omega)$ which, for every fixed $\mathbf{x} \in X$ is a random variable. For a fixed $\omega \in \Omega$, $\phi(\mathbf{x}, \omega)$ is called a sample function or a realization.*

The d-dimensional Euclidean space, $X = \mathbb{R}^d$, $d \geq 1$ will be studied in the following, and the dependency of the random field on the underlying probability space will usually be suppressed throughout the thesis:

$$\phi(\mathbf{x}) = \phi(\mathbf{x}, \omega), \mathbf{x} \in \mathbb{R}^d.$$

Definition 4 *A random field $\phi(\mathbf{x})$ is Gaussian if all finite dimensional distributions are multivariate Gaussian. That is, if $(\phi(\mathbf{x}_1), ..., \phi(\mathbf{x}_n))$ is a multivariate Gaussian random vector for any $\mathbf{x}_1, ..., \mathbf{x}_n \in \mathbb{R}^d$.*

The basic characteristics of a Gaussian random field are the mean and the covariance function, but without loss of generality we can assume that the random field under consideration has zero mean. The covariance function is defined by

$$C(\mathbf{x}, \mathbf{y}) = \mathbb{E}[\phi(\mathbf{x})\phi(\mathbf{y})],$$

and in particular, when $\mathbf{x} = \mathbf{y}$ we obtain the variance of $\phi(\mathbf{x})$,

$$\sigma^2(\mathbf{x}) = \mathbb{E}[\phi(\mathbf{x})^2].$$

Definition 5 *Suppose that $\mathcal{L}^2(\Omega, \mathcal{F}, \mathbb{P})$ is the Hilbert space of random variables at $\mathbf{x} \in \mathbb{R}^d$. A second order random field $\phi(\mathbf{x})$ is defined as a mapping on $\mathbb{R}^d$ with values in $\mathcal{L}^2(\Omega, \mathcal{F}, \mathbb{P})$,*

$$\phi : \mathbb{R}^d \to \mathcal{L}^2(\Omega, \mathcal{F}, \mathbb{P}). \tag{2.6}$$

Hence, for any second order random field $\phi(\mathbf{x})$,

$$\mathbb{E}[\phi(\mathbf{x})^2] < \infty.$$

2.2 Stationary Random Fields

Definition 6 *A random field $\phi(\mathbf{x})$ is a strictly stationary field if the spatial distribution is invariant under translation of the coordinates,*

$$\begin{aligned} &\mathbb{P}(\phi(\mathbf{x}_1) < z_1, \phi(\mathbf{x}_2) < z_2, ..., \phi(\mathbf{x}_n) < z_n) \quad = \\ &\mathbb{P}(\phi(\mathbf{x}_1 + \mathbf{h}) < z_1, \phi(\mathbf{x}_2 + \mathbf{h}) < z_2, ..., \phi(\mathbf{x}_n + \mathbf{h}) < z_n) \end{aligned}$$

for all $n \in \mathbb{N}$ and $\mathbf{h}$, $\mathbf{x}_1, ..., \mathbf{x}_n \in \mathbb{R}^d$. Here $\mathbb{P}(\phi(\mathbf{x}) < z)$ gives the probability that the variable ϕ at the location $\mathbf{x}$ is not greater than any given threshold z.

The condition specified in Definition 6 is a very strong condition which requires that all moments and cross-correlations, provided that they exist, will not depend on the location. Since this requirement may well not hold in practice, weaker forms of stationarity may be enough to provide the foundation for spatial modelling.

Definition 7 *A random field $\phi(\mathbf{x})$ of second order is called second order stationary, if the expectation $\mathbb{E}[\phi(\mathbf{x})]$ is identically constant and the covariance function is given by,*

$$C(\mathbf{x}, \mathbf{y}) = C(\mathbf{x} - \mathbf{y}). \tag{2.7}$$

In general strict stationarity implies second-order stationarity but the converse is not true. However, in the case of Gaussian random fields which are fully characterized by their mean and covariance function, second order stationarity implies strict stationarity.

A valid covariance function must be symmetric and positive semi-definite. To check semi-definiteness, $C(\mathbf{x} - \mathbf{y})$ must satisfy

$$\sum_{i=1}^{n} \sum_{j=1}^{n} a_i a_j C(\mathbf{x}_i - \mathbf{x}_j) \geq 0, \tag{2.8}$$

for all $n \in \mathbb{N}$ and any numbers $a_i \in \mathbb{R}$ and any vector $\mathbf{x}_i \in \mathbb{R}$. As indicated in [28], a sufficient condition for positive semi-definiteness is that the spectral density, $G(\mathbf{k})$, of the covariance function

$$G(\mathbf{k}) = \int_{\mathbb{R}^d} C(\mathbf{r}) e^{-i\mathbf{k}\cdot\mathbf{r}} d\mathbf{r}, \quad \mathbf{k} \in \mathbb{R}^d,$$

must be nonnegative for all $\mathbf{k}$.

Definition 8 *A stationary random field is an isotropic random field if the covariance function only depends on the Euclidean distance,*

$$C(\mathbf{x}, \mathbf{y}) = C(r),$$

where $r = \| \mathbf{x} - \mathbf{y} \|$ is the Euclidean distance. Hence $C(r)$ is invariant under translation and rotations.

For an isotropic covariance function, the correlation function is defined by

$$c(r) = \frac{C(r)}{\sigma^2},$$

where the variance $\sigma^2 = C(0)$. The function $c(r)$ calculates the linear correlation between values of $\phi(\mathbf{x})$ at points separated by a r. One way to summarise $c(r)$ is through the correlation length.

Definition 9 *The correlation length ρ, is a measure of the length over which the property (e.g. permeability) would be expected to be correlated and is given by*

$$\rho = \int_0^\infty c(r)dr. \tag{2.9}$$

Notice that ρ is only an appropriate measure of correlation length if $c(r) > 0$ throughout. The physical significance of ρ lies in the fact that as $\frac{\|\mathbf{x}-\mathbf{y}\|}{\rho}$ increases above 1, $\phi(\mathbf{x})$ and $\phi(\mathbf{y})$ tend to become more and more uncorrelated.

2.3 Continuity and Differentiability

A deterministic function $f(\mathbf{x})$ is continuous, if for any sequence $\{\mathbf{x}_n\}$, $f(\mathbf{x}_n) \to f(\mathbf{x})$ as $\mathbf{x}_n \to \mathbf{x}$. Similarly, when considering a random field $\phi(\mathbf{x})$, continuity is defined by using the convergence of a sequence $\phi(\mathbf{x}_n)$ of random variables. In our investigation of smoothness properties, we shall consider almost sure continuity and differentiability, and mean square continuity and differentiability.

Definition 10 *Let $\{\xi_n\}$ be a sequence of random variables in $\mathcal{L}^2(\Omega, \mathcal{F}, \mathbb{P})$. Then $\{\xi_n\}$ is said to converge to the random variable ξ:*

- *Almost surely or with probability one, if*

$$\mathbb{P}\Big(\lim_{n\to\infty} \xi_n = \xi\Big) = 1. \tag{2.10}$$

- *In the mean square sense, if*

$$\lim_{n\to\infty} \mathbb{E} \mid \xi_n - \xi \mid^2 = 0. \tag{2.11}$$

Definition 11 *Suppose that $\phi(\mathbf{x})$ is a second order random field defined on a compact set $D, D \subset \mathbb{R}^d$. Then*

- *$\phi(\mathbf{x})$ has continuous sample paths with probability one in D if for every sequence $\{\mathbf{x}_n\} \in D$ for which $\mathbf{x}_n \to \mathbf{x}$ as $n \to \infty$,*

$$\mathbb{P}\{\forall \mathbf{x} \in D, \text{and for any} \quad \mathbf{x}_n \to \mathbf{x}, \phi(\mathbf{x}_n, \omega) \to \phi(\mathbf{x}, \omega) \quad \text{as} \quad n \to \infty\} = 1.$$

- $\phi(\mathbf{x})$ *is mean square continuous in* D *if for every sequence* $\{\mathbf{x}_n\} \in D$ *for which* $\mathbf{x}_n \to \mathbf{x}$ *as* $n \to \infty$,

$$\mathbb{E}\Big[\mid \phi(\mathbf{x}_n) - \phi(\mathbf{x}) \mid^2 \Big] \to 0 \quad as \quad n \to \infty.$$

Sample path continuity with probability one implies that there are, with probability one, no discontinuities within D. As shown in [16], one form of continuity does not imply the other since one form of convergence does not imply the other.
As mentioned for continuity, there are various types of differentiability depending on different types of convergence.

Definition 12 *Suppose that* $\phi(\mathbf{x})$ *is a second order random field defined on a compact set* $D, D \subset \mathbb{R}^d$. *Then*

- $\phi(\mathbf{x})$ *has differentiable sample paths with probability one in* D *if there exist a version* $\phi_i(\mathbf{x})$, *denoting the* i*-th partial derivatives of* $\phi(\mathbf{x})$ *at* $\mathbf{x}$,

$$\phi_i(\mathbf{x}) = \frac{\partial \phi(\mathbf{x})}{\partial x_i} = \lim_{h \to 0} \frac{\phi(\mathbf{x} + h\mathbf{e}_i) - \phi(\mathbf{x})}{h},$$

where $\mathbf{e}_i$ *is the unit vector along the* i*-th direction, such that for every sequence* $\{\mathbf{x}_n\} \in D$ *for which* $\mathbf{x}_n \to \mathbf{x}$ *as* $n \to \infty$,

$$\mathbb{P}\{\forall \mathbf{x} \in D, \text{and for any} \quad \mathbf{x}_n \to \mathbf{x}, \phi_i(\mathbf{x}_n, \omega) \to \phi_i(\mathbf{x}, \omega) \\ as \quad n \to \infty, \forall i = 1, ..., d\} = 1.$$

- $\phi(\mathbf{x})$ *is mean square differentiable in* D *if for every sequence* $\{\mathbf{x}_n\} \in D$ *for which* $\mathbf{x}_n \to \mathbf{x}$ *as* $n \to \infty$, *there exist a version* $\phi_i(\mathbf{x})$ *such that*

$$\mathbb{E}\Big[\mid \phi_i(\mathbf{x}_n) - \phi_i(\mathbf{x}) \mid^2 \Big] \to 0 \quad as \quad n \to \infty, \forall i = 1, ..., d.$$

Remark 1 *Suppose that* $\phi(\mathbf{x})$ *is an isotropic random field with covariance function* $C(r)$. *Then*

- $\phi(\mathbf{x})$ *is mean square continuous at any* $\mathbf{x} \in \mathbb{R}^d$ *if and only if* $C(r)$ *is continuous at* 0.

- *If* $\frac{d^2C(r)}{dr^2}$ *exists and is finite at the point 0, then* $\phi(\mathbf{x})$ *is mean square differentiable at any* $\mathbf{x}$.

For further discussions on mean square continuity and differentiability, see [17,28,31,35].

As explained in [29], in order to study sample path continuity (differentiability) of a random field, one can either use the Kolmogorov continuity theorem or the Sobolev embedding theorem. In this thesis we shall use the Sobolev embedding theorem to establish all the regularity properties.

2.4 Gaussian White Noise

White noise can be physically thought of as a sound with equal intensity at all frequencies within a broad band. The reason why the word "white" is used to explain this type of noise is due to its similarity to "white light" which consists of all different colours of light combined together. Mathematically, white noise can defined as a Gaussian measure or formally, as the derivative of Brownian motion (Brownian sheet in higher dimensions). However it is well known that Brownian motion is nowhere differentiable. To obtain a satisfactory theory of white noise, one approach is to introduce the concept of generalized Gaussian random fields. For detailed discussions on generalized Gaussian random fields see [28].

Definition 13 *A Gaussian random field $W(\mathbf{x})$, $\mathbf{x} \in \mathbb{R}^d_+$ with zero mean and covariance function*

$$\mathbb{E}[W(\mathbf{x})W(\mathbf{y})] = \prod_{n=1}^{d} \min(x_n, y_n), \tag{2.12}$$

is called the Brownian sheet.

As indicated in [20], white noise is formally defined by

$$\dot{W}(\mathbf{x}) = \frac{\partial^d W(\mathbf{x})}{\partial x_1 ... \partial x_d}, \tag{2.13}$$

and has the following properties

$$\mathbb{E}[\dot{W}(\mathbf{x})] = 0 \tag{2.14}$$

$$\mathbb{E}[\dot{W}(\mathbf{x})\dot{W}(\mathbf{y})] = \delta(\mathbf{x}-\mathbf{y}), \qquad \mathbf{x}, \mathbf{y} \in \mathbb{R}^d. \tag{2.15}$$

Remark 2 *To make sense of a multidimensional Gaussian random field of the form*

$$\phi(\mathbf{x}) = \int_{\mathbb{R}^d} g(\mathbf{x} - \mathbf{x_0}) W(d\mathbf{x_0}) \tag{2.16}$$

where $g(\mathbf{x} - \mathbf{x_0}) \in \mathcal{L}^2(\mathbb{R}^d)$ *and* $W(d\mathbf{x_0})$ *is a Brownian sheet, one needs to introduce measure theory. A detailed discussion is given in [57,17,20]. In this thesis we shall frequently use the following two properties*

$$\mathbb{E}[\phi(\mathbf{x})] = 0, \tag{2.17}$$

$$\mathbb{E}[\phi(\mathbf{x})\phi(\mathbf{y})] = \int_{\mathbb{R}^d} g(\mathbf{x} - \mathbf{x_0}) g(\mathbf{y} - \mathbf{x_0}) d\mathbf{x_0}. \tag{2.18}$$

See [57,17] for a verification of these properties.

2.5 Simulation of Gaussian random fields

In this section we shall present some of the widely used techniques to generate realizations for second order stationary random fields. We will just describe the case $d = 1$, but the same theory applies with appropriate modifications for $d = 2, 3$. Generally, there are two kinds of second order random fields that can be simulated. Namely, conditional simulations and unconditional simulations. In conditional simulations, the generated realizations satisfy the condition that their values at sampled points equal to those observed, whereas in unconditional simulations, the generated realizations do not follow the observed values and instead honour the correlation parameters through the covariance function. In most spatial problems, the covariance function can be computed from the given observation data. However in the case of log permeability of oil reservoir, where we do not have direct measurements of the spatial field, the covariance function has to be chosen a priori. This is because the data do not usually provide enough information to approximate the covariance function.

2.5.1 Matrix Decomposition Method

The matrix decomposition method for simulation of a Gaussian field is based on the Cholesky decomposition of the covariance matrix of the multidimensional Gaussian vector. Let $\phi(x)$ be a zero mean Gaussian random field with covariance function $C(x_i, x_j)$. Assume that we want to simulate a realization with N grid points. Then

the LU (the lower-upper triangular matrix technique) method to this problem can be summarised in the following steps

- Step 1: The matrix $C(x_i, x_j)$, $(i, j = 1, 2, ..., N)$ is by definition a positive-definite symmetric matrix. Thus it can be decomposed into a product of a lower triangular matrix L and an upper triangular matrix U using the Cholesky algorithm. So

$$C = LU,$$

  where $U = L^T$.

- Step 2: Assume that V is a vector of N independent standard Gaussian random variables, and let

$$X = LV, \tag{2.19}$$

  where $X^T = [X(x_1), ..., X(x_N)]$, $X(x_i) = \phi(x_i)$.

- Step 3: The random vector generated by (2.19) have the desired zero mean and covariance

$$\begin{aligned} \mathbb{E}[(LV)(LV)^T] &= L\mathbb{E}[VV^T]U & (2.20)\\ &= LIU & (2.21)\\ &= C. & (2.22) \end{aligned}$$

The drawbacks of this technique are in the large storage requirement for the covariance matrix and perhaps the computing time required to split C into lower and upper triangular matrices. Although the factorization only needs to be done once, for simulating large random fields these requirements often become very expensive because the covariance matrix is generally not a sparse matrix. For further details on this method of simulation see [28].

2.5.2 Moving Window Method

Consider a Gaussian random field $\phi(x)$ given by

$$\phi(x) = \int_{-\infty}^{\infty} g(x - x_0)W(dx_0) \tag{2.23}$$

where $W(dx_0)$ is a Brownian measure and $g(x-x_0)$ is a weighting function determined from the covariance function. Notice that by truncating and discretizing the above integral we obtain the basis for the moving window method

$$\phi_N(x) = \sum_{j=\lfloor \frac{x}{h} \rfloor - b}^{j=\lfloor \frac{x}{h} \rfloor + b} g(x - x_j)\xi_j \sqrt{h}.$$

Here $\{\xi_j\}_{j=-N}^{N}$ is a family of independent standard Gaussian random variables, h denotes the width of the discretization, $\lfloor x \rfloor$ denotes the greatest integer not exceeding x, $\{x_j = jh\}_{j=-N}^{N}$ are the evenly spaced grid points, and b denotes the truncation bandwidth. The bandwidth is chosen as large as possible so that $g(x-x_0)$ for $\mid x-x_0 \mid > b$ has a negligible value.

One of the drawbacks of this technique is that, as indicated in [23], in higher dimensions the computations rapidly become cumbersome, and it is inefficient when the kernel is not given in a closed form.

2.5.3 Spectral Representation Method

Suppose that $\phi(x)$, $x \in \mathbb{R}$, is a zero mean second order stationary Gaussian random field with covariance function $C(x-y)$ and spectral density $G(k)$. Then as indicated in [46], a finite approximation of $\phi(x)$ is given by

$$\phi_N(x) = \sum_{n=0}^{N-1} \sqrt{\frac{G(k_n)\Delta k}{\pi}} (\xi_n \cos(k_n x) + \eta_n \sin(k_n x)), \tag{2.24}$$

where ξ_n and η_n are independent standard normal random variables, $k_n = n\Delta k$ and $\Delta k = \frac{k_{max}}{N}$. Here k_{max} denotes an upper cutoff beyond which $G(k_n)$ is negligible for practical purposes, and it can be selected so that

$$\int_{-k_{max}}^{k_{max}} G(k)dk = \int_{0}^{k_{max}} 2G(k)dk \tag{2.25}$$

$$\approx 2\pi\sigma^2. \tag{2.26}$$

Notice that $\phi_N(x)$ is periodic with period

$$T = \frac{2\pi}{\Delta k}, \tag{2.27}$$

and the covariance function is given by

$$C_N(x-y) = \sum_{n=0}^{N-1} \frac{G(k_n)\Delta k}{\pi} \cos(k_n(x-y)). \tag{2.28}$$

The convergence rate of the spectral representation primarily depends on the smoothness of the covariance function. If the covariance function is very smooth, then the spectral representation converges rapidly.
Observe that (2.24) can alternatively be written as

$$\phi_N(x) = \sum_{n=0}^{N-1} \sqrt{\frac{G(k_n)\Delta k}{\pi}} \mu_n \cos\left(k_n x + \tan^{-1}\left(\frac{-\eta_n}{\xi_n}\right)\right), \tag{2.29}$$

where $\tan^{-1}\left(\frac{-\eta_n}{\xi_n}\right)$ are independent random phase angles uniformly distributed in the range $(0, 2\pi)$ and

$$\mu_n = \sqrt{\xi_n^2 + \eta_n^2}, \tag{2.30}$$

are called Rayleigh random variables. See [46] or section A.7 for more details. On the other hand, there is another interpretation of (2.29) in which the amplitude is treated as a deterministic function. That is

$$\hat{\phi}_N(x) = \sum_{n=0}^{N-1} \sqrt{\frac{2G(k_n)\Delta k}{\pi}} \cos(k_n x + v_n), \tag{2.31}$$

where v_n is uniform over $(0, 2\pi)$. Formulations (2.29) and (2.31) have some similarities and differences. Both generators have the same approximate covariance function. However, while (2.29) is Gaussian for any N, realizations generated using (2.31) are only asymptotically Gaussian. In other words, (2.31) becomes Gaussian as $\Delta k \to 0, N \to \infty$ with $\Delta k N \to \infty$.

Remark 3 *In this thesis, we shall select the Gaussian spectral representation, (2.29), to generate approximate realizations of $\phi_N(x)$. This is because we prefer to preserve the Gaussian properties of $\phi(x)$.*

2.5.4 Karhunen-Loeve Expansion

Let D be a compact set in $\mathbb{R}$, $\phi(x)$ be a second order stationary Gaussian random field over D and $C(x-y)$ be the corresponding covariance function. Then the Karhunen-Loeve (K-L) expansion of $\phi(x)$ is given by

$$\phi(x) = \sum_{n=0}^{\infty} \sqrt{\lambda_n} \xi_n \psi_n(x),$$

where λ_n, ψ_n respectively denote the eigenvalues and a complete set of normalized eigenfunctions of $C(x-y)$, and the parameters ξ_n are independent standard normal random variables. By definition, $C(x-y)$ is bounded, symmetric and positive definite. Thus using Mercer's theorem, [7,17], it can be written as

$$C(x-y) = \sum_{n=0}^{\infty} \lambda_n \psi_n(x)\psi_n(y).$$

The eigenvalues and the eigenfunctions can be calculated by solving the homogeneous Fredholm integral equation

$$\int_D C(x-y)\psi_n(x)dx = \lambda_n \psi_n(y). \tag{2.32}$$

The eigenfunctions can be chosen to form a complete orthogonal set satisfying

$$\int_D \psi_n(x)\psi_m(x)dx = \delta_{nm},$$

where δ_{nm} denotes the Kronecker delta.

Remark 4 *The truncated K-L expansion*

$$\phi_N(x) := \sum_{n=0}^{N-1} \sqrt{\lambda_n}\xi_n\psi_n(x),$$

converges to $\phi(x)$ uniformly in x in mean square i.e

$$\sup_{x\in D} \mathbb{E}[(\phi(x) - \phi_N(x))^2] = \sup_{x\in D} \sum_{n=N}^{\infty} \lambda_n \psi_n(x)^2 \to 0 \quad as \quad N \to \infty.$$

See [43] for further details.

A detailed convergence study was carried out in [9] to investigate the robustness of the K-L expansion by varying the size of D, the correlation length, and the number of K-L terms. The results were:

- The smoother the covariance function of $\phi(x)$, the fewer K-L terms are required for the expansion.
- As the ratio of ρ to D increases, fewer K-L terms are required for the expansion.
- The variance of $\phi(x)$ is larger than the variance of the truncated expansion $\phi_N(x)$.

2.5.5 Fast Fourier Transform Implementation

The generation of random fields using a spectral representation method can be computationally expensive. However the computational cost can be significantly reduced by using the Fast Fourier Transform. A Fast Fourier Transform (FFT) is an efficient algorithm to compute the discrete Fourier transform and its inverse. Computing the discrete Fourier transform directly from the definition takes $O(N^2)$ arithmetical operations on N points, while an FFT can compute the same result using $O(N \log N)$ operations. In this context, (2.29) can be written as

$$\phi^j(q\Delta x) = \Re\left\{ \sum_{n=0}^{N-1} D_n e^{i(n\Delta k)(q\Delta x)} \right\}, q = 0, 1, ..., N-1, \tag{2.33}$$

where $\Re$ denotes the real part, ϕ^j denotes the j-th realization and

$$D_n = \sqrt{\frac{G(n\Delta k)\Delta k}{\pi}} \mu_n e^{iv_n}, n = 0, 1, 2, ..., N-1 \tag{2.34}$$

$$\Delta k = \frac{k_{max}}{M}. \tag{2.35}$$

Here v_n are uniformly distributed in $(0, 2\pi)$ and μ_n are Rayleigh random variables. Rayleigh random variables can be generated by,

$$\mu_n = \sqrt{-2 \ln u_n}, \tag{2.36}$$

where u_n are uniformly distributed in $(0, 1)$ and are independent of v_n. To completely benefit from the FFT technique, it is suggested in [46] that the number of Fourier coefficients must be an integer power of two,

$$N = 2^r. \tag{2.37}$$

In order to avoid aliasing when generating sample functions, the spatial increment Δx must fulfill the condition,

$$\Delta x \leq \frac{\pi}{k_{max}}. \tag{2.38}$$

Notice that since (2.29) is periodic with period T,

$$T = \frac{2\pi}{\Delta k}, \tag{2.39}$$

Δx and Δk are related in the following way

$$N\Delta x = T = \frac{2\pi}{\Delta k}. \tag{2.40}$$

As a result of the above relations, (2.33) can be written as

$$\phi^j(q\Delta x) = \Re\left\{ \sum_{n=0}^{N-1} D_n e^{\frac{2\pi i n q}{N}} \right\}, q = 0, 1, ..., N-1. \tag{2.41}$$

However the formula given in (2.41) produces periodic realizations. As explained in [23], in order to avoid this undesirable effect a lattice size larger than that required must be selected and the excess ignored. How much larger depends on the correlation length. That is, Δk must be selected so that

$$\frac{2\pi}{\Delta k} \geq N\Delta x + 2\rho, \tag{2.42}$$

where ρ is correlation length and then the realization will only be plotted over $N\Delta x$. This will create a buffer zone which will eliminate the problem associated with the periodicity of the numbers arising as a result of using the FFT. Now by combining (2.35) and (2.42), the following relation between M and N is established:

$$\frac{2\pi M}{k_{max}} \geq N\Delta x + 2\rho. \tag{2.43}$$

Remark 5 *To prevent having periodic realizations when using the Gaussian spectral representation, we shall assume that $M = N$, and select Δx and ρ such that* (2.38) *and* (2.43) *are satisfied.*

Chapter 3

Isotropic Elliptic Stochastic PDEs

In this chapter we shall briefly study isotropic elliptic stochastic partial differential equations. We will address the analytical properties of a particular solution and the conditions required for uniqueness of the Green's function. A useful formula is also derived linking the computation of the covariance function of the solution to that of the Green's function. In order to discuss the regularity properties of the solution, we need to introduce Sobolev spaces.

Suppose that $\phi(\mathbf{x})$, $\mathbf{x} \in \mathbb{R}^d$, is a zero mean second order Gaussian random field. Then the probability density function (pdf) is defined by

$$\pi(\phi) = Z \exp(-J(\phi)), \tag{3.1}$$

where Z is a normalization constant, the functional $J(\phi)$ given by,

$$J(\phi) = \frac{1}{2} \int_{\mathbb{R}^d} \phi(\mathbf{x}) \mathcal{T}^{-1} \phi(\mathbf{x}) d\mathbf{x}, \tag{3.2}$$

and $\mathcal{T}$ is the covariance operator,

$$\mathcal{T}\phi(\mathbf{x}) = \int_{\mathbb{R}^d} C(\mathbf{x}, \mathbf{y}) \phi(\mathbf{y}) d\mathbf{y}. \tag{3.3}$$

Here $C(\mathbf{x}, \mathbf{y})$ is the covariance function of $\phi(\mathbf{x})$. There are various algorithms designed for drawing samples from (3.1) and readers are referred to [22] for a comprehensive review. One way to achieve this is via the Langevin equation,

$$\frac{\partial \phi(\mathbf{x}, t)}{\partial t} = -\nabla J(\phi) + \sqrt{2} \dot{W}(\mathbf{x}, t), \tag{3.4}$$

where $\dot{W}(\mathbf{x}, t)$ is space-time white noise. As $t \to \infty$, the solution of the Langevin equation will produce realizations from $\pi(\phi)$. However for a particular type of Gaussian random field, the Langevin method does not constitute the optimal way for sampling. For example assume the inverse of the covariance operator $\mathcal{T}^{-1}$ to be a linear elliptic differential operator L^2,

$$\mathcal{T}^{-1} = L^2. \tag{3.5}$$

Notice that

$$\begin{aligned} L^2\mathcal{T}\phi(\mathbf{x}) &= \int_{\mathbb{R}^d} L^2 C(\mathbf{x}, \mathbf{y})\phi(\mathbf{y})d\mathbf{y}, & (3.6)\\ &= \phi(\mathbf{x}). & (3.7) \end{aligned}$$

Hence (3.5) is formally equivalent to

$$L^2 C(\mathbf{x}, \mathbf{y}) = \delta(\mathbf{x} - \mathbf{y}). \tag{3.8}$$

In this thesis we shall investigate generating samples from (3.1) by solving elliptic stochastic partial differential equations. The idea is to compute a class of covariance functions which satisfy (3.8), and then use the Gaussian spectral representation for simulating samples from the pdf. The differential operator will be chosen to be defined on the whole of $\mathbb{R}^d$ as it will lead to closed form expressions for the covariance function.
Consider

$$L\phi(\mathbf{x}) = \dot{W}(\mathbf{x}), \qquad \mathbf{x} \in \mathbb{R}^d, \tag{3.9}$$

where L is a constant coefficient positive isotropic elliptic differential operator of order $2m$,

$$L = \sum_{p=0}^{m} a_p \nabla^{2p}, \tag{3.10}$$

and $\dot{W}(\mathbf{x})$ is a Gaussian white noise. Observe that (3.9) is formal since $\dot{W}(\mathbf{x})$ is only defined as a generalized random field. To overcome this problem, the usual theory of elliptic PDEs can be applied to this class of stochastic PDEs by casting the problem in a weak form. However, the weak formulation of (3.9) will not be considered in this

thesis and instead, we shall only study a particular solution of (3.9) and its properties. This solution is defined by

$$\phi(\mathbf{x}) = \int_{\mathbb{R}^d} g(\| \mathbf{x} - \mathbf{x_0} \|) W(d\mathbf{x_0}), \tag{3.11}$$

where $W(d\mathbf{x_0})$ is defined as a Brownian measure and $g(\| \mathbf{x} - \mathbf{x_0} \|)$ (if it exists) is the Green's function of L. The Green's function is the solution of

$$Lg(\| \mathbf{x} - \mathbf{x_0} \|) = \delta(\mathbf{x} - \mathbf{x_0}), \tag{3.12}$$

subject to the condition that $g(\| \mathbf{x} - \mathbf{x_0} \|)$ and all its derivatives vanish at infinity.

Remark 6 *As the differential operator L is an isotropic (rotationally invariant) operator, $g(\| \mathbf{x} - \mathbf{x_0} \|)$ is a function of the Euclidean distance.*

3.1 Properties of the particular solution

There are various ways to demonstrate the uniqueness of solutions for a deterministic elliptic PDE. For instance, uniqueness can be established by using the Lax-Milgram theorem. However for constant coefficient elliptic differential operators defined on $\mathbb{R}^d$, uniqueness can be verified by using the Fourier transform. Before proceeding any further, we need to define the notion of strong ellipticity.

Definition 14 *The operator (3.10) is said to be a strongly elliptic differential operator if the symbol*

$$\lambda(k) = \sum_{p=0}^{m} a_p(-ik)^{2p} > 0, \tag{3.13}$$

for all $k = \| \mathbf{k} \|, \mathbf{k} \in \mathbb{R}^d$.

Theorem 15 *If L is a strongly elliptic differential operator, then the Green's function of L exists and is unique.*

Proof: See [45], chapter 12, for further details.

Observe that since L is a deterministic and isotropic differential operator, the Green's

function will be deterministic and rotationally invariant. Thus $\phi(\mathbf{x})$ is a zero mean isotropic Gaussian random field. The covariance function is given by

$$C(\| \mathbf{x} - \mathbf{y} \|) = \int_{\mathbb{R}^d} g(\| \mathbf{x} - \mathbf{x_0} \|) g(\| \mathbf{y} - \mathbf{x_0} \|) d\mathbf{x_0},$$

and hence the variance is

$$\sigma^2 = \int_{\mathbb{R}^d} g(\| \mathbf{x} - \mathbf{x_0} \|)^2 d\mathbf{x_0}.$$

If the Green's function is square integrable, then the variance will be finite and so $\phi(\mathbf{x})$ will be a real valued Gaussian random field. However if the variance is infinite, then $\phi(\mathbf{x})$ should be understood in a distributional sense.

Theorem 16 *Suppose that L is an isotropic strongly elliptic differential operator. Then the Green's function and the covariance function satisfy*

$$LC(\| \mathbf{x} - \mathbf{y} \|) = g(\| \mathbf{x} - \mathbf{y} \|). \tag{3.14}$$

Moreover, if L is defined by (3.10) then,

- *the covariance function of* (3.9) *is given by*

$$C(r) = -\frac{\partial g(r)}{\partial a_0}, \tag{3.15}$$

- *the covariance function of $L^n \phi(\mathbf{x}) = \dot{W}(\mathbf{x})$ is*

$$C_n(r) = \frac{-1}{(2n-1)!} \frac{\partial^{2n-1} g(r)}{\partial a_0^{2n-1}}, \qquad n \geq 1. \tag{3.16}$$

Formal Proof: The first part of the theorem can be shown by using the shifting property of the delta function,

$$\begin{aligned} LC(\| \mathbf{x} - \mathbf{y} \|) &= \int_{\mathbb{R}^d} Lg(\| \mathbf{x} - \mathbf{x_0} \|) g(\| \mathbf{y} - \mathbf{x_0} \|) d\mathbf{x_0} \\ &= \int_{\mathbb{R}^d} \delta(\mathbf{x} - \mathbf{x_0}) g(\| \mathbf{y} - \mathbf{x_0} \|) d\mathbf{x_0} \\ &= g(\| \mathbf{x} - \mathbf{y} \|). \end{aligned}$$

When L is defined by (3.10), (3.12) reads

$$a_m \nabla^{2m} g(r) + a_{m-1} \nabla^{2(m-1)} g(r) + ... + a_0 g(r) = \delta(\mathbf{x} - \mathbf{x_0}). \tag{3.17}$$

In particular,

$$g(r) = \frac{1}{(2\pi)^d} \int_{\mathbb{R}^d} \frac{e^{i\mathbf{k}\cdot\mathbf{r}}}{\lambda(\mathbf{k})} d\mathbf{k}. \tag{3.18}$$

Now by differentiating both sides of (3.17) with respect to a_0 we obtain

$$a_m \nabla^{2m} \frac{\partial g(r)}{\partial a_0} + a_{m-1} \nabla^{2(m-1)} \frac{\partial g(r)}{\partial a_0} + ... + a_0 \frac{\partial g(r)}{\partial a_0} + g(r) = 0. \tag{3.19}$$

Hence

$$L\left(\frac{\partial g}{\partial a_0}\right) \quad = \quad -g(r), \tag{3.20}$$

and so

$$C(r) = -\frac{\partial g(r)}{\partial a_0}. \tag{3.21}$$

Consider

$$L^n \phi(\mathbf{x}) = \dot{W}(\mathbf{x}), \qquad n \geq 1. \tag{3.22}$$

The corresponding covariance function is given by

$$C_n(r) = \frac{1}{(2\pi)^d} \int_{\mathbb{R}^d} \frac{e^{i\mathbf{k}\cdot\mathbf{r}}}{(\lambda(\mathbf{k}))^{2n}} d\mathbf{k}. \tag{3.23}$$

By successively applying the quotient rule to (3.18), C_n can be written as

$$C_n(r) = \frac{-1}{(2n-1)!} \frac{\partial^{2n-1} g(r)}{\partial a_0^{2n-1}}. \tag{3.24}$$

Theorem 16 provides a very useful mechanism to evaluate the covariance functions from the Green's function. This is because the computation of the Green's function is far simpler in comparison to the computation of the covariance function.

Remark 7 *As far as we aware the above theorem has not been described previously in the literature.*

3.2 Sobolev Space

In this section we will examine the regularity properties of (3.11). By regularity we mean Hölder continuity and differentiability. Before attempting to address these questions, we first need to identify the solution space of (3.9). Solution spaces of elliptic PDEs are usually defined in terms of Sobolev spaces and in the following, we shall focus on the $\mathcal{L}^2$ definition of Sobolev spaces. But first we need to define Schwartz space.

Definition 17 *Let us denote* $\partial^{\alpha}\psi(\mathbf{x}) := \partial_1^{\alpha_1}...\partial_d^{\alpha_d}\psi(\mathbf{x}) = \psi^{\alpha}(\mathbf{x})$ *for any multiindex* $\alpha = (\alpha_1, ..., \alpha_d)$ *with* $\alpha_j = 0, 1, 2, ...$ *Hence*

$$\partial_1^{\alpha_1}\psi(x) := \frac{\partial^{\alpha_1}\psi(x)}{\partial x_1^{\alpha_1}}. \tag{3.25}$$

Let $\mathcal{C}^{\infty}(\mathbb{R}^d)$ *be the space of infinitely differentiable function in* $\mathbb{R}^d$*. Then Schwartz space,* $S = S(\mathbb{R}^d)$*, is the space of functions* $\psi(\mathbf{x}) \in \mathcal{C}^{\infty}(\mathbb{R}^d)$ *such that*

$$\| \psi \|_{\alpha,N} := \sup_{\mathbf{x}\in\mathbb{R}^d} (1+ \| \mathbf{x} \|)^N \mid \partial_x^{\alpha}\psi(\mathbf{x}) \mid < \infty, \tag{3.26}$$

for any $N = 1, 2, ...$ *and any multiindex* $\alpha = (\alpha_1, ..., \alpha_d)$ *with* $\alpha_j = 0, 1, 2, ...,$ *and the sequence* $\psi_n(\mathbf{x}) \to \psi(\mathbf{x})$ *if*

$$\| \psi_n - \psi \|_{\alpha,N} \to 0, \quad as \quad n \to \infty \tag{3.27}$$

for any such N *and* α*.*

Definition 18 *The space of tempered distribution,* $S'(\mathbb{R}^d)$*, is the space of linear continuous functionals on* $S(\mathbb{R}^d)$*. That is,* $f \in S'(\mathbb{R}^d)$ *if the following two conditions hold:*

- *Linearity:* $f(\alpha\psi_1 + \beta\psi_2) = \alpha f(\psi_1) + \beta f(\psi_2), \quad \alpha, \beta \in \mathbb{R}, \ \psi_1, \psi_2 \in S(\mathbb{R}^d).$
- *Continuity:* $f(\psi_n) \to f(\psi)$*, if* $\psi_n \to \psi$*, as* $n \to \infty$*,* $\psi, \psi_n \in S(\mathbb{R}^d).$

Assume that γ is a non-negative integer. Then we define the Sobolev space $H^{\gamma}(\mathbb{R}^d)$, to be the set of all $u \in \mathcal{L}^2(\mathbb{R}^d)$ whose (distributional) derivatives $\partial^{\alpha}u$ belong to $\mathcal{L}^2(\mathbb{R}^d)$ for $\mid \alpha \mid \leq \gamma$:

$$H^{\gamma}(\mathbb{R}^d) = \{u \in \mathcal{L}^2(\mathbb{R}^d) \mid \partial^{\alpha}u \in \mathcal{L}^2(\mathbb{R}^d) \quad \text{for} \quad \mid \alpha \mid \leq \gamma\}.$$

For fractional and negative exponents, there is an equivalent characterization of this definition in terms of Fourier transforms.

Definition 19 *For* $\gamma \in \mathbb{R}$*, the Sobolev space* $H^{\gamma}(\mathbb{R}^d)$ *is defined by*

$$H^{\gamma}(\mathbb{R}^d) = \left\{u(\mathbf{x}) \in S'(\mathbb{R}^d) \mid (1+ \mid k \mid^2)^{\frac{\gamma}{2}} \mathcal{F}(u) \in \mathcal{L}^2(\mathbb{R}^d)\right\}, \tag{3.28}$$

where $\mathcal{F}$ denotes the Fourier transform of u. The corresponding norm is defined by

$$\| u \|_{H^\gamma} = \| (1+ \mid k \mid^2)^{\frac{\gamma}{2}} \mathcal{F}(u)(k) \|_{\mathcal{L}^2} . \tag{3.29}$$

For detailed discussions on the Fourier transform of a distribution and its properties see [5,39].
Sobolev spaces and Schwartz space are related as follow

$$S \subset \cdots \subset H^{\gamma_2} \subset H^{\gamma_1} \subset \mathcal{L}^2 \subset H^{-\gamma_1} \subset H^{-\gamma_2} \subset \cdots \subset S',$$

where $0 < \gamma_1 < \gamma_2 < \gamma_3 \cdots$, and $H^{\gamma_1} \subset \mathcal{L}^2$ denotes that fact that H^{γ_1} is dense in $\mathcal{L}^2$. One of the fruitful results of the theory of Sobolev spaces is the Sobolev embedding theorem.

Theorem 20 *Suppose that $\gamma > s + \frac{d}{2}$. Then the Sobolev space $H^\gamma(\mathbb{R}^d)$ can be embedded in the space of s-times continuously differentiable functions $\mathcal{C}^s(\mathbb{R}^d)$,*

$$H^\gamma(\mathbb{R}^d) \subset \mathcal{C}^s(\mathbb{R}^d).$$

Proof: See [10], Corollary 1.4.

As a consequence of this theorem, one can deduce that if $u(\mathbf{x}) \in H^\gamma(\mathbb{R}^d)$ and γ is large enough, then $u(\mathbf{x})$ can be differentiated $[\gamma - \frac{d}{2}\ ]$ (integer part) times, all the derivatives are square integrable and the last derivative is Hölder continuous with exponent

$$\gamma - \frac{d}{2} - [\gamma - \frac{d}{2}].$$

3.2.1 Local Sobolev Space

In [20], the author shows that Gaussian white noise belongs to a special class of Sobolev spaces known as a local Sobolev space. Before presenting the result we need to recall some definitions.

Definition 21 *A function $u(\mathbf{x})$ is locally square integrable on $\mathbb{R}^d$ if*

$$\int_D \mid u(\mathbf{x}) \mid^2 d\mathbf{x} < \infty,$$

for every compact set D in $\mathbb{R}^d$.

Definition 22 *Suppose that* $\gamma \in \mathbb{R}$. *If* $u(\mathbf{x})$ *is any distribution, we say* $u(\mathbf{x}) \in H^{\gamma}_{loc}(\mathbb{R}^d)$ *if for any* $\psi(\mathbf{x}) \in \mathcal{C}^{\infty}_0(\mathbb{R}^d)$, $u(\mathbf{x})\psi(\mathbf{x}) \in H^{\gamma}(\mathbb{R}^d)$.

Observe that in a bounded domain H^{γ} and H^{γ}_{loc} are equivalent. In fact as indicated in [39], if $f(\mathbf{x}) \in H^{\gamma}_{loc}$, then $f(\mathbf{x})$ has the required smoothness for being in H^{γ} but imposes no global square integrability. Hence $f(\mathbf{x})$ belongs to $\mathcal{C}^{\gamma-\frac{d}{2}}$ provided that $\gamma - \frac{d}{2} > 0$. See [58,5,30] for further details.

Theorem 23 *Suppose that* $\dot{W}(\mathbf{x})$ *is Gaussian white noise on* $\mathbb{R}^d$. *Then with probability one,*

$$\dot{W}(\mathbf{x}) \in H^{-\frac{d}{2}-\epsilon}_{loc}(\mathbb{R}^d), \quad \epsilon > 0.$$

Proof: See [20].

Theorem 24 *Suppose that* L *is an isotropic strongly elliptic differential operator of order* $2m$ *and that* $\dot{W}(\mathbf{x})$ *is Gaussian white noise on* $\mathbb{R}^d$. *Then with probability one, the particular solution (3.11) of*

$$L\phi(\mathbf{x}) = \dot{W}(\mathbf{x}),$$

belongs to $H^{2m-\frac{d}{2}-\epsilon}_{loc}(\mathbb{R}^d)$, $\epsilon > 0$.

Proof: Since L is of order $2m$ and $\dot{W}(\mathbf{x}) \in H^{-\frac{d}{2}-\epsilon}_{loc}(\mathbb{R}^d)$, this theorem follows directly from the elliptic regularity theorem. See [39], Theorem 6.33 for further details.

Theorem 24 combined with the Sobolev embedding theorem provides a framework for exploring the regularity properties of $\phi(\mathbf{x})$ for any constant coefficient elliptic differential operator.

Chapter 4

Examples of Stationary Random Fields

In this chapter, we shall study two specific examples of (3.1), namely the stochastic modified Helmholtz equation and the stochastic biharmonic equation. In each example the covariance function and approximate realizations are computed and simulated. In addition, the regularity properties are investigated. To benefit from the power of the FFT algorithm, we shall use the Gaussian spectral representation to derive the approximate realizations.

4.1 Stochastic Helmholtz equation

Consider the stochastic modified Helmholtz equation (we will refer to this as Helmholtz equation for brevity)

$$-b\nabla^2\phi(\mathbf{x}) + c\phi(\mathbf{x}) = \dot{W}(\mathbf{x}), \quad \mathbf{x} \in \mathbb{R}^d, \tag{4.1}$$

where b and c are strictly positive constants. The symbol of the Helmholtz operator is given by

$$\lambda(k) = bk^2 + c, \tag{4.2}$$

and for any strictly positive b and c, $\lambda(k)$ is strongly elliptic. Hence by Theorem 15 there exists a unique Green's function. We shall only study a particular solution of (4.1),

$$\phi(\mathbf{x}) = \int_{\mathbb{R}^d} \Big(\frac{1}{(2\pi)^d} \int_{\mathbb{R}^d} \frac{e^{i\mathbf{k}\cdot(\mathbf{x}-\mathbf{x_0})}}{bk^2 + c} d\mathbf{k} \Big) W(d\mathbf{x_0}), \tag{4.3}$$

where the expression inside the brackets is the Green's function, which can be evaluated explicitly (see Appendix A). Continuity and differentiability properties of sample functions were discussed in Chapter 3. According to Theorem 24, (4.3) belongs to

$$\phi(\mathbf{x}) \in H_{loc}^{2-\frac{d}{2}-\epsilon}(\mathbb{R}^d), \quad \epsilon > 0.$$

Thus using the Sobolev embedding theorem,

$$\phi(\mathbf{x}) \in \mathcal{C}^{2-d-\epsilon}(\mathbb{R}^d), \tag{4.4}$$

provided that

$$2 - d - \epsilon > 0. \tag{4.5}$$

4.1.1 One Dimensional Solution

For the one-dimensional Helmholtz equation,

$$\phi(x) \in H_{loc}^{\frac{3}{2}-\epsilon}(\mathbb{R}),$$

and so $\phi(x)$ is Hölder continuous with exponent less than one. The Green's function is calculated in section A.1 and is given by

$$g(r) = \frac{e^{-\sqrt{\frac{c}{b}}r}}{2\sqrt{bc}}.$$

Using Theorem 16, the covariance function is given by

$$\begin{aligned} C(r) &= -\frac{\partial g}{\partial c} && (4.6) \\ &= \frac{(\sqrt{c}r + \sqrt{b})e^{-\sqrt{\frac{c}{b}}r}}{4bc\sqrt{c}}, && (4.7) \end{aligned}$$

and therefore the variance is

$$\sigma^2 = \frac{1}{4c\sqrt{bc}}.$$

Observe that since the variance is finite and positive, the particular solution of the one-dimensional stochastic Helmholtz equation is a real valued Gaussian random field. Moreover, the covariance function is positive which means that the correlation length is a valid measure of geological distance. The correlation length is given by

$$\rho = 2\sqrt{\frac{b}{c}}. \tag{4.8}$$

One can obtain additional insight into the physical significance of ρ by rewriting the correlation function as,

$$c(r) = \Big(\frac{2r}{\rho} + 1\Big)e^{-\frac{2r}{\rho}} \tag{4.9}$$

and considering the following cases:

- As $\rho \to \infty$, $c(r) \to 1$ for every r except $r = \infty$ when it equal zero. This situation represents a physical model where the random field is constant in space, but the value of this constant is random.

- As $\rho \to 0$, $c(r) \to 0$ except at $r = 0$ where $c(0) = 1$. This situation describes an uncorrelated random field.

There are many numerical schemes designed for approximating solutions of elliptic partial differential equations. For instance in the literature, the finite element method has been extensively used for such a purpose. However in order to use these numerical schemes, boundary conditions need to be specified before solving the problem. Now since (4.1) is defined on the entire Euclidean space, artificial boundary conditions need to be constructed. In this thesis we will not be studying ways of constructing artificial boundary conditions and instead use the Gaussian spectral representation to generate realizations of (4.1).

To obtain an approximate realization of (4.3) using the Gaussian spectral representation, we need to introduce a cutoff k_{max} such that

$$\int_0^{k_{max}} \frac{1}{\pi(bk^2 + c)^2} dk \approx \sigma^2. \tag{4.10}$$

The value of k_{max} will be chosen so that the relative error between the variance and the left hand side of (4.10) is less than 10^{-3}. Thus the approximate realizations can be generated by

$$\phi_N(x) = \sum_{n=0}^{N-1} \frac{\sqrt{-2\Delta k \ln(u_n)}\cos(k_n x + v_n)}{\sqrt{\pi}(bk_n^2 + c)}, \tag{4.11}$$

where

$$k_n = n\Delta k = n\Big(\frac{k_{max}}{N}\Big). \tag{4.12}$$

Figure 4.1 shows how the the correlation function and the approximate realization changes as the the correlation length is reduced. Based on the selected values of b and c, $\rho = 2, 2.828$ and 3.464. Notice that the larger the correlation length, the slower the decay of the correlation function.

4.1.2 Two Dimensional Solution

For the two dimensional Helmholtz equation,

$$\phi(\mathbf{x}) \in H^{1-\epsilon}_{loc}(\mathbb{R}^2).$$

Observe that in this case the condition specified in (4.5) is violated, and so the $\mathcal{L}^2$ definition of Sobolev spaces is no longer sufficient to establish the regularity properties of the sample function. One way to overcome this problem is by defining (3.9) on $\mathcal{L}^q$ for $q > 2$. However we shall not be pursuing this avenue in this thesis, and readers are referred to [13] for a detailed discussion on the regularity properties of SPDEs using the $\mathcal{L}^q$ definition of Sobolev spaces.

The Green's function is calculated in section A.2 and is given by

$$g(r) = \frac{K_0(r\sqrt{\frac{c}{b}})}{2\pi b}, \tag{4.13}$$

where K_0 denotes the zeroth order modified Bessel function of the second kind. The covariance function is

$$\begin{aligned} C(r) &= -\frac{\partial g}{\partial c} && (4.14)\\ &= \frac{rK_1(r\sqrt{\frac{c}{b}})}{4\pi b\sqrt{bc}}, && (4.15) \end{aligned}$$

where K_1 is the modified Bessel function of order one of the second kind. Hence the variance is

$$\begin{aligned} \sigma^2 &= \lim_{r\to 0} C(r) \\ &= \frac{1}{4\pi bc}. \end{aligned}$$

Thus the particular solution of the two dimensional Helmholtz equation is a real valued Gaussian random field and is continuous in the mean square sense. The

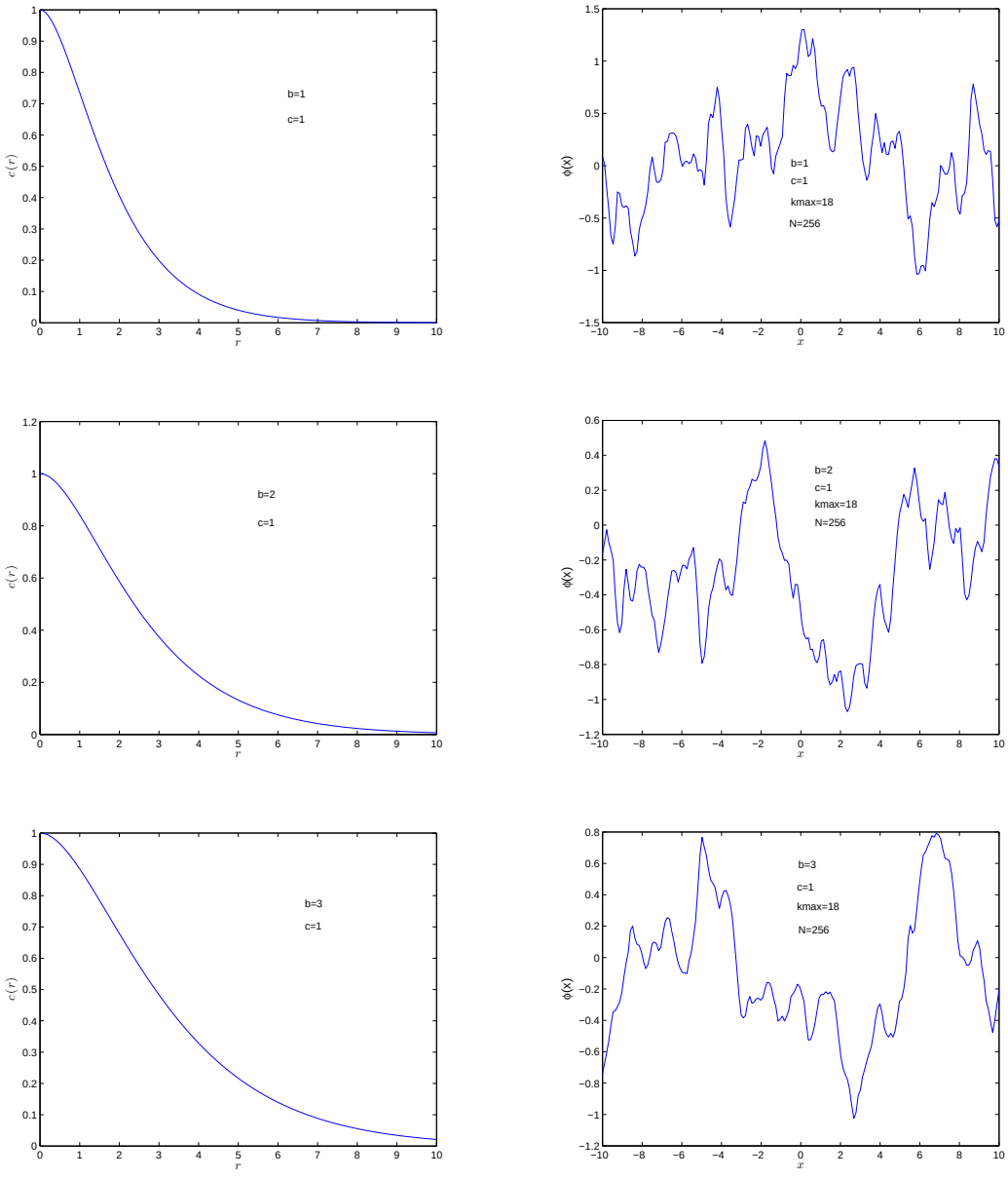

Figure 4.1: Correlation functions and realizations for the one dimensional Helmholtz equation.

correlation length is

$$\begin{aligned}\rho &= \int_0^\infty r\sqrt{\frac{c}{b}}K_1\Big(\sqrt{\frac{c}{b}}r\Big)dr \\ &= \frac{\pi}{2}\sqrt{\frac{b}{c}}.\end{aligned}$$

To obtain an approximate realization, we need to introduce a cutoff k_{max} such that

$$|\frac{1}{\sigma^2}\int_0^{k_{max}}\int_0^{k_{max}}\frac{1}{\pi^2(b(k_x^2+k_y^2)+c)^2}dk_xdk_y - 1| \leq 10^{-3}. \tag{4.16}$$

Hence approximate realizations are generated by,

$$\phi_N(x,y) = \sum_{m,n=-\frac{N}{2}}^{\frac{N}{2}-1}\frac{\sqrt{-\Delta k_n\Delta k_m\ln(u_{mn})}\cos(k_nx+k_my+v_{mn})}{\pi(b(k_n^2+k_m^2)+c)}. \tag{4.17}$$

Here k_n and k_m respectively denote the wave-numbers in direction x and y with the mesh size

$$\Delta k_n = \Delta k_m = \frac{k_{max}}{N}.$$

Figure 4.2 shows the correlation function and a 256×256 realization of (4.17) when $\rho = 1.571, 2.221$ and 2.721. Notice that larger correlation lengths produce bigger "blobs" in the realization than smaller correlation lengths.

4.1.3 Three Dimensional Solution

For the three dimensional Helmholtz equation,

$$\phi(\mathbf{x}) \in H_{loc}^{\frac{1}{2}-\epsilon}(\mathbb{R}^3).$$

The Green's function is calculated in section A.3 and is given by

$$g(r) = \frac{e^{-\sqrt{\frac{c}{b}}r}}{4\pi br},$$

and so the covariance function is

$$C(r) = \frac{e^{-\sqrt{\frac{c}{b}}r}}{8\pi b\sqrt{bc}}.$$

Therefore since the variance is finite, the particular solution is a real valued Gaussian random field and is continuous in the mean square sense.

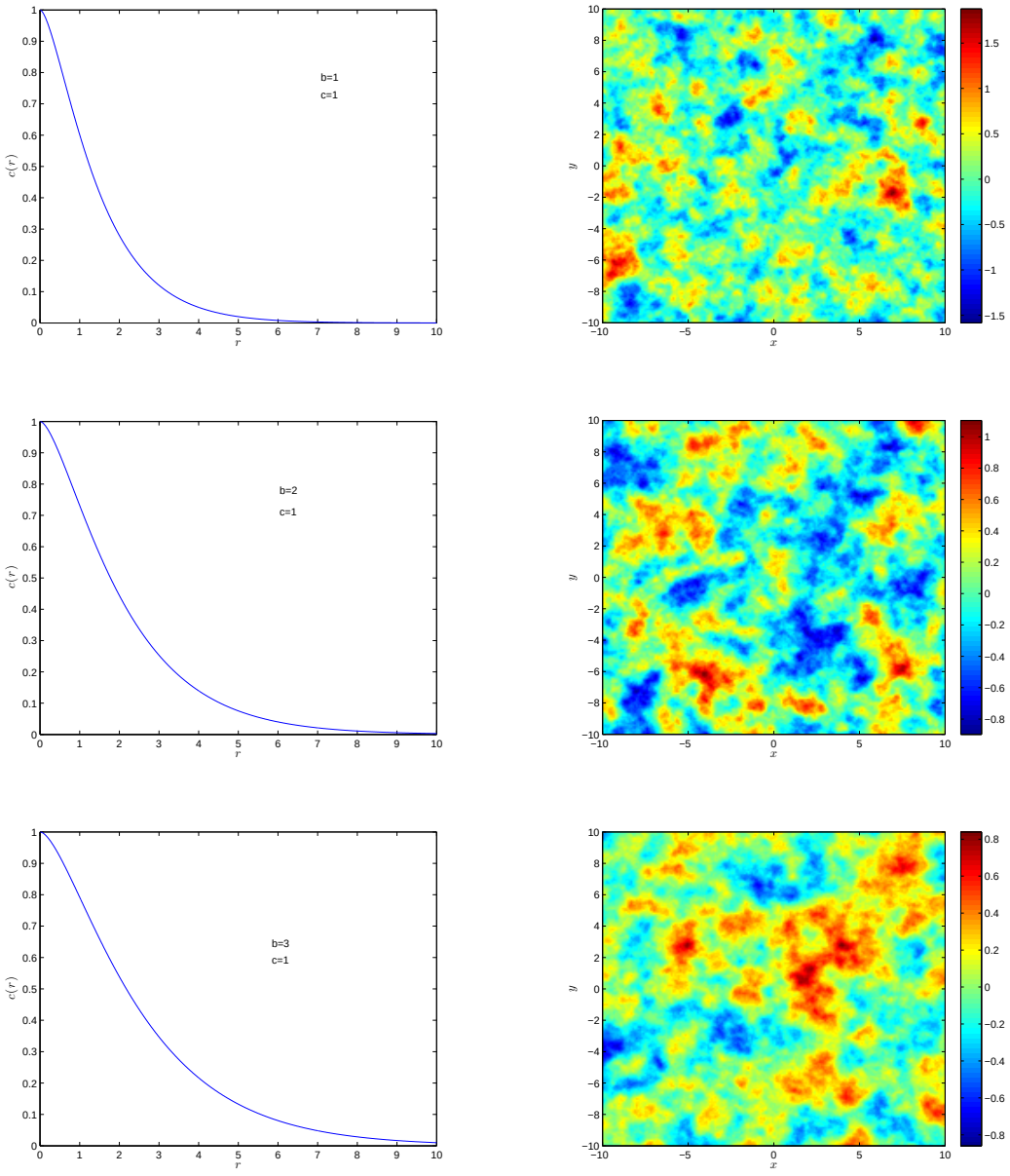

Figure 4.2: Correlation functions and 256×256 realizations for the two dimensional Helmholtz equation using $k_{max} = 30$.

4.2 Stochastic biharmonic equation

Consider the stochastic biharmonic-Helmholtz equation (we will refer to this as the biharmonic equation for brevity),

$$a\nabla^4\phi(\mathbf{x}) + b\nabla^2\phi(\mathbf{x}) + c\phi(\mathbf{x}) = \dot{W}(\mathbf{x}), \quad \mathbf{x} \in \mathbb{R}^d, \tag{4.18}$$

where a, c are strictly positive and $b \in \mathbb{R}$. The symbol of the biharmonic operator is given by

$$\lambda(k) = ak^4 - bk^2 + c. \tag{4.19}$$

Therefore for any b such that

$$b \leq 0, \tag{4.20}$$

(4.19) is strongly elliptic for all strictly positive a and c. Hence the Green's function of the biharmonic operator is unique in that case. If $b > 0$, then the Green's function is unique provided that

$$b < 2\sqrt{ac}. \tag{4.21}$$

A particular solution of (4.18) is given by

$$\phi(\mathbf{x}) = \int_{\mathbb{R}^d} \Big(\frac{1}{(2\pi)^d} \int_{\mathbb{R}^d} \frac{e^{i\mathbf{k}\cdot(\mathbf{x}-\mathbf{x_0})}}{ak^4 - bk^2 + c} d\mathbf{k} \Big) W(d\mathbf{x_0}). \tag{4.22}$$

Observe that according to Theorem 24,

$$\phi(\mathbf{x}) \in H_{loc}^{4-\frac{d}{2}-\epsilon}(\mathbb{R}^d),$$

and so by the Sobolev embedding theorem,

$$\phi(\mathbf{x}) \in \mathcal{C}^{4-d-\epsilon}(\mathbb{R}^d), \tag{4.23}$$

provided that

$$4 - d - \epsilon > 0. \tag{4.24}$$

4.2.1 One Dimensional Solution

In the case of the one dimensional stochastic biharmonic equation,

$$\phi(x) \in H^{\frac{7}{2}-\epsilon}_{loc}(\mathbb{R}),$$

and so $\phi(x)$ can be differentiated twice and the second derivative is Hölder continuous with exponent less than one. In order to compute the Green's function, there are various cases to consider depending on the value of the parameter b. For detailed computations see section A.4

Case1: $b < -2\sqrt{ac}$

Observe that for $b < -2\sqrt{ac}$, the Green's function is

$$g(r) = \frac{1}{2a(Q^2 - P^2)}\Big(\frac{e^{-Pr}}{P} - \frac{e^{-Qr}}{Q}\Big) \tag{4.25}$$

where

$$P = \sqrt{\frac{-b + \sqrt{b^2 - 4ac}}{2a}}, \tag{4.26}$$

$$Q = \sqrt{\frac{-b - \sqrt{b^2 - 4ac}}{2a}}. \tag{4.27}$$

Therefore using Theorem 16 the covariance function is given by

$$C(r) = \frac{Q^3((Q^2 - P^2)(Pr + 1) - 4P^2)e^{-Pr} + P^3((Q^2 - P^2)(Qr + 1) + 4Q^2)e^{-Qr}}{4a^2(Q^2 - P^2)^3P^3Q^3} \tag{4.28}$$

and so the variance is

$$\sigma^2 = \frac{(Q^2 + 3PQ + P^2)}{4a^2(Q + P)^3P^3Q^3}. \tag{4.29}$$

The correlation length is given by

$$\rho = \frac{2(Q + P)^3}{PQ(Q^2 + 3PQ + P^2)}. \tag{4.30}$$

Case2: $-2\sqrt{ac} < b < 2\sqrt{ac}$

For $-2\sqrt{ac} < b < 2\sqrt{ac}$, the Green's function

$$g(r) = \frac{(A\cos(Ar) + B\sin(Ar))e^{-Br}}{4aAB(A^2+B^2)}, \tag{4.31}$$

where

$$A = \sqrt{\frac{b}{4a} + \frac{1}{2}\sqrt{\frac{c}{a}}} \quad and \quad B = \sqrt{-\frac{b}{4a} + \frac{1}{2}\sqrt{\frac{c}{a}}}. \tag{4.32}$$

The covariance function is given by

$$C(r) = \frac{\Big(B^2(2rA^2 + B + 4\sqrt{\frac{a}{c}}A^2B)\sin(Ar) + A(A^2 + \frac{Brb}{2a} + 4A^2B^2\sqrt{\frac{a}{c}})\cos(Ar)\Big)e^{-Br}}{32acA^3B^3}.$$

The variance is

$$\sigma^2 = \frac{A^2 + 5B^2}{32B^3a^2(A^2+B^2)^3}.$$

Remark 8 *For $0 \leq b < 2\sqrt{ac}$, the covariance function has negative as well as positive values. In such a case the definition of the correlation length as defined in chapter 2 is not a useful measure of the lengthscale over which ϕ is correlated, and should instead be defined as*

$$\rho = \int_0^\infty \mid c(r) \mid dr, \tag{4.33}$$

which will be computed using numerical integration.

Notice that for negative values of b, the spectral density decays with frequency. On the other hand, for positive values of b, the spectral density peaks at some finite frequency and as demonstrated in Figure (4.3), lead to singular peak as $b \to 2\sqrt{ac}$. To derive an approximate realization of (4.22) using the Gaussian spectral representation, we need to introduce a cutoff k_{max} such that

$$\mid \frac{1}{\sigma^2}\int_0^{k_{max}} \frac{1}{\pi(ak^4 - bk^2 + c)^2}dk - 1\mid \ \leq 10^{-3}. \tag{4.34}$$

The approximate realizations are therefore generated by,

$$\phi_N(x) = \sum_{n=0}^{N-1} \frac{\sqrt{-2\Delta k\ln(u_n)}\cos(k_n x + v_n)}{\sqrt{\pi}(ak_n^4 - bk_n^2 + c)}, \tag{4.35}$$

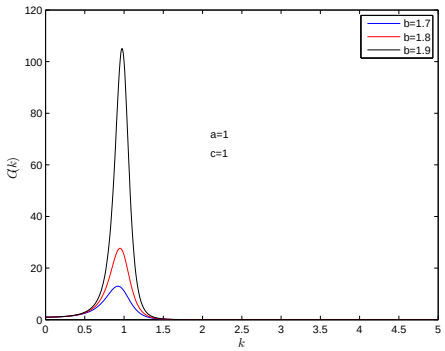

Figure 4.3: Spectral density of the covariance function for the one dimensional stochastic biharmonic equation.

where

$$k_n = n\Delta k = n\Big(\frac{k_{max}}{N}\Big). \tag{4.36}$$

Figures (4.4) and (4.5) show the correlation function and a realization of (4.35) for various choices of a, b and c. Notice that b determines the shape of the correlation function. For negative values of b, the correlation function is monotonically decreasing and for positive values of b, the structure of the spectral density produces a negative hole in the correlation function which results in oscillatory behaviour. In fact, the oscillation increases as

$$b \to 2\sqrt{ac}. \tag{4.37}$$

4.2.2 Two Dimensional Solution

For the two dimensional biharmonic equation,

$$\phi(\mathbf{x}) \in H^{3-\epsilon}_{loc}(\mathbb{R}^2), \tag{4.38}$$

and so $\phi(\mathbf{x})$ can be differentiated once and the derivative is Hölder continuous with exponent less than one. To compute the Green's function, there are various cases to consider depending on the value of the parameter b.

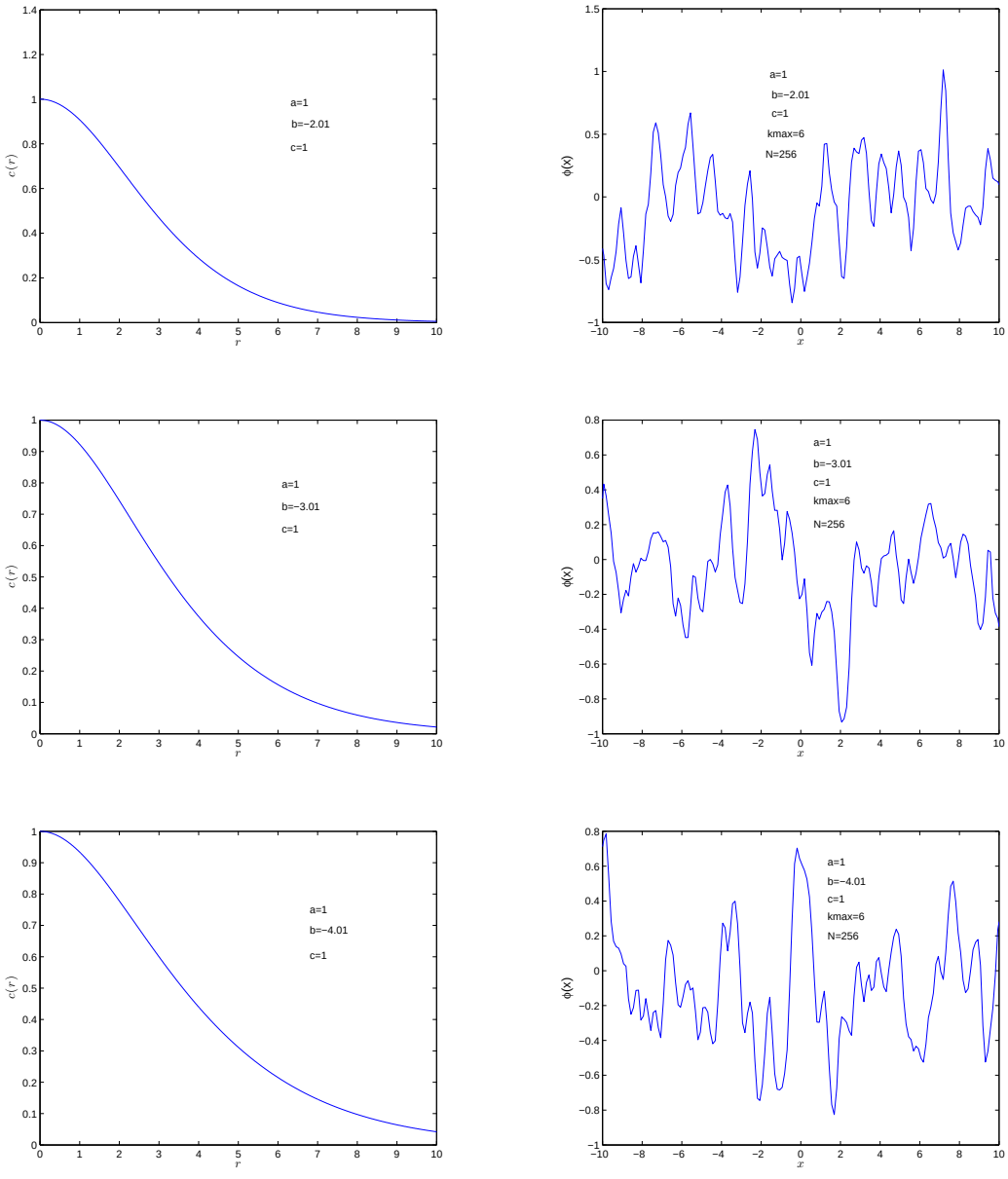

Figure 4.4: Correlation functions and realizations for the one dimensional biharmonic equation. Here $\rho = 3.206, 3.732$ and 4.204, and $b < -2ac$.

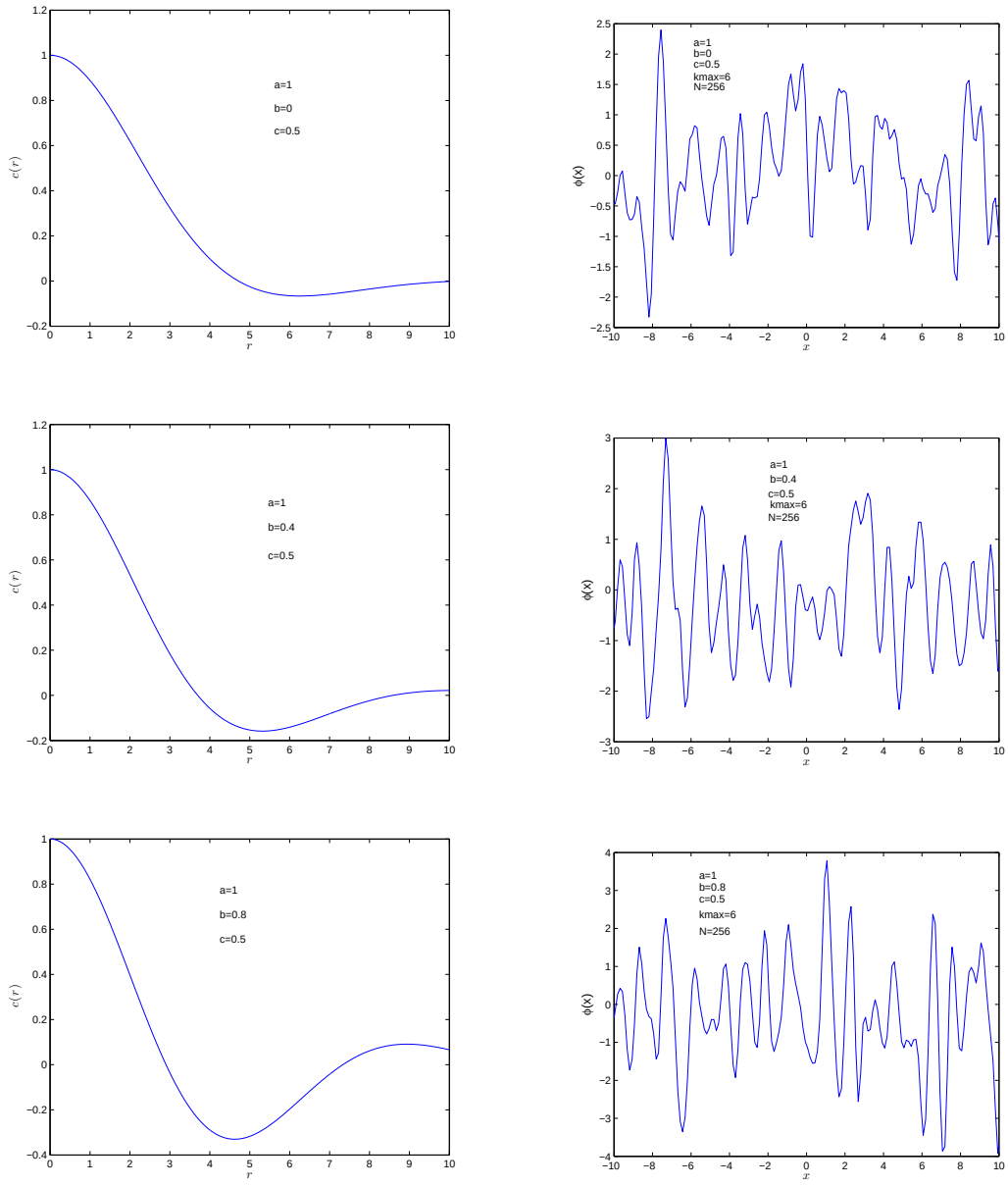

Figure 4.5: Correlation functions and realizations for the one dimensional biharmonic equation. Here $\rho = 3.776, 4.169$ and 5.748, and $0 \leq b < 2\sqrt{ac}$.

Case1: $b < -2\sqrt{ac}$

For $b < -2\sqrt{ac}$, the Green's function is given by

$$g(r) = \frac{K_0(Pr) - K_0(Qr)}{2\pi a(Q^2 - P^2)}. \tag{4.39}$$

The covariance function is

$$C(r) = \frac{r(Q^2 - P^2)(QK_1(Pr) + PK_1(Qr)) - 4PQ(K_0(Pr) - K_0(Qr))}{4\pi a^2 PQ(Q^2 - P^2)^3}. \tag{4.40}$$

Therefore the variance is

$$\begin{aligned} \sigma^2 &= \lim_{r\to 0} C(r) && (4.41)\\ &= \frac{Q^4 - 4P^2Q^2(\ln(Q) - \ln(P)) - P^4}{4\pi a^2 P^2 Q^2 (Q^2 - P^2)^3}. && (4.42) \end{aligned}$$

The correlation length is given by

$$\rho = \frac{(Q - P)^3 \pi (Q^2 + 3PQ + P^2)}{2PQ(Q^4 - 4P^2Q^2(\ln(Q) - \ln(P)) - P^4)}. \tag{4.43}$$

Case2: $-2\sqrt{ac} < b < 2\sqrt{ac}$

For $-2\sqrt{ac} < b < 2\sqrt{ac}$, the Green's function is

$$g(r) = \frac{-\Im K_0(r(B + iA))}{4\pi aAB}, \tag{4.44}$$

where $\Im$ denotes the imaginary part and A and B are defined as above. Subsequently the covariance function is

$$C(r) = \frac{-A^2B\sqrt{a}r\Im K_1(r(B + iA)) - AB^2\sqrt{a}r\Re K_1(r(B + iA)) - \sqrt{c}\Im K_0(r(B + iA))}{32a^2\pi A^3B^3\sqrt{c}} \tag{4.45}$$

where $\Re$ denotes the real part. Hence the variance is

$$\sigma^2 = \frac{A^2 - B^2}{32a^2A^2B^2\pi(A^2 + B^2)^2} + \frac{\tan^{-1}(\frac{A}{B})}{32\pi a^2A^3B^3}. \tag{4.46}$$

In order to obtain an approximate realization, we need to introduce a cutoff k_{max} such that

$$|\frac{1}{\sigma^2}\int_0^{k_{max}}\int_0^{k_{max}} \frac{1}{\pi^2(a(k_x^2 + k_y^2)^2 - b(k_x^2 + k_y^2) + c)^2} dk_x dk_y - 1|. \tag{4.47}$$

Now approximate realizations can be generated by

$$\phi_N(x,y) = \sum_{m,n=-\frac{N}{2}}^{\frac{N}{2}-1} \frac{\sqrt{-\Delta k_n \Delta k_m \ln(u_{mn})}\cos(k_n x + k_m y + v_{mn})}{\pi(a(k_n^2+k_m^2)^2 - b(k_n^2+k_m^2)+c)}, \tag{4.48}$$

where k_n and k_m respectively denote the wave-numbers in direction x and y with the mesh size

$$\Delta k_n = \Delta k_m = \frac{k_{max}}{N}.$$

Figures (4.6) and (4.7) show a variety of correlation function and realization of (4.48) for different choices of a, b and c. For positive value of b, the correlation function oscillates and the number of oscillations increase as b approaches $2\sqrt{ac}$. The oscillations disappear for negative value of b and replaced with monotonically decaying correlation function. Notice that the "hole effect" is less than those in figure (4.5).

4.2.3 Three Dimensional Solution

For the three dimensional biharmonic equation,

$$\phi(\mathbf{x}) \in H^{\frac{5}{2}-\epsilon}_{loc}(\mathbb{R}^3).$$

Hence $\phi(\mathbf{x})$ is Hölder continuous with exponent less than one.

Case1: $b < -2\sqrt{ac}$

For $b < -2\sqrt{ac}$, the Green's function is given by

$$g(r) = \frac{e^{-Pr} - e^{-Qr}}{4\pi a r(Q^2 - P^2)}. \tag{4.49}$$

The covariance function is given by

$$C(r) = \frac{(4PQ - rP^3 + rPQ^2)e^{-Qr} - (4PQ - rQ^3 + rP^2Q)e^{-Pr}}{8\pi a^2 r(Q^2-P^2)^3 PQ}. \tag{4.50}$$

Case2: $-2\sqrt{ac} < b < 2\sqrt{ac}$

For $-2\sqrt{ac} < b < 2\sqrt{ac}$, the Green's function is

$$g(r) = \frac{\sin(Ar)e^{-Br}}{8\pi a r AB}.$$

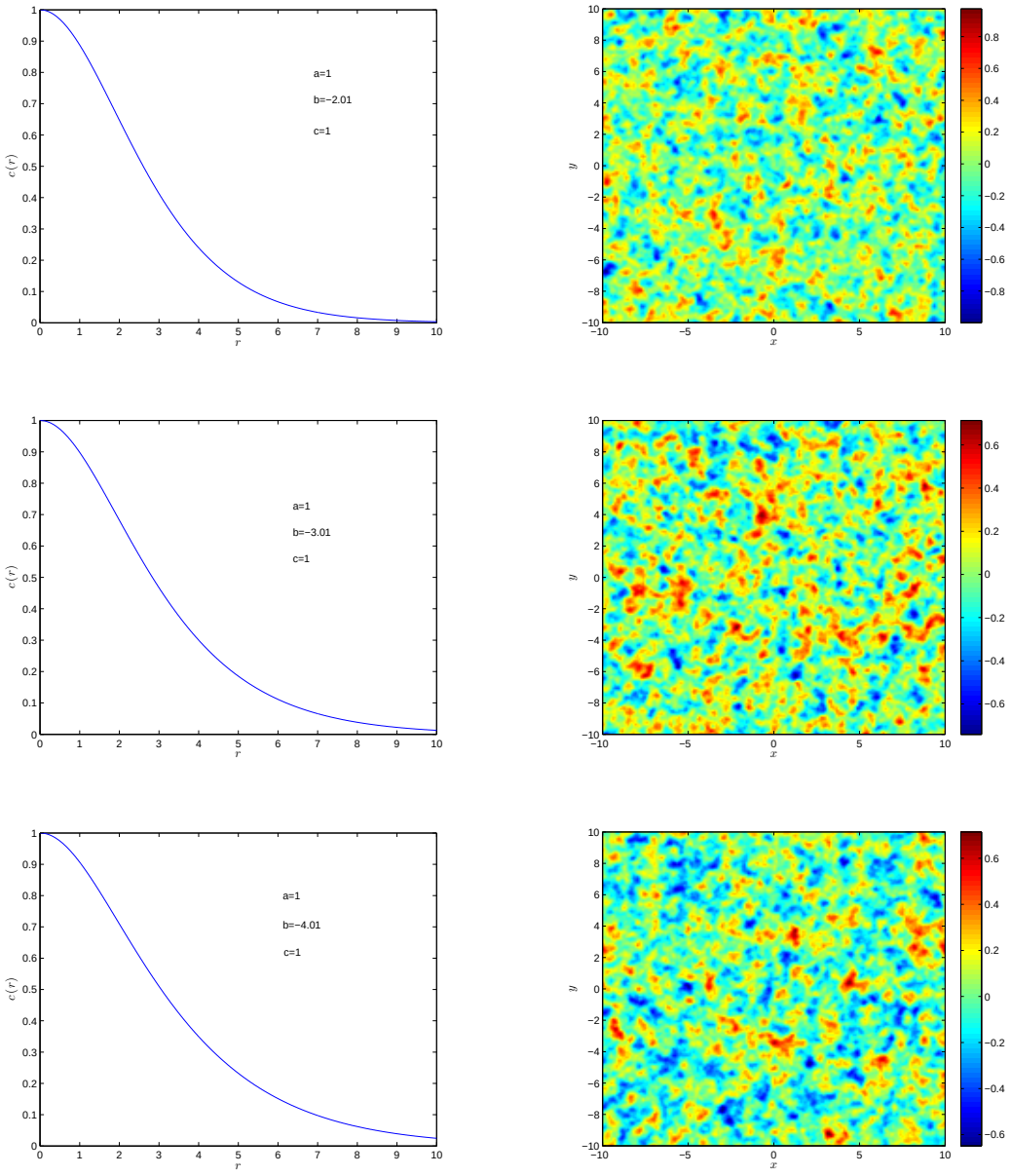

Figure 4.6: Correlation functions and 256×256 realizations for the two dimensional biharmonic equation using $k_{max} = 7$. Here $\rho = 2.949, 3.300$ and 3.624, and $b < -2ac$.

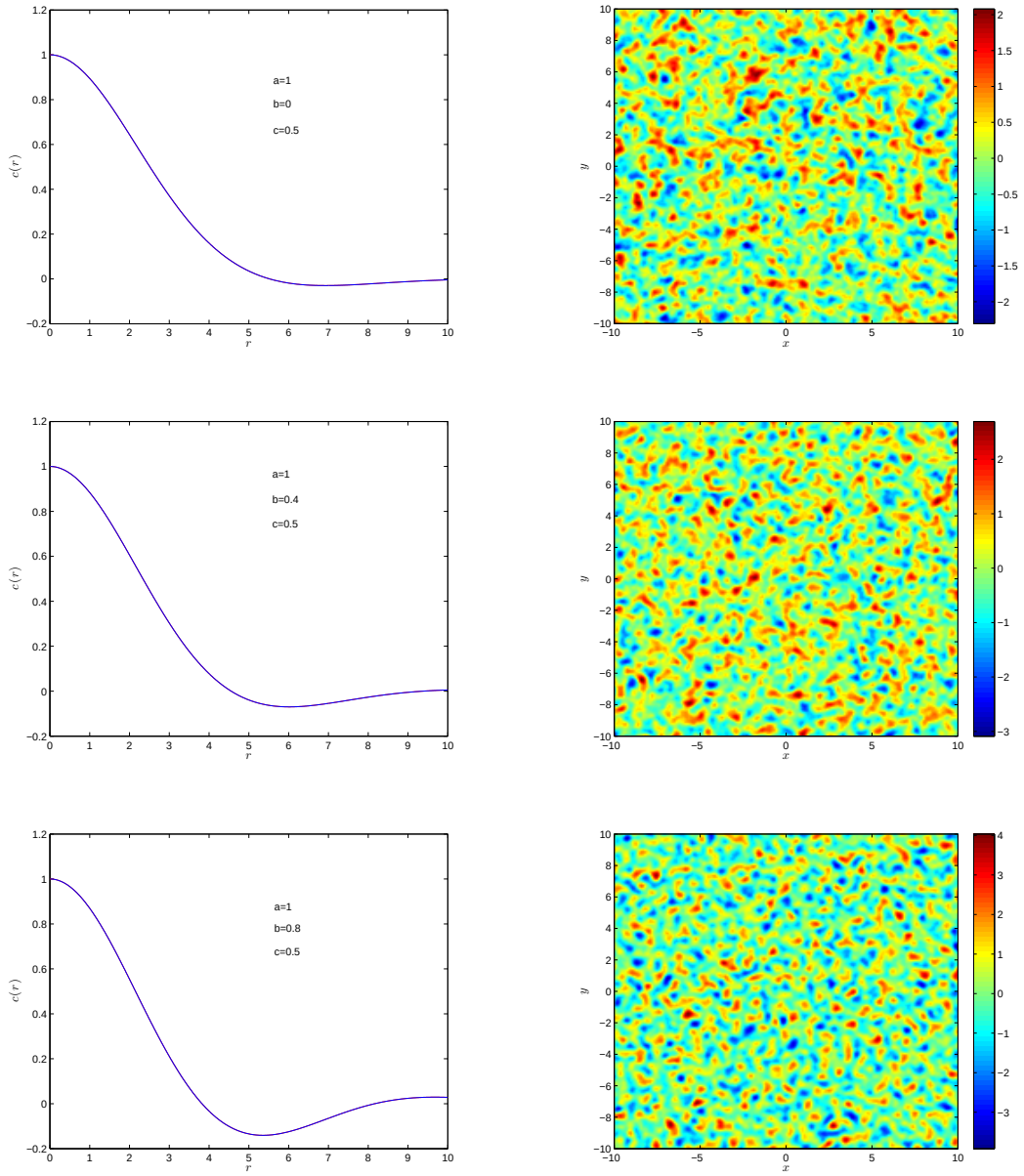

Figure 4.7: Correlation functions and 256×256 realizations for the two dimensional biharmonic equation using $k_{max} = 7$. Here $\rho = 2.685, 2.559$ and 2.541 and $0 \leq b < 2\sqrt{ac}$.

The covariance function is

$$C(r) = \frac{\Big((A^2Br\sqrt{a}+\sqrt{c})\sin(Ar)-\sqrt{a}AB^2r\cos(Ar)\Big)e^{-Br}}{64a^2A^3B^3r\sqrt{c}\pi}.$$

In conclusion, the stochastic biharmonic equation appears to have several desirable features in comparison with the stochastic Helmholtz equation. First of all, it has rich regularity properties making it a suitable model in two or three dimensions. In addition, for a different choice of parameters, the stochastic biharmonic equation can produce various correlation behaviors including damped oscillatory ones, whereas only monotonically decaying ones were observed for the stochastic Helmholtz equation. However geological formations in general display anisotropies such as stratification, and so it is useful to construct anisotropic random fields in order to more realistically describe the effects of field heterogeneity. In the next chapter, we shall study anisotropic random fields generated by solving an elliptic stochastic boundary value problem with tensor coefficients.

Chapter 5

Anisotropic Elliptic Stochastic PDEs

In this chapter, we will study the generation of anisotropic random fields using elliptic stochastic pde with tensor coefficients. The model considered is capable of producing non-stationary random fields on curved layers. Approximate realizations of this model will be drawn by using the finite element method, which is applied using the MATLAB PDE toolbox.

There is a growing need for greater realism in geological modelling, which is driven by the increasing quality and resolution of seismic data. The problem of prediction, as discussed in the introduction to this thesis, requires the solution of difficult inverse problems. In turn, the Bayesian approach to these problems requires good prior probability densities.

As indicated in [4,33], the presence of features such as faults in complicated 3-dimensional arrangements, and cross-bedding of sedimentary structures, makes it very difficult to build a geometric model in the first place. Moreover, in order to use traditional methods of texture interpolation, a global mapping is usually required from physical space into a rectangular system of coordinates. However, as the geological complexity increases, constructing such transformations becomes very difficult and tedious to achieve.

The problem of constructing a model of the geometry could be eased if it were possible to interpolate realistic sedimentary textures without having to build a full geometric model. In the following, we would like to investigate the possibility of using vector

fields to guide the random fields. The idea is to replace geometric models with vector fields defined on an arbitrary, Cartesian grid that are not aligned in anyway with the rock properties. The vector fields will be used to build tensor coefficients for an elliptic stochastic pde. We will think of the first vector field as a field of vectors normal to the bedding planes. Then the other vectors are in the tangent planes to the bedding surfaces. These vectors will be chosen to be unit vectors and to be mutually orthogonal. Given vectors $\mathbf{p}, \mathbf{q}, \mathbf{r}$ with

$$\mathbf{p} \cdot \mathbf{p} = \mathbf{q} \cdot \mathbf{q} = \mathbf{r} \cdot \mathbf{r} = 1, \tag{5.1}$$

and

$$\mathbf{p} \cdot \mathbf{q} = \mathbf{p} \cdot \mathbf{r} = \mathbf{q} \cdot \mathbf{r} = 0, \tag{5.2}$$

we set

$$\mathcal{D}_{i,j} = \alpha p_i p_j + \beta q_i q_j + \gamma r_i r_j, \qquad i, j, k \in \{1, 2, 3\}, \tag{5.3}$$

with, $\alpha, \beta, \gamma > 0$. This defines a general, symmetric positive definite tensor. In the following we will restrict our attention to the 2-dimensional case.

5.1 Anisotropic Stationary Random fields

In the last chapter we have investigated isotropic correlation functions for a particular class of second order random fields. However, spatial correlation does not only depend on the Euclidean distance between two locations. Very often the correlation in one direction does not equal to the correlation in another direction. Now given a stationary and isotropic random field, it is possible to simulate a stationary but anisotropic random field by performing coordinate transformations.

Definition 25 *A second order stationary random field is said to be geometrically anisotropic if it is characterized by the covariance function*

$$C(\mathbf{x} - \mathbf{y}) = C(\| \mathbf{r}^T \mathcal{D} \mathbf{r} \|), \tag{5.4}$$

where $\mathbf{r} = \mathbf{x} - \mathbf{y}$ *and* $\mathcal{D}$ *is a nonnegative matrix. If* $\mathcal{D}$ *is the identity matrix, then*

$$C(\mathbf{x} - \mathbf{y}) = C(r), \tag{5.5}$$

and the random field is isotropic.

Consider

$$L\phi(\mathbf{x}) \;=\; \dot{W}(\mathbf{x}), \quad \mathbf{x} \in \mathbb{R}^2, \tag{5.6}$$

where $\dot{W}(\mathbf{x})$ is Gaussian white noise and L is given by

$$L = a_m(\nabla \cdot (\mathcal{D}\nabla))^{2m} + a_{m-1}(\nabla \cdot (\mathcal{D}\nabla))^{2(m-1)} + ... + a_1(\nabla \cdot (\mathcal{D}\nabla)) + a_0. \tag{5.7}$$

Here the a_is are constants and the diffusivity matrix $\mathcal{D}$ is defined by

$$\mathcal{D}_{ij} = \alpha p_i p_j + \beta q_i q_j \qquad i, j \in \{1, 2\}, \tag{5.8}$$

α, $\beta > 0$. In the following we shall consider the example given by

$$\mathbf{p} \;=\; (\cos\theta, \sin\theta), \tag{5.9}$$

$$\mathbf{q} \;=\; (-\sin\theta, \cos\theta), \tag{5.10}$$

and so $\mathcal{D}$ reduces to

$$\begin{aligned} \mathcal{D} \;&=\; \begin{pmatrix} \alpha\cos^2\theta + \beta\sin^2\theta & (\alpha-\beta)\sin\theta\cos\theta \\ (\alpha-\beta)\sin\theta\cos\theta & \beta\cos^2\theta + \alpha\sin^2\theta \end{pmatrix} \\ &=\; \begin{pmatrix} \cos\theta & -\sin\theta \\ \sin\theta & \cos\theta \end{pmatrix} \begin{pmatrix} \alpha & 0 \\ 0 & \beta \end{pmatrix} \begin{pmatrix} \cos\theta & \sin\theta \\ -\sin\theta & \cos\theta \end{pmatrix} \end{aligned}$$

Notice that α and β are the eigenvalues corresponding to the eigenvectors $(\cos\theta, \sin\theta)$ and $(-\sin\theta, \cos\theta)$. Any realization of (5.6) would be controlled by the values of α, β and θ. If $\alpha > \beta$, then the direction of stronger correlation follows the vector $(\cos\theta, \sin\theta)$, whereas if $\alpha < \beta$, then the direction of correlation follows the vector $(-\sin\theta, \cos\theta)$.

We will study a particular solution of (5.6),

$$\phi(\mathbf{x}) = \int_{\mathbb{R}^2} \Big(\frac{1}{(2\pi)^2} \int_{\mathbb{R}^2} \frac{e^{i\mathbf{k}\cdot(\mathbf{x}-\mathbf{x}_0)}}{\lambda(\mathbf{k})} d\mathbf{k} \Big) W(d\mathbf{x}_0),$$

and this solution is an anisotropic stationary Gaussian random field. In fact by performing the following linear transformation,

$$k_1 \;=\; \frac{h_1}{\sqrt{\alpha}}\cos\theta - \frac{h_2}{\sqrt{\beta}}\sin\theta, \qquad h_1, h_2 \in \mathbb{R} \tag{5.11}$$

$$k_2 \;=\; \frac{h_1}{\sqrt{\alpha}}\sin\theta - \frac{h_2}{\sqrt{\beta}}\cos\theta, \tag{5.12}$$

the particular solution will reduce to the isotropic case and will have the same regularity properties. Notice that since the angle θ is constant, L is a constant coefficient differential operator and so the covariance function formally satisfies

$$L^2 C(r') = \delta(\mathbf{x} - \mathbf{y}), \tag{5.13}$$

where

$$\begin{aligned} r' &= \| \mathbf{r}^T \mathcal{D} \mathbf{r} \| \\ &= \sqrt{r_1^2 (\frac{\alpha \sin^2\theta + \beta \cos^2\theta}{\alpha\beta}) + 2 r_1 r_2 (\frac{\beta - \alpha}{\alpha\beta}) \sin\theta\cos\theta + r_2^2 (\frac{\beta \sin^2\theta + \alpha \cos^2\theta}{\alpha\beta})}. \end{aligned}$$

Here $r_1 = x_1 - y_1$, $r_2 = x_2 - y_2$. Hence using the same technique as in Theorem 16, the covariance function and the Green's function satisfy

$$C(r') = -\frac{\partial g(r')}{\partial a_0}. \tag{5.14}$$

For the rest of this section, we shall compute the anisotropic covariance function for the stochastic Helmholtz equation and the stochastic biharmonic equation. Moreover, approximate realizations of their solution will be simulated using the Gaussian spectral representation.

5.1.1 Anisotropic Stochastic Helmholtz equation

Consider

$$-\nabla \cdot (\mathcal{D} \nabla \phi(\mathbf{x})) + c\phi(\mathbf{x}) = \dot{W}(\mathbf{x}), \tag{5.15}$$

where $c > 0$. The covariance function is

$$\begin{aligned} C(r') &= \frac{1}{(2\pi)^2} \int_{\mathbb{R}^2} \frac{e^{i\mathbf{k}\cdot(\mathbf{x}-\mathbf{x}_0)}}{(\mathbf{k}^T \mathcal{D} \mathbf{k} + c)^2} d\mathbf{k} && (5.16) \\ &= \frac{r' K_1(r'\sqrt{c})}{4\pi\sqrt{\alpha\beta c}}, && (5.17) \end{aligned}$$

The variance is

$$\begin{aligned} \sigma^2 &= \lim_{r_1, r_2 \to 0} C(r') && (5.18) \\ &= \frac{1}{4\pi\sqrt{\alpha\beta c}}. && (5.19) \end{aligned}$$

Observe that when $\alpha = \beta$, (5.17) reduces to the two dimensional isotropic covariance function of the stochastic Helmholtz equation.

When dealing with anisotropic random fields, the correlation length needs to be computed for each of the two directions. The correlation length along the r_1 direction is computed by setting $r_2 = 0$ and integrating over r_1

$$\rho_1 = \frac{1}{\sigma^2}\int_0^\infty C(r')dr_1, \tag{5.20}$$

$$= \frac{\pi}{2}\sqrt{\frac{\alpha\beta}{c(\alpha\sin^2\theta + \beta\cos^2\theta)}}, \tag{5.21}$$

similarly, the correlation length along the r_1 direction is computed by setting $r_1 = 0$ and integrating over r_2

$$\rho_2 = \frac{1}{\sigma^2}\int_0^\infty C(r')dr_2, \tag{5.22}$$

$$= \frac{\pi}{2}\sqrt{\frac{\alpha\beta}{c(\beta\sin^2\theta + \alpha\cos^2\theta)}}. \tag{5.23}$$

Figure (5.1) illustrate the correlation function and approximate realizations of (5.15) generated using the Gaussian spectral representation. Notice that the orientation of the stripes is influenced by the value of θ, and the elliptically shaped correlation function has its semi-major axis in the θ direction. The correlation lengths are respectively given by $\rho_1 = 4.967$ and $\rho_2 = 1.571, 1.924$ and 2.221.

5.1.2 Anisotropic Stochastic biharmonic equation

Consider

$$a(\nabla\cdot(\mathcal{D}\nabla))^2\phi(\mathbf{x}) + b\nabla\cdot(\mathcal{D}\nabla)\phi(\mathbf{x}) + c\phi(\mathbf{x}) = \dot{W}(\mathbf{x}), \tag{5.24}$$

where $a, c > 0$, $b \in \mathbb{R}$ and $\mathcal{D}$ is as defined above. The symbol of the anisotropic biharmonic operator is given by

$$\lambda(\mathbf{k}) = a(\mathbf{k}^T\mathcal{D}\mathbf{k})^2 - b\mathbf{k}^T\mathcal{D}\mathbf{k} + c. \tag{5.25}$$

Thus for any $b \leq 0$, the symbol is strongly elliptic for all strictly positive a and c. Hence the Green's function of the biharmonic operator is unique in that case. If $b > 0$, then the Green's function is unique provided that

$$b < 2\sqrt{ac}. \tag{5.26}$$

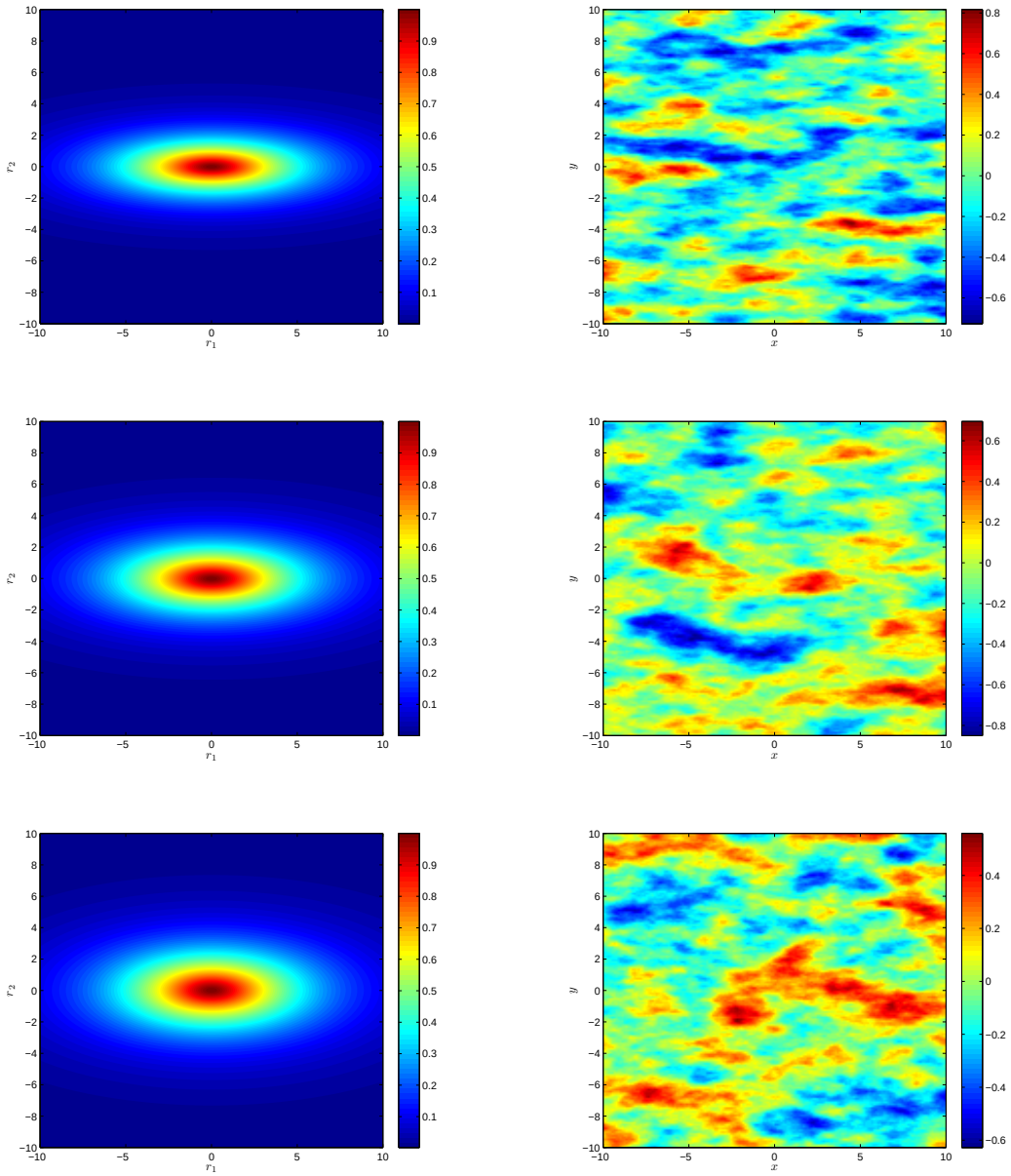

Figure 5.1: Correlation functions and 256×256 realizations for the anisotropic Helmholtz equation using $\alpha = 10$, $\theta = 0$, $c = 1$, $k_{max} = 26$ and $\beta = 1, 1.5$ and 2 respectively.

In order to compute the Green's function, there are various cases to consider depending on the value of the parameter b.

Case1: $b < -2\sqrt{ac}$

For $b < -2\sqrt{ac}$, the Green's function is

$$g(r') = \frac{K_0(Pr') - K_0(Qr')}{2\pi a\sqrt{\alpha\beta}(Q^2 - P^2)}, \tag{5.27}$$

where P and Q are respectively given by (4.26) and (4.27). The covariance function is

$$C(r') = \frac{r'(Q^2 - P^2)(QK_1(Pr') + PK_1(Qr')) - 4PQ(K_0(Pr') - K_0(Qr'))}{4\pi a^2\sqrt{\alpha\beta}PQ(Q^2 - P^2)^3}. \tag{5.28}$$

Therefore the variance is

$$\begin{aligned} \sigma^2 &= \lim_{r1,r2\to 0} C(r') && (5.29)\\ &= \frac{Q^4 - 4P^2Q^2(\ln(Q) - \ln(P)) - P^4}{4\pi a^2 P^2Q^2(Q^2 - P^2)^3\sqrt{\alpha\beta}}. && (5.30) \end{aligned}$$

The correlation length along the r_1 direction is,

$$\rho_1 = \frac{\sqrt{\alpha\beta}(Q - P)^3\pi(Q^2 + 3PQ + P^2)}{2\sqrt{\alpha\sin^2\theta + \beta\cos^2\theta}PQ(Q^4 - 4P^2Q^2(\ln(Q) - \ln(P)) - P^4)}, \tag{5.31}$$

and the correlation length along the r_2 direction is,

$$\rho_2 = \frac{\sqrt{\alpha\beta}(Q - P)^3\pi(Q^2 + 3PQ + P^2)}{2\sqrt{\beta\sin^2\theta + \alpha\cos^2\theta}PQ(Q^4 - 4P^2Q^2(\ln(Q) - \ln(P)) - P^4)}. \tag{5.32}$$

Case2: $-2\sqrt{ac} < b < 2\sqrt{ac}$

For $-2\sqrt{ac} < b < 2\sqrt{ac}$, the Green's function is

$$g(r') = \frac{-\Im K_0(r'(B + iA))}{4\pi aAB\sqrt{\alpha\beta}}, \tag{5.33}$$

where $\Im$ denotes the imaginary part and A and B defined as above. Subsequently the covariance function is

$$C(r') = \frac{-A^2B\sqrt{a}r'\Im K_1(r'(B + iA)) - AB^2\sqrt{a}r'\Re K_1(r'(B + iA)) - \sqrt{c}\Im K_0(r'(B + iA))}{32a^2\pi A^3B^3\sqrt{c\alpha\beta}} \tag{5.34}$$

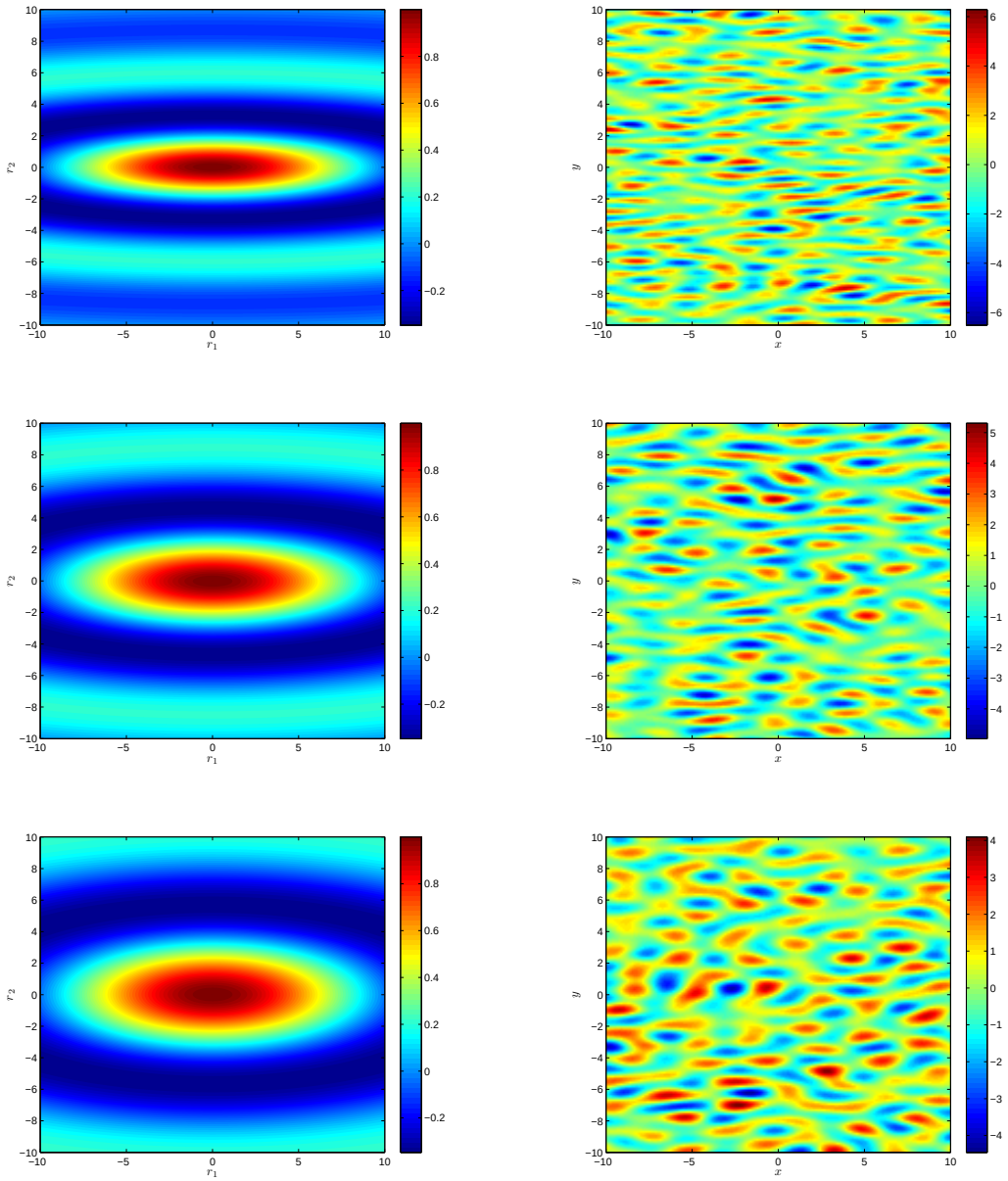

Figure 5.2: Correlation functions and 256×256 realizations for the anisotropic Helmholtz equation using $a = 1$, $b = 1.9$, $c = 1$, $\alpha = 15$, $\theta = 0$, $k_{max} = 7$ and $\beta = 0.7, 1.4$ and 2.1 respectively.

where $\Re$ denotes the real part. Hence the variance is

$$\sigma^2 = \frac{A^2 - B^2}{32a^2\sqrt{c\alpha\beta}A^2B^2\pi(A^2+B^2)^2} + \frac{\tan^{-1}(\frac{A}{B})}{32\pi a^2\sqrt{c\alpha\beta}A^3B^3}. \tag{5.35}$$

Notice that for $0 \leq b < 2\sqrt{ac}$, the covariance function has negative as well as positive values. In this case the correlation length will be computed numerically as explained in section (4.2.1).

Figure (5.2) shows the correlation function and approximate realizations of (5.24) generated using the Gaussian spectral representation. Notice the concentric ellipses of the correlation function repeat themselves and have their semi-major axis in the θ direction. The correlation lengths are respectively given by $\rho_1 = 5.876$ and $\rho_2 = 2.415, 3.096$ and 3.425.

5.2 Nonstationary Random fields

Modelling correlation functions can be a very complicated task to do. Usually the random field show different patterns over different parts of its domain which does not allow simple expressions to describe its dependency structure. For example, distinct geological layers and facies may cause the permeability field of a given geologic formation to be spatially nonstationary. Now a random field is said to be a nonstationary random field if either its mean varies spatially or its covariance depend on the actual locations.

In the following we shall study the construction of nonstationary random fields using elliptic boundary value problem driven by a piecewise constant approximation of Gaussian white noise. The generated realizations are locally stationary and the correlation function will not be computed as it is very difficult to do so. The approximate realizations of the model considered will be drawn by using the finite element method.

Modelling non-stationary random fields can be divided into global and local methods. Global methods take into account the whole domain, whereas local methods assume that a globally non-stationary random field can be approximated as a collection of locally stationary random fields. For detailed discussions on these methods see [60,35]. In this section however, we shall consider one way of generating locally stationary

random fields. Notice that a function $f(x)$ which varies in x is a constant in an interval $[\eta, \eta + \epsilon]$, provided that $\mid \epsilon \mid > 0$ is sufficiently small. A similar approach can be used when modelling nonstationary random fields. In other words, despite the fact that the mean and covariance functions are nonstationary throughout the domain, it is possible to assume that the random field is approximately stationary on smaller subsets of its domain.

Consider

$$-\nabla \cdot (\mathcal{D}(x,y)\nabla\phi_h(x,y)) + \lambda\phi_h(x,y) = \dot{W}_h(x,y), \quad x,y \in D, \tag{5.36}$$

$$\nabla\phi_h(x,y).n = 0, \quad on \quad \partial D, \tag{5.37}$$

where $\mathcal{D}$ is defined as before except that θ is spatially varying, and $\dot{W}_h(x,y)$ is a piecewise constant approximation of Gaussian white noise, which is motivated by the need to use the finite element method. Also the homogeneous boundary condition is chosen for simplicity. Notice that since the coefficients are spatially varying, the solution of (5.36) will be a nonstationary random field. Moreover, the field will also be locally stationary and the actual process of combining all the locally stationary fields into a global field is done by using the finite element method.

As indicated in [32], a piecewise constant approximation of Gaussian white noise is defined by

$$\dot{W}_h(x,y) = \sum_{T \in T_h} \frac{\xi_T}{\sqrt{\mid T \mid}} \chi_T(x,y), \tag{5.38}$$

where T_h denotes a triangulation of D, $\mid T \mid$ denotes the area of each triangle T, χ_T is the characteristic function of T,

$$\chi_T(x,y) = \begin{cases} 1 & (x,y) \in T, \\ 0 & \text{otherwise} \end{cases} \tag{5.39}$$

and $\{\xi_T\}_{T \in T_h}$ is a family of independent and identically distributed normal random variables with mean 0 and variance 1. Figure (5.3) displays a realization of $\dot{W}_h(x,y)$. The main obstacle to carrying out an error estimate of finite element method for a stochastic pde is the lack of regularity of its solution. In [32], Cao et al have demonstrated that for a particular class of semilinear elliptic stochastic pde driven by Gaussian white noise, which includes the stochastic Helmholtz equation, the solution

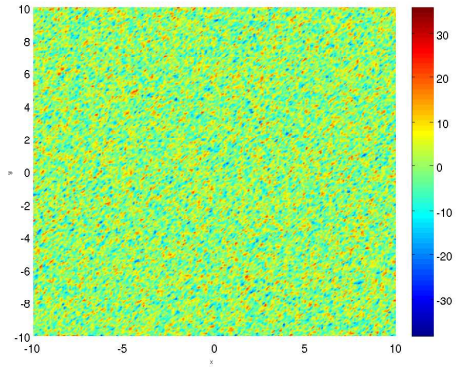

Figure 5.3: A realization of a piecewise constant approximation of Gaussian white noise with meshsize 0.078125.

can be sufficiently approximated by replacing white noise with (5.38). And consequently, because the resulting problem has the desired regularity for error analysis, it can be reasonably approximated by the finite element method.

Observe that for a particular realization of $\dot{W}_h(x, y)$, (5.36) is a deterministic elliptic boundary value problem of the type studied in Appendix B . Hence in the following, we will numerically solve (5.36) for various choices of θ using the MATLAB PDE toolbox. Ideally, one might expect θ to be interpolated from real measurements. However experimental data rarely would be enough to infer θ, and so θ itself can be treated as a correlated random field. In the following θ will be treated either as a deterministic function or as a realization of a stationary Gaussian random field.

5.2.1 Deterministic angle

Let the angle θ be a spatially varying deterministic function of (x, y). Then the solution of (5.36) will be a nonstationary Gaussian random field. In this section we shall illustrate one approach of using (5.36) to generate realizations on curved layers. The idea is to assume that the log permeability has longer correlation along the layer in comparison to the correlation across the layer. Then the shape of the layer will provide enough information to find the angle $\theta(x, y)$. Figure (5.4) is an example of such a scenario. Suppose that the top boundary of the layer in Figure (5.4) is given by the function $z(x)$, which can be interpolated given some information about the layer. Observe that the orientation of the shape varies according to the derivative of

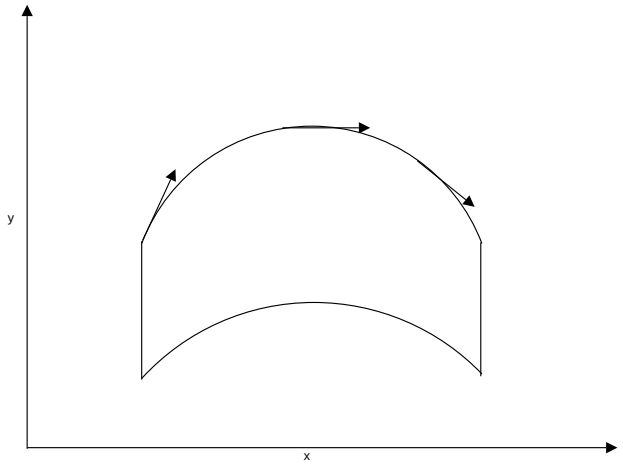

Figure 5.4: Schematic picture of a curved layer

$z(x)$. Hence θ can be represented by the variable angle of inclination of the tangent to the function $z(x)$,

$$\tan\theta(x,y) = z'(x). \tag{5.40}$$

In the case of figure (5.4), the angle can be approximated by

$$\theta(x,y) = \tan^{-1}(-0.72x - 0.072). \tag{5.41}$$

Figure (5.5) displays 4 independent realizations of (5.36) generated using (5.41). In each of the 4 plots, a different realization of $\dot{W}_h(x,y)$ is used and the middle right graph demonstrate how the vector flow $(\cos\theta(x,y), \sin\theta(x,y))$ conforms with the geometry of the layer.

5.2.2 Random angle

In the previous section we have assumed that the angle θ can be described by a deterministic function. However a deterministic angle is too limiting to capture curvilinear features such as channels and cross bedding. In this section we shall investigate how to use a realization from a stationary random field to construct a realization of a non-stationary random field.

Suppose that $\theta(x,y)$ is an approximate realization of the stochastic Helmholtz boundary value problem,

$$-b\nabla^2\theta_h(x,y) + c\theta_h(x,y) \;=\; \tilde{\dot{W}}_h(x,y), \quad x,y \in D, \tag{5.42}$$

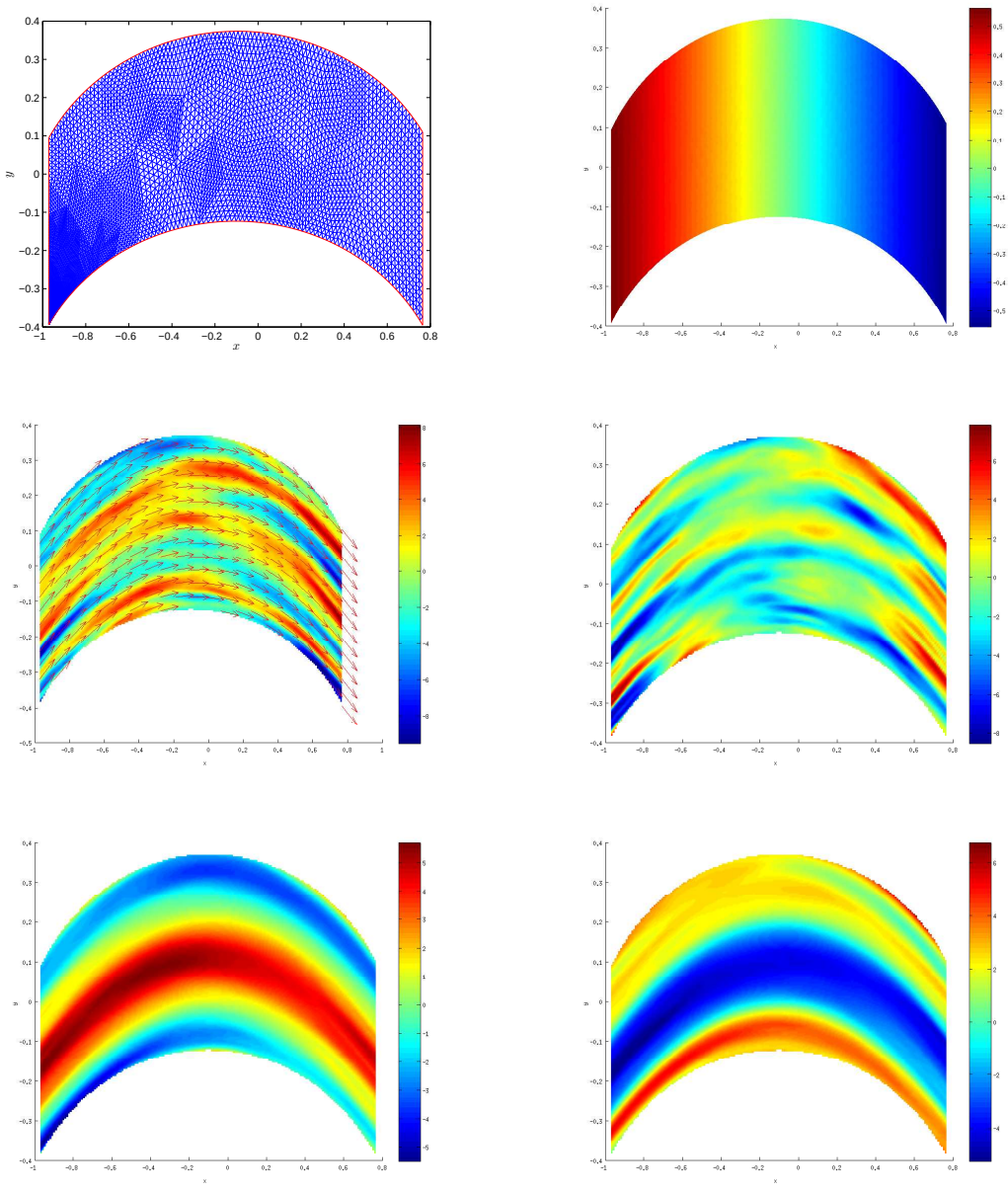

Figure 5.5: 4 approximate realizations of ϕ_h generated using the triangulation (top left) and $\theta(x, y) = \tan^{-1}(-0.72x - 0.072)$(top right). The 3rd and 4th graphs simulated using $\alpha = 0.1$, $\beta = 0.0001$, $\lambda = 1$, and the 5th and the 6th graph simulated using $\alpha = 1$, $\beta = 0.0001$, $\lambda = 1$.

$$\nabla\theta_h(x,y)\cdot n \;=\; 0, \qquad on \qquad \partial D \tag{5.43}$$

where b and c are strictly positive constants and, $\tilde{\dot{W}}_h(x,y)$ is a piecewise constant approximation of Gaussian white noise, such that $\tilde{\dot{W}}_h(x,y)$ is independent of $\dot{W}_h(x,y)$. The idea is to first simulate $\theta(x,y)$, defining the local orientations of the stripes at each location (x,y), and then generate approximate realizations of $\phi_h(x,y)$. Observe that in this example (5.36) will have spatially varying random coefficients, and so the solution will be a nonstationary non-Gaussian random field. Figure (5.6) shows the generated realization of (5.42) when $b = 0.8$ and $c = 1$, and 5 independent realizations of $\phi_h(x,y)$ using the same realization of $\theta_h(x,y)$. In other words the diffusivity matrix $\mathcal{D}$ is the same in all of the 5 independent realizations. Notice that curvilinear features are produced and that the local orientations of the stripes are controlled by the value of the angle $\theta_h(x,y)$ at each location (x,y). In fact, since $\alpha > \beta$, the local direction of the stripes depends on the vector $(\cos\theta_h(x,y), \sin\theta_h(x,y))$ at each location (x,y). Similarly, if $\alpha < \beta$, the location orientation of the stripes will depend on the vector $(-\sin\theta_h(x,y), \cos\theta_h(x,y))$ at each location (x,y).

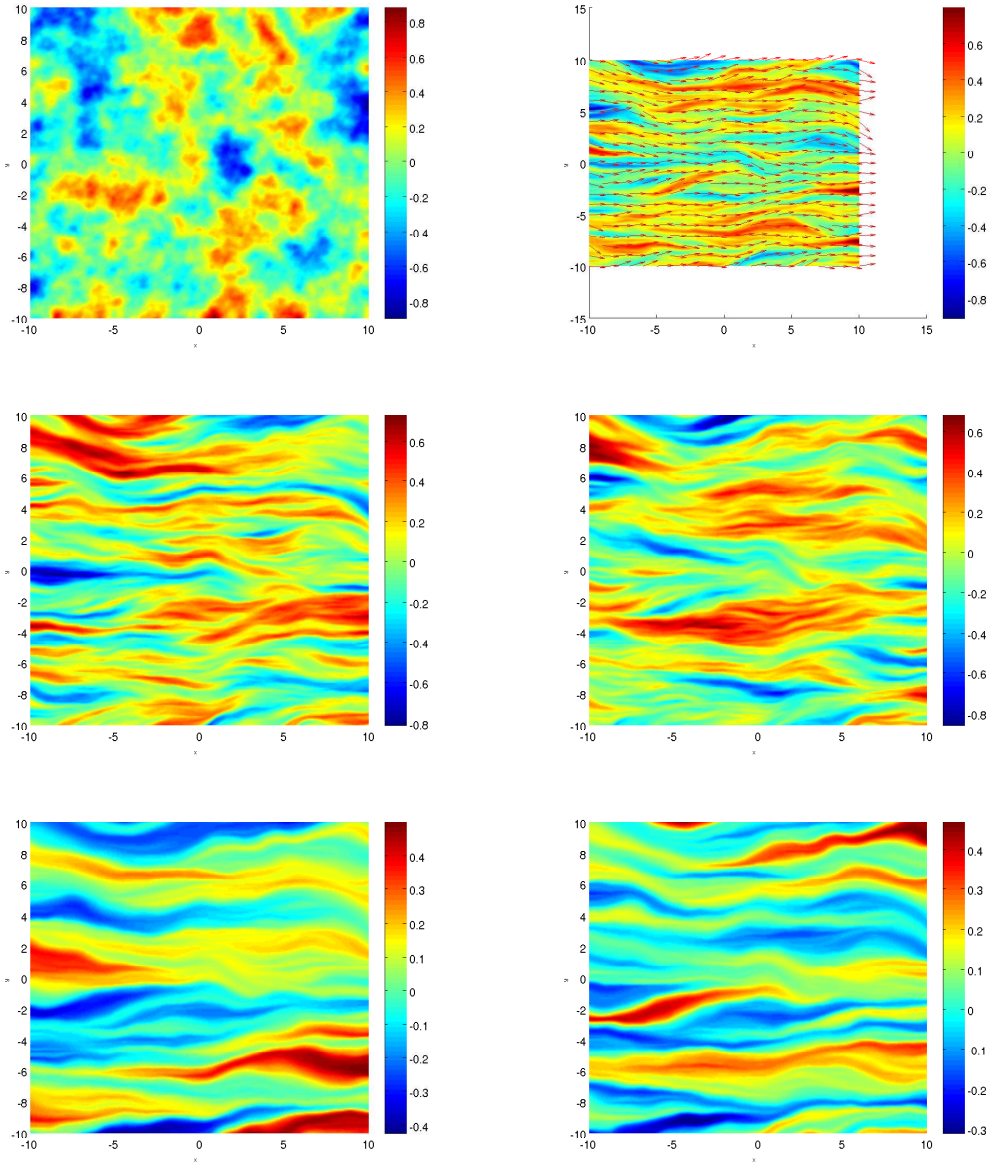

Figure 5.6: 5 approximate realizations of (5.36) generated using a realization of (5.42)(top left). The 2nd, 3 and 4th graph simulated using $\alpha = 10$, $\beta = 0.1$,$\lambda = 1$, and the 5th and the 6th graph simulated using $\alpha = 100$, $\beta = 0.1$, $\lambda = 1$. A triangulation with meshsize 0.078125 is used throughout.

Chapter 6

Conclusion

One of the critical tasks in reservoir modelling is the simulation of representative permeability fields. In general, reservoir formations usually show a significant level of heterogeneity and spatial variability in such a way that makes it very hard to describe the porous medium in any precise quantitative manner. This is due to the lack of data and the lack of knowledge of the characteristics at small scale. Therefore deterministic treatments of permeability are less useful since such a method does not provide any measure of uncertainty.

The aim of this thesis was to generate random fields to build suitable prior models for the logarithm of permeability fields. Inverse problems in geoscience are usually ill-posed, needing the specification of a prior model to constrain the nature of the inverse solutions. As indicated before, standard stochastic simulation techniques can only be applied when the principal directions of correlation align with Cartesian coordinate directions. However rock layers are not flat and most geological boundaries do not follow the coordinate lines of rectangular mesh systems. Therefore in order to use random field generators which rely on rectangular coordinates, a transformation to stratigraphic coordinates is usually required to map the actual geological layers into rectangular layers. However, because of the complexity of geological layers which might be twisted and faulted, the construction such transformation is very difficult to achieve. To address this problem, many authors have suggested using partial differential equations to generate random fields particularly, elliptic pdes driven by Gaussian white noise. One of the many attractive features of this method of simulation is that it does not require any particular assumption of a coordinate system until one has to actually perform a computation and then only locally for each cell of a grid. This

is similar to the fact that when fluid flow are modelled locally using a pde, a global coordinate system which follows the geometry is not needed, and only a local coordinate system is needed when doing calculations. Hence one can generate random fields directly on the physical domain without the need for a transformation to rectangular coordinates.

In chapter 3 of this thesis, we have studied isotropic elliptic stochastic pdes and the regularity properties of their solutions. The regularity properties were established using the Sobolev embedding theorem. Moreover, a useful formula linking the computation of the covariance function to that of the Green's function was derived.

In chapter 4, we considered two specific examples of isotropic stochastic pdes, namely the stochastic Helmholtz equation and the stochastic biharmonic equation. In each case the correlation function and approximate realizations were computed and simulated, and the regularity properties were investigated. To benefit from the power of the FFT algorithm, we used the Gaussian spectral representation to derive the approximate realizations. The stochastic biharmonic equation appears to have several desirable features in comparison with the stochastic Helmholtz equation. First of all, it has rich regularity properties making it a suitable model in two or three dimensions. In addition, for a different choice of parameters, the stochastic biharmonic equation can produce various correlation behaviors including damped oscillatory ones, whereas only monotonically decaying ones occur with the stochastic Helmholtz equation.

As geological features are generally not isotropically distributed, we have investigated in chapter 5 of this thesis the possibility of using vector fields to guide random fields. Directional influence appears when the correlation in one direction does not equal to the correlation in another direction. The vector fields were chosen to be orthonormal and were used to build tensor coefficients for an elliptic stochastic pde. For a particular choice of anisotropic constant coefficients, we have computed the correlation function and approximate realizations for both the stochastic Helmholtz equation and the stochastic biharmonic equation. On the other hand for spatially varying coefficients, the model considered was capable of producing non-stationary random fields with curvilinear features. Approximate realizations of this model were drawn by using the finite element method, which was applied by using the MATLAB PDE toolbox.

The promising results we have obtained so far, suggest that the next phase of this work should focus on further investigating the generation of non-stationary random fields using elliptic stochastic pdes. In particular, the following points need to be addressed in future work:

- Throughout this thesis we have concentrated on simulating unconditional realizations. However one needs to consider how to use the stochastic pde method to condition the realizations on observation data. Potsepaev et al [48] suggest generating conditional realizations by formulating a minimization problem and introducing Lagrange multipliers. Hence following the footstep of the work presented in [48] would be useful for future research. Ideally, it would be interesting to study the effects of local point conditioning on the angle $\theta(x, y)$ and, by considering spatially varying eigenvalues. That is, when the diffusivity matrix $\mathcal{D}$ defined by

  $$\mathcal{D}_{i,j} = \alpha(x, y)p_i p_j + \beta(x, y)q_i q_j \quad i, j \in \{1, 2\},$$

  where $\mathbf{p}$ and $\mathbf{q}$ are defined as in chapter 5. Notice that this require the eigenvalues and the eigenvectors to be known in every grid cell.

- In section 5.2.1 we have illustrated how to generate realizations from a nonstationary Gaussian random field on curved layers, based on the assumption that the top and bottom boundary of the given curved layer are parallel. Is it possible to extend the method to examples where the top and bottom boundaries are not parallel?

- Is the stochastic pde method as good as pixel based algorithms such as multipoint geostatistics? Multipoint geostatistics does not rely on covariance models and a key ingredient of this technique is training images, which enables us to impart geological features to realizations.

Appendix A

Green's function computations

Throughout this chapter we will be using integral tables from [3].

A.1 One dimensional Helmholtz equation

The Green's function is expressed as

$$\begin{aligned} g(r) &= \frac{1}{2\pi}\int_{-\infty}^{\infty}\frac{e^{ikr}}{bk^2+c}dk \\ &= \frac{1}{\pi b}\int_{0}^{\infty}\frac{\cos(kr)}{k^2+\frac{c}{b}}dk \\ &= \frac{e^{-r\sqrt{\frac{c}{b}}}}{2\sqrt{bc}}. \end{aligned}$$

A.2 Two dimensional Helmholtz equation

The two dimensional Green's function is given by

$$g(r) = \frac{1}{(2\pi)^2}\int_{-\infty}^{\infty}\int_{-\infty}^{\infty}\frac{e^{i\mathbf{k}\cdot\mathbf{r}}}{(bk^2+c)}dk_1dk_2.$$

Using polar coordinates this integral reduces to

$$g(r) = \frac{1}{(2\pi)^2}\int_{0}^{\infty}\int_{0}^{2\pi}\frac{\rho e^{i\rho r\cos(\theta)}}{(b\rho^2+b)}d\theta d\rho.$$

Notice that

$$\int_{0}^{2\pi} e^{i\rho r\cos(\theta)}d\theta = 2\pi J_0(\rho r).$$

Thus

$$\begin{aligned} g(r) &= \frac{1}{(2\pi)^2}\int_0^\infty \frac{2\pi\rho J_0(\rho r)}{(b\rho^2+c)}d\rho \\ &= \frac{1}{2\pi b}\int_0^\infty \frac{\rho J_0(\rho r)}{(\rho^2+\frac{c}{b})}d\rho \\ &= \frac{K_0(r\sqrt{\frac{c}{b}})}{2\pi b}. \end{aligned}$$

A.3 Three dimensional Helmholtz equation

Consider the three dimensional Green's function

$$g(r) = \frac{1}{(2\pi)^3}\int_{-\infty}^\infty\int_{-\infty}^\infty\int_{-\infty}^\infty \frac{e^{i\mathbf{k}\cdot\mathbf{r}}}{(bk^2+c)}dk_1dk_2dk_3.$$

Using spherical coordinates this integral reduces to

$$\begin{aligned} g(r) &= \frac{1}{(2\pi)^3}\int_0^{2\pi}\int_0^\pi\int_0^\infty \frac{\rho^2\sin(\theta)e^{i\rho r\cos(\theta)}}{(b\rho^2+c)}d\rho d\theta d\varpi \\ &= \frac{1}{(2\pi)^2}\int_0^\pi\int_0^\infty \frac{\rho^2\sin(\theta)e^{i\rho r\cos(\theta)}}{(b\rho^2+c)}d\rho d\theta. \end{aligned}$$

Now

$$\int_0^\pi \sin(\theta)e^{i\rho r\cos(\theta)}d\theta = \frac{2\sin(\rho r)}{\rho r}.$$

Thus

$$\begin{aligned} g(r) &= \frac{1}{(2\pi)^2}\int_0^\infty \frac{2\rho\sin(\rho r)}{r(b\rho^2+c)}d\rho \\ &= \frac{1}{2\pi^2 rb}\int_0^\infty \frac{\rho\sin(\rho r)}{(\rho^2+\frac{c}{b})}d\rho \\ &= \frac{e^{-\sqrt{\frac{c}{b}}r}}{4\pi rb}. \end{aligned}$$

A.4 One dimensional biharmonic equation

The one dimensional Green's function is expressed as

$$g(r) = \frac{1}{2\pi}\int_{-\infty}^\infty \frac{e^{ikr}}{(ak^4-bk^2+c)}dk,$$

where a and c are strictly positive constants and $b \in \mathbb{R}$. In order to preserve the existence of the Green's function, the symbol of the biharmonic operator

$$\lambda(k) = ak^4 - bk^2 + c, \tag{A.1}$$

must be positive for all k. As indicated before if $b \leq 0$, then $\lambda(k) > 0$ for all strictly positive a and c. On the other hand if $b > 0$, then $\lambda(k)$ is positive provided that

$$b < 2\sqrt{ac}. \tag{A.2}$$

Now the Green's function can be factorised to

$$g(r) = \frac{1}{2\pi a}\int_{-\infty}^{\infty} \frac{e^{ikr}}{(k^2+P^2)(k^2+Q^2)}dk \tag{A.3}$$

$$= \frac{1}{2\pi a(Q^2-P^2)}\left(\int_0^{\infty}\frac{\cos(kr)}{k^2+P^2}dk - \int_0^{\infty}\frac{\cos(kr)}{k^2+Q^2}dk\right). \tag{A.4}$$

Here

$$P = \sqrt{\frac{-b+\sqrt{b^2-4ac}}{2a}}, \tag{A.5}$$

$$Q = \sqrt{\frac{-b-\sqrt{b^2-4ac}}{2a}}. \tag{A.6}$$

To evaluate the above integrals using integral tables, we must choose P and Q so that their real parts are postive

$$\Re P \quad \text{and} \quad \Re Q > 0. \tag{A.7}$$

Then the Green's function reduces to

$$g(r) = \frac{1}{2a(Q^2-P^2)}\left(\frac{e^{-Pr}}{P} - \frac{e^{-Qr}}{Q}\right). \tag{A.8}$$

To retain $(A.7)$, we need to investigate the following cases:

- $b^2 - 4ac = 0$,
- $b^2 - 4ac > 0$,
- $b^2 - 4ac < 0$.

A.4.1 Case1

Consider the case when $b^2 - 4ac = 0$, which leads to

$$b = \pm 2\sqrt{ac}. \tag{A.9}$$

Notice that $b = 2\sqrt{ac}$ compromises the condition required for existence of the Green's function and, $b = -2\sqrt{ac}$ result in having zero in the denominator. Therefore Case1 will not considered.

A.4.2 Case2

Consider the example when $b^2 - 4ac > 0$, which implies that either $b > 2\sqrt{ac}$ or $b < -2\sqrt{ac}$. However to preserve existence of the Green's function, we shall only consider

$$b < -2\sqrt{ac}. \tag{A.10}$$

In this case P and Q will be positive real numbers and therefore $(A.7)$ is satisfied.

A.4.3 Case3

Consider the example when $b^2 - 4ac < 0$, which is true provided that

$$-2\sqrt{ac} < b < 2\sqrt{ac}. \tag{A.11}$$

Suppose that

$$\frac{b}{2a} = A^2 - B^2 \quad \text{and} \quad \frac{b^2 - 4ac}{4a^2} = -4A^2B^2, \tag{A.12}$$

where $A, B > 0$ such that

$$A = \sqrt{\frac{b}{4a} + \frac{1}{2}\sqrt{\frac{c}{a}}} \quad \text{and} \quad B = \sqrt{-\frac{b}{4a} + \frac{1}{2}\sqrt{\frac{c}{a}}}. \tag{A.13}$$

Hence P and Q are a complex conjugate pair given by

$$P = B + iA, \tag{A.14}$$

$$Q = B - iA. \tag{A.15}$$

In addition since $B > 0$, $(A.7)$ is satisfied. Now by substituting $(A.14)$ and $(A.15)$ into $(A.4)$ we obtain

$$g(r) = \frac{(A\cos(Ar) + B\sin(Ar))e^{-Br}}{4aAB(A^2 + B^2)}. \tag{A.16}$$

A.5 Two dimensional biharmonic Equation

The two dimensional Green's function is given by

$$g(r) = \frac{1}{(2\pi)^2}\int_{-\infty}^{\infty}\int_{-\infty}^{\infty}\frac{e^{i\mathbf{k}\cdot\mathbf{r}}}{(ak^4 - bk^2 + c)}dk_1 dk_2.$$

Using polar coordinates this integral reduces to

$$g(r) = \frac{1}{(2\pi)^2}\int_{0}^{\infty}\int_{0}^{2\pi}\frac{\rho e^{i\rho r\cos(\theta)}}{(a\rho^4 - b\rho^2 + b)}d\theta d\rho.$$

Notice that

$$\int_0^{2\pi} e^{i\rho r\cos(\theta)}d\theta = 2\pi J_0(\rho r).$$

Thus

$$g(r) \;=\; \frac{1}{(2\pi)}\int_0^{\infty}\frac{\rho J_0(\rho r)}{(a\rho^4 - b\rho^2 + c)}d\rho.$$

Now by using partial fraction the Green's function reduces to

$$g(r) \;=\; \frac{1}{2\pi}\int_0^{\infty}\frac{\rho J_0(\rho r)d\rho}{a(\rho^2 + P^2)(\rho^2 + Q^2)} \tag{A.17}$$

$$\;=\; \frac{1}{2\pi a(Q^2 - P^2)}\left(\int_0^{\infty}\frac{\rho J_0(\rho r)d\rho}{\rho^2 + P^2} - \int_0^{\infty}\frac{\rho J_0(\rho r)d\rho}{\rho^2 + P^2}\right), \tag{A.18}$$

where P and Q are defined as before. To evaluate the above integrals using integral tables, we must choose P and Q so that $(A.7)$ is satisfied. That is we must select a, b and c so that $(A.7)$ is obeyed. Then the Green's function reduces to

$$g(r) = \frac{K_0(Pr) - K_0(Qr)}{2\pi a(Q^2 - P^2)}. \tag{A.19}$$

As discussed above there are various cases to consider depending on how $b^2 - 4ac$ is treated. Notice that $b^2 - 4ac > 0$ holds provided that $b < -2\sqrt{ac}$. In this case P and Q are postive real numbers and therefore $(A.7)$ is satisfied. On the other hand, $b^2 - 4ac < 0$ provided that $-2\sqrt{ac} < b < 2\sqrt{ac}$. In that case P and Q are complex conjugate pair given by

$$P \;=\; B + iA, \tag{A.20}$$

$$Q \;=\; B - iA. \tag{A.21}$$

Hence

$$g(r) = \frac{K_0((B+iA)r) - K_0((B-iA)r)}{2\pi a(-4iAB)} \tag{A.22}$$

$$= \frac{-\Im K_0((B+iA)r)}{4\pi aAB}. \tag{A.23}$$

Here $\Im$ denote the imaginary part.

A.6 Three dimensional biharmonic Equation

The three dimensional Green's function is expressed as

$$g(r) = \frac{1}{(2\pi)^3}\int_{-\infty}^{\infty}\int_{-\infty}^{\infty}\int_{-\infty}^{\infty}\frac{e^{i\mathbf{k}\cdot\mathbf{r}}}{(ak^4 - bk^2 + c)}dk_1dk_2dk_3, \tag{A.24}$$

where a, b and c are as defined before. Using spherical coordinates

$$k_1 = \rho\sin(\varpi)\cos(\theta), k_2 = \rho\sin(\varpi)\sin(\theta), k_3 = \rho\cos(\varpi),$$

(A.24) is written as

$$g(r) = \frac{1}{(2\pi)^3}\int_0^{2\pi}\int_0^{\pi}\int_0^{\infty}\frac{\rho^2\sin(\theta)e^{i\rho r\cos(\theta)}}{(a\rho^4 - b\rho^2 + c)}d\rho d\theta d\varpi$$

$$= \frac{1}{(2\pi)^2}\int_0^{\pi}\int_0^{\infty}\frac{\rho^2\sin(\theta)e^{i\rho r\cos(\theta)}}{(a\rho^4 - b\rho^2 + c)}d\rho d\theta.$$

Using the identity

$$\int_0^{\pi}\sin(\theta)e^{-\rho r\cos(\theta)}d\theta = \frac{2\sin(\rho r)}{\rho r},$$

the Green's function reduces to

$$g(r) = \frac{1}{2\pi^2 r}\int_0^{\infty}\frac{\rho\sin(\rho r)}{(a\rho^4 - b\rho^2 + c)}d\rho. \tag{A.25}$$

Now by using partial fractions the above integral simplifies to

$$g(r) = \frac{1}{2\pi^2 ar(Q^2 - P^2)}\left(\int_0^{\infty}\frac{\rho\sin(\rho r)d\rho}{(\rho^2 + P^2)} - \int_0^{\infty}\frac{\rho\sin(\rho r)d\rho}{(\rho^2 + Q^2)}\right). \tag{A.26}$$

Here P and Q are defined as before. To evaluate the above integrals using integral tables, we must choose P and Q so that $(A.7)$. Then the Green's function reduces to

$$g(r) = \frac{e^{-Pr} - e^{-Qr}}{4\pi ar(Q^2 - P^2)}. \tag{A.27}$$

As indicated before there are various cases to consider depending on how $b^2 - 4ac$ is treated. $b^2 - 4ac > 0$ holds provided that $b < -2\sqrt{ac}$. In this case P and Q are positive real numbers and therefore $(A.7)$ is satisfied. On the other hand, $b^2 - 4ac < 0$ provided that $-2\sqrt{ac} < b < 2\sqrt{ac}$. In that case P and Q are a complex conjugate pair given by

$$P = B + iA, \tag{A.28}$$

$$Q = B - iA. \tag{A.29}$$

Hence

$$g(r) = \frac{e^{-(B+iA)r} - e^{-(B-iA)r}}{-16ari\pi AB} \tag{A.30}$$

$$= \frac{\sin(Ar)e^{-rB}}{8arAB\pi}. \tag{A.31}$$

A.7 Radius and Angle of Independent Gaussian random variables

Assume that ξ and η are zero mean unit variance independent Gaussian random variables. Consider

$$\mu = \sqrt{\eta^2 + \xi^2}, \qquad v = \tan^{-1}(\frac{-\eta}{\xi}). \tag{A.32}$$

The joint cumulative distribution function of μ and v is

$$F_{\mu,v}(\mu_0, v_0) = P(\mu \leq \mu_0, v \leq v_0) \tag{A.33}$$

$$= \int\int_{(x,y)\in D} \frac{e^{-\frac{(x^2+y^2)}{2}}}{2\pi} dxdy \tag{A.34}$$

where

$$D = \{(x, y) : \sqrt{x^2 + y^2} \leq \mu_0, 0 < \tan^{-1}(\frac{-y}{x}) < v_0\}. \tag{A.35}$$

Using polar coordinates the above integral reduces to

$$F(\mu_0, v_0) = \int_0^{\mu_0}\int_0^{v_0} \frac{re^{-\frac{r^2}{2}}}{2\pi} drd\theta \tag{A.36}$$

$$= \frac{v_0}{2\pi}(1 - e^{-\frac{\mu_0^2}{2}}), \quad 0 < v < 2\pi, \quad 0 < \mu_0 < \infty. \tag{A.37}$$

The joint pdf is obtained by taking partial derivatives with respect to μ_0 and v_0

$$f(\mu_0, v_0) = \frac{1}{2\pi}(\mu_0 e^{-\frac{\mu_0^2}{2}}) \quad 0 < v_0 < 2\pi, \quad 0 < \mu_0 < \infty. \tag{A.38}$$

Thus μ has a Rayleigh distribution and v is uniformly distributed in $(0, 2\pi)$.

A.8 Gaussian Markov Random Fields

The Markov property of a random field indexed by time describes the independence of the process in the past from its behaviour in the future, given information on its current state. However the concepts of "past" and "future" in a multidimensional space setting are not easy to understand. For detailed discussions on how the Markov property is defined in a multidimensional setting see [50]. In [50], the author obtained an interesting result which states the Markov property for stationary Gaussian random fields in terms of the spectral density.

Theorem 26 *Let $G(\mathbf{k})$ be the spectral density of a stationary Gaussian random field $\phi(\mathbf{x})$ and suppose that $\frac{1}{G(\mathbf{k})}$ is an elliptic polynomial of degree $2m$. If $\frac{1}{G(\mathbf{k})}$ has no zeros then $\phi(\mathbf{x})$ is Markovian of order m.*

This theorem indicates that if the reciprocal of the spectral density can expressed as a polynomial in $\mathbf{k}$

$$\frac{1}{G(\mathbf{k})} = G(k_1, k_2, ..., k_d) = \sum_{|\alpha|} a_{\alpha_1 ... \alpha_d} k_1^{\alpha_1} ... k_d^{\alpha_d}, \tag{A.39}$$

where $\mid \alpha \mid = \alpha_1 + \alpha_2 + ... + \alpha_d \leq 2m$, such that (A.39) is strongly elliptic, then $\phi(\mathbf{x})$ is Markovian of order m.

Remark 9 *As indicated in [50], a Gaussian random field $\phi(\mathbf{x})$ is Markovian of order m if $\phi(\mathbf{x})$ has $m-1$ continuous sample derivatives.*

As a consequence of this theorem, we can deduce the following result

Lemma 27 *The solution of* (3.9) *is Markovian.*

Proof: By Theorem 16, the covariance function of the solution of (3.9) is given by

$$C(r) = -\frac{\partial g(r)}{\partial a_0}. \tag{A.40}$$

Hence the spectral density of $C(r)$ is given by

$$G(\mathbf{k}) = \int_{\mathbb{R}^d} C(r)e^{-\mathbf{k}\cdot\mathbf{r}}d\mathbf{r} = \int_{\mathbb{R}^d} -\frac{\partial g(r)}{\partial a_0}e^{-\mathbf{k}\cdot\mathbf{r}}d\mathbf{r} \tag{A.41}$$

$$= -\frac{\partial}{\partial a_0}\left(\int_{\mathbb{R}^d} g(r)e^{-\mathbf{k}\cdot\mathbf{r}}d\mathbf{r}\right) \tag{A.42}$$

$$= -\frac{\partial \mathcal{F}(g)(k)}{\partial a_0} \tag{A.43}$$

Now since

$$\mathcal{F}(g)(k) = \frac{1}{\lambda(k)} \tag{A.44}$$

$$= \frac{1}{\sum_{p=0}^{m} a_p(-ik)^{2p}}, \tag{A.45}$$

$$-\frac{\partial \mathcal{F}(g)(k)}{\partial a_0} = \frac{1}{\mid \lambda(k) \mid^2}. \tag{A.46}$$

Thus

$$\frac{1}{G(\mathbf{k})} = \mid \lambda(k) \mid^2 \tag{A.47}$$

and since $\lambda(k)$ is strongly elliptic by definition, the result follows.

Remark 10 *Gaussian Markov random fields have many advantages. They are jointly Gaussian and have the Markov property which allows fast computation of the conditional densities. These properties are particularly useful for models which depend on inference using Markov chain Monte Carlo sampling. See [24] for further details.*

Appendix B

The Finite Element Method

The finite element method is one of the most powerful techniques for numerically solving partial differential equations. Formally, the method consists of the following five steps:

- Converting the given boundary value problem into a weak form. In order to do so, we need to decide on the function spaces in which the weak form is viewed.
- The weak formulation is approximated in the chosen finite dimensional space.
- Approximating the infinite dimensional function spaces by finite dimensional subspaces, for example by using piecewise linear polynomials with respect to the chosen triangulation.
- Discretising the computational domain using a triangulation.
- As a result of the previous steps, we ultimately obtain a system of equations whose solution will approximately solve the given boundary value problem.

Consider

$$-\nabla \cdot (\mathcal{D}(x,y)\nabla u(x,y)) + \lambda u(x,y) = f(x,y), \quad x,y \in D \tag{B.1}$$

$$\mathcal{D}(x,y)\nabla u(x,y).n = 0, \quad on \quad \partial D, \tag{B.2}$$

where n is the outward-pointing unit normal vector, $\lambda > 0$, $f(x,y) \in \mathcal{L}^2(D)$ and $\mathcal{D}(x,y)$ is a symmetric positive definite matrix.

Assume that $v(x,y)$ is a test function defined on D. Then by multiplying both sides of (B.1) by $v(x,y)$ and integrating over D we obtain

$$\int_D -\nabla \cdot (\mathcal{D}(x,y)\nabla u(x,y))v(x,y) \quad + \quad \lambda u(x,y)v(x,y)dxdy \tag{B.3}$$

$$= \int_D f(x,y)v(x,y)dxdy. \tag{B.4}$$

Using the Divergence theorem, the left hand side of (B.4) reduces to,

$$\int_D \nabla v(x,y) \cdot (\mathcal{D}(x,y)\nabla u(x,y)) \quad + \quad \lambda u(x,y)v(x,y)dxdy \tag{B.5}$$

$$- \int_{\partial D} v(x,y)\mathcal{D}(x,y)\nabla u(x,y).n \tag{B.6}$$

Observe that since $\mathcal{D}(x,y)\nabla u(x,y).n$ is zero on ∂D, the second integral vanishes. Hence (B.4) reduces to

$$\int_D \nabla v(x,y) \cdot (\mathcal{D}(x,y)\nabla u(x,y))dxdy \quad + \quad \int_D \lambda u(x,y)v(x,y)dxdy \tag{B.7}$$

$$= \int_D f(x,y)v(x,y)dxdy \tag{B.8}$$

Notice that (B.8) only need to have weak derivatives of order one, which is indeed a significant reduction of the requirement of u. Weak derivatives only need $\frac{\partial u}{\partial x}$ and $\frac{\partial u}{\partial y}$ be locally integrable. In (B.8), it must be possible to integrate the products

$$\frac{\partial u}{\partial x}\frac{\partial v}{\partial x} \quad \textit{and} \quad \frac{\partial u}{\partial y}\frac{\partial v}{\partial y}. \tag{B.9}$$

In other words, $u(x,y) = v(x,y)$ must be allowed. Moreover,

$$\int_D f(x,y)v(x,y)dxdy, \tag{B.10}$$

must be finite. Therefore the solution u of (B.8) need to satisfy

$$u(x,y), \frac{\partial u}{\partial x}, \frac{\partial u}{\partial y} \in \mathcal{L}^2(D), \tag{B.11}$$

and $v(x,y)$ need to satisfy the same conditions. These conditions define the Sobolev space $H^1(D)$,

$$H^1(D) = \{v \in \mathcal{L}^2(D) : \frac{\partial v}{\partial x}, \frac{\partial v}{\partial y} \in \mathcal{L}^2(D)\}. \tag{B.12}$$

So overall the weak formulation of (B.1) is defined in terms of the Sobolev space $H^1(D)$, find $u \in H^1(D)$ such that

$$\int_D \nabla v(x,y) \cdot (\mathcal{D}(x,y)\nabla u(x,y))dxdy + \int_D \lambda u(x,y)v(x,y)dxdy \quad (B.13)$$

$$= \int_D f(x,y)v(x,y)dxdy \quad (B.14)$$

for all $v \in H^1(D)$. Usually the weak formulation of a given linear boundary value problem can be written in the form, find $u \in V$ such that

$$B(u,v) = F(v), \qquad \forall v \in V, \quad (B.15)$$

where V is a Hilbert space (one of the Sobolev spaces), $B(u,v)$ is known as a bilinear form and $F(v)$ is continuous linear functional. For example in the context of (B.14),

$$B(u,v) = \int_D \nabla v \cdot (\mathcal{D}\nabla u)dxdy + \int_D \lambda uvdxdy, \quad (B.16)$$

$$F(v) = \int_D fvdxdy. \quad (B.17)$$

In fact, in this case $B(u,v)$ is a symmetric bilinear form because

$$B(u,v) = B(v,u), \forall u, v \in V. \quad (B.18)$$

In general, a bilinear form satisfies the following properties:

- Linearity: $\forall v_1, v_2, v_3 \in V$ and $a_1, a_2 \in \mathbb{R}$

$$B(a_1v_1 + a_2v_2, v_3) = a_1B(v_1, v_3) + a_2B(v_2, v_3). \quad (B.19)$$

- $B(.,.)$ is said to be coercive if there exists $\delta_1 > 0$ such that

$$B(u,u) \geq \delta_1 \parallel u \parallel_V^2, \forall u \in V. \quad (B.20)$$

- $B(.,.)$ is bounded if there exists $\delta_2 > 0$ such that

$$B(u,v) \leq \delta_2 \parallel u \parallel_V \parallel v \parallel_V, \forall u, v \in V. \quad (B.21)$$

Remark 11 *If (B.18), (B.19), (B.20), and (B.21) are satisfied, then $B(.,.)$ defines an inner product on V. Such an inner product is known as the energy inner product. See [51,54] for further details.*

To ensure the existence and the uniqueness of a weak solution, we use the Lax-Milgram theorem.

Lemma 28 *The weak formulation, find $u \in H^1(D)$ such that*

$$B(u,v) = F(v), \quad \forall v \in H^1(D) \tag{B.22}$$

as defined in $(B.16)$ *and* $(B.17)$ *has a unique solution.*

Proof: The proof follows from the fact that $\mathcal{D}$ is a symmetric positive definite matrix and that $f(x,y) \in \mathcal{L}^2(D)$.Before presenting the proof, we first recall the Lax-Milgram Theorem.

Theorem 29 *Suppose that V is a Hilbert space equipped with norm $\| \cdot \|_V$. Let $B(.,.)$ be a bilinear functional on $V \times V$ such that:*

- *$B(u,u)$ is coercive*
- *$B(u,v)$ is bounded,*
- *and let $F(\cdot)$ be a linear functional on V with $\delta_3 > 0$ such that $\forall v$*

$$| F(v) | \delta_3 \leq \| v \|_V . \tag{B.23}$$

Then, there exists a unique solution $u \in V$ such that

$$B(u,v) = F(v), \forall v \in V. \tag{B.24}$$

Definition 30 *We say that the differential operator L,*

$$Lu(x,y) = -\nabla \cdot (\mathcal{D}(x,y)\nabla u(x,y)) + \lambda u(x,y), \tag{B.25}$$

is uniformly elliptic if there exists a constant $\delta > 0$ such that

$$\xi \mathcal{D}(x,y)\xi^T \geq \delta \| \xi \|^2, \tag{B.26}$$

for almost every $x, y \in D$ and $\forall \xi \in \mathbb{R}^2$.

To prove coercivity, consider

$$B(u,u) = \int_D \nabla u \cdot (D\nabla u) + \lambda \mid u \mid^2 dxdy. \tag{B.27}$$

Observe that by using $(B.26)$,

$$\nabla u \cdot (D\nabla u) \geq \delta \mid \nabla u \mid^2 . \tag{B.28}$$

Hence

$$B(u,u) \geq \int_D \delta \mid \nabla u \mid^2 + \lambda \mid u \mid^2 dxdy. \tag{B.29}$$

Now, define $\delta_1 = \min\{\delta, \lambda\}$. Then

$$\begin{aligned} B(u,u) &\geq \delta_1 \int_D \mid \nabla u \mid^2 + \mid u \mid^2 dxdy & \text{(B.30)} \\ &= \delta_1 \parallel u \parallel^2_{H^1} . & \text{(B.31)} \end{aligned}$$

To show boundedness, consider

$$\begin{aligned} B(u,v) &= \int_D \nabla v \cdot (D\nabla u) + \lambda uv dxdy \\ &= \int_D \Big(\frac{\alpha+\beta}{2} + \frac{\alpha-\beta}{2}\cos\phi(x,y)\Big)\frac{\partial u}{\partial x}\frac{\partial v}{\partial x} + \Big(\frac{\alpha-\beta}{2}\Big)\sin 2\phi(x,y)\frac{\partial u}{\partial y}\frac{\partial v}{\partial x} \\ &+ \Big(\frac{\alpha-\beta}{2}\Big)\sin 2\phi(x,y)\frac{\partial u}{\partial x}\frac{\partial v}{\partial y} + \Big(\frac{\alpha+\beta}{2} - \frac{\alpha-\beta}{2}\cos\phi(x,y)\Big)\frac{\partial u}{\partial y}\frac{\partial v}{\partial y}dxdy \\ &+ \int_D \lambda uv dxdy. \end{aligned}$$

Notices that

$$\begin{aligned} \mid B(u,v) \mid \leq\ & \alpha \int_D \mid \frac{\partial u}{\partial x} \mid\mid \frac{\partial v}{\partial x} \mid + \frac{\mid \alpha-\beta \mid}{2}\int_D \mid \frac{\partial u}{\partial y} \mid\mid \frac{\partial v}{\partial x} \mid dxdy \\ &+ \frac{\mid \alpha-\beta \mid}{2}\int_D \mid \frac{\partial u}{\partial x} \mid\mid \frac{\partial v}{\partial y} \mid dxdy + \beta\int_D \mid \frac{\partial u}{\partial x} \mid\mid \frac{\partial v}{\partial x} \mid dxdy \\ &+ \lambda\int_D \mid u \mid\mid v \mid dxdy. \end{aligned}$$

Thus using Cauchy Schwartz inequality,

$$\begin{aligned} \mid B(u,v) \mid \leq\ & \alpha \parallel \frac{\partial u}{\partial x} \parallel_{\mathcal{L}^2} \parallel \frac{\partial v}{\partial x} \parallel_{\mathcal{L}^2} + \frac{\mid \alpha-\beta \mid}{2} \parallel \frac{\partial u}{\partial y} \parallel_{\mathcal{L}^2} \parallel \frac{\partial v}{\partial x} \parallel_{\mathcal{L}^2} \\ &+ \frac{\mid \alpha-\beta \mid}{2} \parallel \frac{\partial u}{\partial x} \parallel_{\mathcal{L}^2} \parallel \frac{\partial v}{\partial y} \parallel_{\mathcal{L}^2} + \beta \parallel \frac{\partial v}{\partial y} \parallel_{\mathcal{L}^2} \parallel \frac{\partial v}{\partial y} \parallel_{\mathcal{L}^2} + \lambda \parallel u \parallel_{\mathcal{L}^2} \parallel v \parallel_{\mathcal{L}^2} . \end{aligned}$$

Assume that $\delta_2^* = max\{\alpha, \beta, \frac{|\alpha-\beta|}{2}, \lambda\}$. Then

$$| B(u,v) | \leq \delta_2^* \Big(\| u \|_{\mathcal{L}^2} + \| \frac{\partial u}{\partial x} \|_{\mathcal{L}^2} + \| \frac{\partial u}{\partial y} \|_{\mathcal{L}^2} \Big) \Big(\| v \|_{\mathcal{L}^2} + \| \frac{\partial v}{\partial x} \|_{\mathcal{L}^2} + \| \frac{\partial v}{\partial y} \|_{\mathcal{L}^2} \Big).$$

Observe that for any positive numbers A, B the following inequality holds

$$(A + B) \leq 2(A^2 + B^2)^{\frac{1}{2}}. \tag{B.32}$$

Hence,

$$\begin{aligned} | B(u,v) | &\leq 2\delta_2^* \Big(\| u \|_{\mathcal{L}^2}^2 + \| \frac{\partial u}{\partial x} \|_{\mathcal{L}^2}^2 + \| \frac{\partial u}{\partial y} \|_{\mathcal{L}^2}^2 \Big)^{\frac{1}{2}} \Big(\| v \|_{\mathcal{L}^2}^2 + \| \frac{\partial v}{\partial x} \|_{\mathcal{L}^2}^2 + \| \frac{\partial v}{\partial y} \|_{\mathcal{L}^2}^2 \Big)^{\frac{1}{2}} \\ &= \delta_2 \| u \|_{H^1} \| v \|_{H^1} . \end{aligned}$$

As with regard to the functional $F(v)$, notice that by using Cauchy Schwartz inequality

$$| F(v) | \leq \| f \|_{\mathcal{L}^2} \| v \|_{\mathcal{L}^2} . \tag{B.33}$$

However since $v \in H_0^1(D)$,

$$\| v \|_{\mathcal{L}^2} \leq \| v \|_{H^1} . \tag{B.34}$$

Hence,

$$| F(v) | \leq \| f \|_{\mathcal{L}^2} \| v \|_{H^1} . \tag{B.35}$$

Therefore by choosing δ_3 such that $\delta_3 = \| f \|_{\mathcal{L}^2}$, the result follows

B.1 The Galerkin Method

In this section, we shall briefly explain how the weak formulation is discretized. There a number of ways for achieving this, and for a comprehensive review see [53]. One approach for discretizing the weak form is by using the Galerkin method. The Galerkin method enables us to calculate the best approximation to the solution of the boundary value problem from a chosen finite dimensional subspace. Before discussing how the Galerkin method works, we need to recall the projection theorem.

Definition 31 *If V is an inner product space with inner product $(.,.)$ and u,v are vectors in V satisfying*

$$(u, v)_V = 0, \tag{B.36}$$

then u and v are said to be orthogonal.

Theorem 32 *Suppose that V is an inner product space, Z is a finite dimensional subspace of V, and $u \in V$. Then*

- *There is a unique vector $u^* \in Z$ satisfying*

$$\| u - u^* \|_V < \| u - v^* \|_V, \forall v^* \in Z, \quad u^* \neq v^*. \tag{B.37}$$

  The vector u^* is called the best approximation to u from Z or the projection of u onto Z.

- *A vector u^* is the best approximation to u from Z if and only if it satisfies the following orthogonality condition: for $u^* \in Z$*

$$(u - u^*, v^*)_V = 0, \forall v^* \in Z. \tag{B.38}$$

Consider a weak formulation, $u \in V$ such that

$$B(u, v) = F(v), \tag{B.39}$$

where $B(.,.)$ is a symmetric bilinear form on the Hilbert space V and F is a continuous linear functional on V. Suppose that Z is a finite dimensional subspace of V. Then Z has a basis $\{\gamma_1, ..., \gamma_n\}$ and $u^* \in Z$ can be written as

$$u^* = \sum_{j=1}^{n} a_j \gamma_j. \tag{B.40}$$

Now if u^* also satisfies the orthogonality condition (B.38), then by taking $v^* = \gamma_k$,

$$(u - \sum_{j=1}^{n} a_j \gamma_j, \gamma_k)_V = 0, \quad k = 1, ..., n \tag{B.41}$$

and so

$$\sum_{j=1}^{n} (\gamma_j, \gamma_k)_V a_j = (u, \gamma_k)_V, \quad k = 1, ..., n. \tag{B.42}$$

Hence, the best approximation from Z to the solution u of (B.39) is computed by solving the system (B.42). However, the solution u to the boundary value problem is unknown, and there is no way of calculating the right hand side of (B.42). One way to resolve this problem is to use the Galerkin technique. The Galerkin idea is to use the inner product defined by the bilinear form $B(.,.)$ to compute the best approximation to u. That is

$$\sum_{j=1}^{n} B(\gamma_j, \gamma_k) a_j = B(u, \gamma_k), \quad k = 1, ..., n. \tag{B.43}$$

But since

$$B(u, \gamma_k) = F(\gamma_k), \tag{B.44}$$

we have

$$\sum_{j=1}^{n} B(\gamma_j, \gamma_k) a_j = F(\gamma_k). \quad k = 1, ..., n. \tag{B.45}$$

Now consider the weak formulation defined by (B.16) and (B.17). If $K \in \mathbb{R}^{n \times n}$, $M \in \mathbb{R}^{n \times n}$ and $\tilde{F} \in \mathbb{R}^n$ are defined by

$$K_{jk} = \int_D \nabla\gamma_k \cdot (\mathcal{D}\nabla\gamma_j), \quad j, k = 1, 2, ..., n \tag{B.46}$$

$$M_{jk} = \int_D \lambda\gamma_k\gamma_j, \quad j, k = 1, 2, ..., n \tag{B.47}$$

$$\tilde{F}_k = \int_D f\gamma_k, \quad k = 1, 2, ..., n, \tag{B.48}$$

then to find the best approximation to the solution u, we need to solve the system

$$(K + M)U = \tilde{F}. \tag{B.49}$$

Here K is called the stiffness matrix, M is the mass matrix, $\tilde{F}$ is called the load vector, and $U \in \mathbb{R}^n$ defines the approximate solution,

$$u^* = \sum_{i=1}^{n} U_i \gamma_i. \tag{B.50}$$

B.2 Piecewise Polynomials

So far we have presented the weak formulation of an elliptic boundary value problem and the Galerkin method for producing an approximate solution from a given finite dimensional subspace. However, the main ingredient of the finite element method is the kind of the approximating subspace used in the calculations. Notice that as shown above, the computation of an approximate solution reduces to solving $(K+M)U = \tilde{F}$. For this method to be useful, the approximating subspace need to be selected so that the solution of (B.49) is well-approximated by any element of the subspace. The best approximating subspace for achieving this consists of piecewise polynomial functions. This is because polynomials are easy to differentiate and integrate and, piecewise polynomials produce sparse stiffness and mass matrices, which enable us to solve $(K + M)U = \tilde{F}$ efficiently. For detailed discussions on approximation subspaces see [53,55].

In the following, we shall briefly explain how piecewise linear polynomials can be used to construct the approximation subspace. This is because, ultimately, we will use the MATLAB PDE toolbox to implement the finite element method, and the toolbox is only programmed to use piecewise linear polynomials.

To define a piecewise polynomial over D, D must be divided into sub-domains. Then a piecewise polynomial is defined by a polynomial on each sub-domain. The combination of sub-domains is known as a mesh and, the most widely used mesh in 2D is the triangulation where D is a union of triangles. For any two triangles in the domain, the intersection has to be a common vertex or a common edge or the empty set. Figure B.1 shows an example of a triangulation consisting of 9×9 vertices and 128 triangles.

Consider a given triangulation T_h, which consists of N_t triangles $T_1, T_2, ..., T_{N_t}$. And let $z_1, z_2, ..., z_{N_v}$ be the vertices of these triangles, where $z_j = (x_j, y_j)$. A piecewise linear function P is a first degree polynomial of the form

$$a_i + b_i x + c_i y, \tag{B.51}$$

on each triangle $T_i \in T_h$. The coefficients a_i, b_i, c_i are uniquely calculated by the values of (B.51) at the three vertices of T_i. Notice that each z_j is a vertex of several

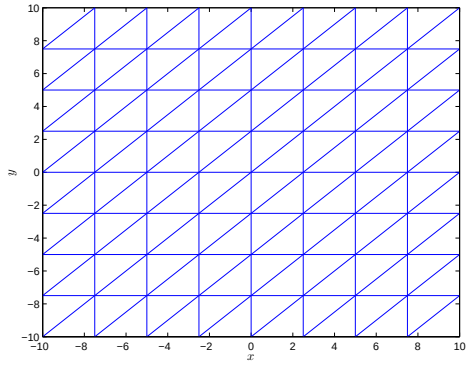

Figure B.1: Triangulation consisting of 128 triangles and 9×9 vertices.

triangles. In fact, if T_i and T_k both have z_j as a vertex, then the coefficients a_i, b_i, c_i and a_k, b_k, c_k need to satisfy

$$a_i + b_i x_j + c_i y_j = a_k + b_k x_j + c_k y_j. \tag{B.52}$$

If triangulation T_h has N_v vertices, then a piecewise linear function on T_h is calculated by the N_v nodal values of the function. Hence the space of all continuous piecewise linear functions, P, is a finite dimensional vector space with dimension N_v. Each function $v \in P$ can be expressed as

$$v = \sum_{j=1}^{N_v} a_j \psi_j, \tag{B.53}$$

where a_j are the nodal values of v and $\{\psi_1, \psi_2, ..., \psi_{N_v}\}$ is a basis for P. Such a basis need to be chosen so that for any $a \in \mathbb{R}^{N_v}$,

$$v(x_k, y_k) = \sum_{j=1}^{N_v} a_j \psi_j(x_k, y_k) = a_k, \tag{B.54}$$

that is,

$$\psi_j(x_k, y_k) = \begin{cases} 1 & j = k \\ 0 & j \neq k \end{cases}. \tag{B.55}$$

Observe that ψ_k vanishes on all the triangles that do not contain the node z_k. Therefore the integrals in K_{jk}, M_{jk}, $\tilde{F}_k$ only need to be computed on the triangles that contain the node z_k. Moreover, K_{jk} and M_{jk} are zero unless z_j and z_k are the vertices of the same triangle. Hence K and M are sparse matrices. For detailed discussion on how to compute K, M and F, see [55].

Appendix C

Matlab Codes

C.1 Correlation function of the one dimensional biharmonic equation

```
M=10; % domain
r=0:0.01:M;
% coefficients
a=1;
b=19.4;
c=150;
A=sqrt( 0.5*sqrt(c/a) + (b/(4*a)) );
B=sqrt( 0.5*sqrt(c/a) - (b/(4*a)));
deno=32*a^2*A^3*B^3*(A^2+B^2)^3;
con1=( (A^2+B^2)*(2.*r*A^2 + B) + 4*A^2*B);
con2=( (A^2+B^2)*(A^2*B.*r-B^3.*r+A^2)+4*A^2*B^2);
Variance= (A^2 + 5*B^2)/(32*(B^3)*(a^2)*(A^2 + B^2)^3);

rho= 16*B^3/( (A^2 + 5*B^2)*(A^2 + B^2)); %correlation length

CC=((B^2.*con1.*sin(A.*r) + A.*con2.*cos(A.*r)) .*exp(-B.*r))/(deno); % covarinac
C=CC/(Variance); % correlation function
plot(r,C);
xlabel('$r$','interpreter','latex','FontSize',12);
ylabel('$C(r)$','interpreter','latex','FontSize',12);
```

```
phrase_parameter = 'a=1';
gtext(phrase_parameter);
phrase_parameter = 'b=19.4';
gtext(phrase_parameter);
phrase_parameter = 'c=120';
gtext(phrase_parameter);
```

C.2 Approximate solution of the one dimensional biharmonic equation

```
clear all;clc; format long
a=0.1;
b=-32;
c=10;
A= sqrt( (b/(4*a)) + 0.5*sqrt(c/a));
B=sqrt( -(b/(4*a)) + 0.5*sqrt(c/a));

% Determining Kmax
vari=(A^2 + 5*B^2)/(32*B^3*a^2*(A^2 + B^2)^3) % Variance in the oscilatory
%case
%P=sqrt( (-b + sqrt(b^2-4*a*c))/(2*a));
%Q=sqrt( (-b - sqrt(b^2-4*a*c))/(2*a));
%vari=(Q^2+3*P*Q+ P^2)/(4*a^2*(Q+P)^3*(P*Q)^3);
%rho=2*((Q+P)^3)/(P*Q*(Q^2+3*Q*P+P^2))
kmax= 6; %Cut off in the Oscillatory case
j=@(v) (2./(2*pi*(a*v.^4-b*v.^2 + c).^2));
Truncation=quad(j,0,kmax);
M=2^8;
dk=kmax/M;
N=M;
period = 2*pi/dk;
k=0:dk:(N-1)*dk;
L=32;
```

```
dx=L/N;
x=-(0.5*N-0.5)*dx:dx:(0.5*N-0.5)*dx;
phi=zeros(N,1);

for n=1:N;
    v(n)=2*pi*rand;% uniformally distributed in (0,2pi)
end

for n=1:N
    tt(n)=rand;
    u(n)=sqrt(-2*log(tt(n)));  %Rayleigh
end

for n=1:N
 y(n)= dk./(pi*(a*k(n).^4 -b*k(n).^2 + c).^2) ; % Spectral density
 yy(n)=sqrt(y(n));% Sqart of the spectral density
  y3(n) = yy(n).*u(n);
 y4(n)=y3(n)*exp(sqrt(-1)*v(n));% sqart of spectral density times exp(iv);
end

phi=real(fft(y4));
plot( x,phi);
xlabel('$x$','interpreter','latex','FontSize',12);
ylabel('\phi(x)','FontSize',12);
phrase_parameter = 'a=1';
gtext(phrase_parameter);
phrase_parameter = 'b=0.8';
gtext(phrase_parameter);
phrase_parameter = 'c=0.5';
gtext(phrase_parameter);
phrase_parameter = 'kmax=6';
gtext(phrase_parameter);
```

```
phrase_parameter = 'N=256';
gtext(phrase_parameter);
```

C.3 Correlation function of the two dimensional biharmonic equation

```
clear all, close all, format long, format compact,clc

a=1;
b=1;
c=1;

M=10;
r=0:0.01:M;
A= sqrt( (b/(4*a)) + 0.5*sqrt(c/a));
B=sqrt( -(b/(4*a)) + 0.5*sqrt(c/a));
i=sqrt(-1);
F1=real (besselk(1,r*(B+i*A)));
F2=imag ( besselk(1,r*(B+i*A)));
F3=imag( besselk(0,r*(B+i*A)));

con1=1/(32*pi*a^2*A^2*B^2);
con2=1/(A^2+B^2);
con3=1/(A*B);
Rcon1=r./(32*pi*a^2*A^2*B^2*(A^2 + B^2));
Rcon2=1/(32*pi*a^2*(A*B)^3);
%Variance
V1=(A^2-B^2)/(32*pi*a^2*A^2*B^2*(A^2+B^2)^2) + atan(A/B)/(32*pi*a^2*(A*B)^3);
RR=Rcon1.*( -A*F2 -B*F1) - Rcon2*(F3);
C=RR/V1;% correlation function

% Numerical Correlation length
```

```
FF=@(r)abs((-A^2*B*sqrt(a)*r.*imag(besselk(1,r*(B+i*A)))-A*B^2*sqrt(a)*r. ...
...*real(besselk(1,r*(B+i*A)))-sqrt(c)*imag(besselk(0,r*(B+i*A)))));
QQ=quad(FF,0,10);
rho=QQ/(32*V1*a^2*pi*A^3*B^3*sqrt(c))
plot(r,C);

xlabel('$r$','interpreter','latex','FontSize',12);
ylabel('$c(r)$','interpreter','latex','FontSize',12);
phrase_parameter = 'a=1';
gtext(phrase_parameter);
phrase_parameter = 'b=1';
gtext(phrase_parameter);
phrase_parameter = 'c=1';
gtext(phrase_parameter);
```

C.4 Approximate solution of the two dimensional biharmonic equation

```
clear all; clc; format long
% Coefficients
a=1;
b=1.8;
c=1;
A= sqrt( (b/(4*a)) + 0.5*sqrt(c/a));
B=sqrt( -(b/(4*a)) + 0.5*sqrt(c/a));
%epsilon=40;
%b=-2*sqrt(a*c)-epsilon;
%M=2^7;
%%%%%%%%%%%%%%%%%%%%%%%%%%%%%%%%%%%%%%%%%%%%%%%%%%%%%%%%%%%%%%%%%%%%%%%%%%%%%%%
% Determining Kmax
CON=A/B;
```

```
Variance=(A^2-B^2)/(32*pi*a^2*A^2*B^2*(A^2+B^2)^2) +...
 ...atan(CON)/(32*pi*a^2*(A*B)^3);%Oscillatory

%P=sqrt( (-b + sqrt(b^2-4*a*c))/(2*a));
%Q=sqrt( (-b - sqrt(b^2-4*a*c))/(2*a));
 %Decaying
%Variance=(Q^4-4*P^2*Q^2*(log(Q)-log(P))-P^4)/(4*pi*a^2*P^2*Q^2*(Q^2-P^2)^3);
%kmax=7;

j=@(v1,v2) (1./( (pi^2)*(a*(v1.^2 + v2.^2).^2-b*(v1.^2 + v2.^2) + c).^2));
Truncation=dblquad(j,0,kmax,0,kmax,)
M=2^8;
dk=kmax/M;
N=M;
k=dk*[0:(N/2-1) -N/2:-1];
k2=k;
peirod=2*pi/dk
L=26;
dx=L/N;
x=-(0.5*N-0.5)*dx:dx:(0.5*N-0.5)*dx;
x2=x;
phi=zeros(N,N);
[X1,X2]=meshgrid(x,x2);
[K1,K2]=meshgrid(k,k2);
K=sqrt( K1.^2 + K2.^2); % scalar specturm

TT=2*pi*rand(N,N);
T=exp(sqrt(-1)*TT);% phase angle
T3=rand(N,N);
T4=-1*log(T3);

SS= dk*dk.*T4./(pi*pi*(a*K.^4 -b*K.^2 +c).^2); % Amplitude
```

```
S=sqrt( SS); %sqrt amplitude

zeta= T.*S;
phi=real( fft2(zeta)  );

imagesc(x,x2,phi)

xlabel('$x$','interpreter','latex','FontSize',12);
ylabel('$y$','interpreter','latex','FontSize',12);
```

C.5 Correlation function of the anisotropic biharmonic equation

```
clear all; clc

r=-10:0.01:10;
a=1;
b=1.9;
c=1;
alpha=15;
beta=2.1;
theta=0;

[R1,R2]=meshgrid(r,r);
P1=R1.^2 *(( alpha*sin(theta)^2 + beta*cos(theta)^2)/(alpha*beta));
P2=2*R1.*R2*(beta-alpha/(alpha*beta))*sin(theta)*cos(theta);
P3=R2.^2 *(( beta*sin(theta)^2 + alpha*cos(theta)^2)/(alpha*beta));
RR=sqrt( P1 + P2 + P3);

A= sqrt( (b/(4*a)) + 0.5*sqrt(c/a));
B=sqrt( -(b/(4*a)) + 0.5*sqrt(c/a));
F2=imag ( besselk(1,RR*(B+i*A)));
F1=real (besselk(1,RR*(B+i*A)));
```

```
F3=imag( besselk(0,RR*(B+i*A)));

% The variance is
vari=(A^2-B^2)/(32*pi*sqrt(c*alpha*beta)*a^2*A^2*B^2*(A^2+B^2)^2) +...
... atan(A/B)/(32*pi*sqrt(c*alpha*beta)*a^2*(A*B)^3);

% The covariance is
C=(-A^2*B*sqrt(a)*RR.*F2 -A*B^2*sqrt(a)*RR.*F1-sqrt(c)*F3)/...
...(32*a^2*pi*A^3*B^3*sqrt(c*alpha*beta));

CC=C/vari;

%%%%%%%%%%%%%%%%%%%%%%%%%%%%%%%%%%%%%%%%%%%%%%%%%%%%%%%%%%%%%%%%%%%%%%%%%%%%%%%%%
% Numerical computation of the correlation lengths

% Setting R2=0,

conn1=sqrt( (alpha*sin(theta)^2 + beta*cos(theta)^2)/(alpha*beta));
conn2=sqrt( (beta*sin(theta)^2 + alpha*cos(theta)^2)/(alpha*beta));
com=B+i*A;

FF1=@(v)abs((-A^2*B*sqrt(a)*conn1*v.*imag(besselk(1,conn1*v*(com)))-...
...A*B^2*sqrt(a)*conn1*v.*real(besselk(1,conn1*v*(com)))- ...
...sqrt(c)*imag(besselk(0,conn1*v*(com)))));

FF2=@(v)abs((-A^2*B*sqrt(a)*conn2*v.*imag(besselk(1,conn2*v*(com)))-...
...A*B^2*sqrt(a)*conn2*v.*real(besselk(1,conn2*v*(com)))-...
...sqrt(c)*imag(besselk(0,conn2*v*(com)))));

QQ1=quad(FF1,0,10);
QQ2=quad(FF2,0,10);
```

```
rho1=QQ1/(32*vari*a^2*pi*A^3*B^3*sqrt(c*alpha*beta))
rho2=QQ2/(32*vari*a^2*pi*A^3*B^3*sqrt(c*alpha*beta))

imagesc(r,r,CC);
xlabel('$r_{1}$','interpreter','latex','FontSize',12);
ylabel('$r_{2}$','interpreter','latex','FontSize',12);
```

C.6 Approximate solution of the anisotropic biharmonic equation

```
clear all; clc; format long

a=1;
b=1.9;
c=1;
alpha=15;
beta=2.1;
theta=0;

A11=beta*(sin(theta))^2 + alpha*(cos(theta))^2;
A22=alpha*(sin(theta))^2 + beta*(cos(theta))^2;
A12=(alpha-beta)*sin(theta)*cos(theta);
sqrt(A22)*A11-A12

%epsilon=40;
%b=-2*sqrt(a*c)-epsilon;
%M=2^7;
%%%%%%%%%%%%%%%%%%%%%%%%%%%%%%%%%%%%%%%%%%%%%%%%%%%%%%%%%%%%%%%%%%%%%%%%%%%%%
% Determining Kmax

A= sqrt( (b/(4*a)) + 0.5*sqrt(c/a));
B=sqrt( -(b/(4*a)) + 0.5*sqrt(c/a));
```

```
CON=A/B;

vari1=(A^2-B^2)/(32*pi*sqrt(c*alpha*beta)*a^2*A^2*B^2*(A^2+B^2)^2) +...
...+atan(CON)/(32*pi*sqrt(c*alpha*beta)*a^2*(A*B)^3)%Oscillatory

%P=sqrt( (-b + sqrt(b^2-4*a*c))/(2*a));

%Q=sqrt( (-b - sqrt(b^2-4*a*c))/(2*a));

%Vari2=(Q^4-4*P^2*Q^2*(log(Q)-log(P))-P^4)/...
%...(4*pi*sqrt(alpha*beta)*a^2*P^2*Q^2*(Q^2-P^2)^3)

kmax=7;

j=@(v1,v2) (1./( (pi^2)*(a*(A11^2*v1.^4 + A22^2*v2.^4 +...
... 2*(A11*A22+2*A12^2)*(v1.^2).*(v2.^2))+...
...a*(4*A11*A12*(v1.^3).*v2 +4*A12*A22*(v1).*(v2.^3))-...
...b*(A11*(v1).^2 + 2*A12*v1.*v2 + A22*(v2).^2) + c ).^2));

Truncation=dblquad(j,0,kmax,0,kmax,1.0e-8)
relerror=abs( (Truncation-vari1)/vari1)

M=2^8;
dk=kmax/M;
N=M;

k=dk*[0:(N/2-1) -N/2:-1];

peirod=2*pi/dk;
L=32;
dx=L/N;
x=-(0.5*N-0.5)*dx:dx:(0.5*N-0.5)*dx;
```

```
x2=x;

phi=zeros(N,N);

[X1,X2]=meshgrid(x,x2);
[K1,K2]=meshgrid(k,k);
K=sqrt( K1.^2 + K2.^2); % scalar specturm

TT=2*pi*rand(N,N);
T=exp(sqrt(-1)*TT);% phase angle
T3=rand(N,N);
T4=-1*log(T3);

denome1=a*(A11^2*K1.^4 + A22^2*K2.^4 + 2*(A11*A22+2*A12^2)*(K1.^2).*(K2.^2));
denome2=a*(4*A11*A12*(K1.^3).*K2 +4*A12*A22*(K1).*(K2.^3));
denome3=-b*(A11*(K1).^2 + 2*A12*K1.*K2 + A22*(K2).^2) + c;
denome= denome1 +denome2 +denome3;

SS= dk*dk.*T4./(pi*pi*(denome).^2); % Amplitude
S=sqrt( SS); %sqrt amplitude
zeta= T.*S;
phi=real( fft2(zeta)  );

imagesc(x,x2,phi)
xlabel('$x$','interpreter','latex','FontSize',12);
ylabel('$y$','interpreter','latex','FontSize',12);
```

Bibliography

[1] G. Evans, J. Blackledge and P. Yardley:*Analytic Methods for Partial Differential Equations*, Springer, 1999.

[2] D.G. Dufy:*Green's Functions with Applications*, Chapman and Hall/CRC, Boca Raton, Florida, 2001.

[3] I.S. Gradshteyn and I.M. Ryzhik:*Table of Integrals, Series, and Products*, Acdamic Press, San Diego, 2000.

[4] C.L. Farmer:*Bayesian field theory applied to scattered data interpolation and inverse problem*, Algorithms for Approximation. Ed. A. Iske and J. Levesley, Springer-Verlag, Heidelberg, 147-166, 2007,

[5] Y. Egorov and M. Shbin:*Foundations of the Classical Theory of Partial Differential Equations (Encyclopaedia of Mathematical Sciences, 30)*, Springer, 1998.

[6] I.Cialenco:*Regularity of Solutions and parameter estimation for SPDE's with Space-Time White noise*, Dissertation, University of Southern California, 2007.

[7] P. Whittle:*On stationary processes in the plane*, Biometrika 41, 434-449, 1954.

[8] L. Smith:*Spatial variability of flow parameters in a Stratified sand*, Mathematical Geology, 1981.

[9] S. Huang, S. Quek and K. Phoon:*Convergence study of the truncated Karhunen-Loeve expasion for simulation of stochastic processes*, Mathematical Journal for numerical methods in Engineering, 2001.

[10] M. E. Taylor:*Partial Differential Equations: Basic Theory*, Springer, 1996.

[11] P. Whittle:*Stochastic processes in several dimensions*, Bulletin of the international statistical institute, 1963.

[12] F. Lindgren and H. Rue:*Explicit Construction of GMRF Approximations to generalised Matern fields on irregular grids*, Lund Institute of Technology, 2007.

[13] N. Krylov:*An analytic approach to SPDEs*, Stochastic Partial Differential Equations: Six Perspectives, Mathematical Surveys and Monographs, Vol. 64, AMS, Providence, RI, 1999.

[14] V. Heine:*Models for two-dimensional stationary stochastic process*, Biometrika 42, 170-178, 1955.

[15] E. Lieb and M. Loss:*Analysis*, American Mathematical Society, 2001.

[16] S. Banerjee, B. Carlin and E. Gelfand:*Hierarchical Modeling and Analysis for Spatial Data*, Chapman Hall, 2003.

[17] R. Adler and J. Taylor:*Random Fields and Geometry*, Springer, 2007.

[18] E. Pardo-Igzquiza1 and M. Chica-Olmo1:*The Fourier Integral Method: An efficient spectral method for simulation of random fields*, Mathematical Geology, Vol. 25, No. 2, 1993.

[19] Yu.V. Egorov and A.I. Komech:*Elements of the Modern Theory of Partial Differential Equations*, Springer, 1999.

[20] J.B Walsh:*An Introduction to stochastic partial differential equations*, Lect. Notes in Math., vol. 1180, Berlin Heidelberg New York, Springer, 1986.

[21] H. Kuo:*White Noise Distribution Theory*, CRC Press, 1996.

[22] C.L Farmer:*Geological modelling and reservoir simulation*, Article in 'Mathematical Methods and Modeling in Hydrocarbon Exploration and Production, Editors: Armin Iske and Trygve Randen, Springer-Verlag, Heidelberg, 119-212, 2005.

[23] G.A Fenton:*Simulation and Analysis of Random fields*, Dissertation, Princeton University, 1990.

[24] H. Rue and T. Follestad:*Efficient Computations for Gaussian Markov random Field Models with two Applications in Spatial Epidemiology*, preprint, Department of Mathematical Sciences, Norwegian University of Science and Technology, 2003.

[25] H. K. Lee, D. Higdon , Z. Bi, M. Ferreira and M. West:*Markov Random Field Models fo High-Dimensional Parameters in Simulations of fluid Flow in Porous Media*, American Statistical Association and American Society for Quality, 2002.

[26] J. Kaipio:*Modelling of Uncertainties in Statistical Inverse Problems*, 6th International Conference on Inverse Problems in Engineering: Theory and Practice, 2008.

[27] R. Buckdahn and E. Pardoux:*Monotonicity Methods for White Noise Driven Quasi-Linear SPDEs*, Diffusion Processes and Related Problems in Analysis, Vol. I, Birkhauser, 219-233, 1990.

[28] G. Christakos:*Random Field Models in Earth Sciences*, Dover, 1992.

[29] R. Dalang, C. Mueller, Y. Xiao, D. khoshnevisan and D. Nualart:*A minicourse on Stochastic Partial Differential equations*, Springer, 2008.

[30] W. Arendt:*Different domains induce different heat semigroups on* $C_0(\Omega)$, Evolution Equations and Their Applications in Physical and Life Sciences: Proceedings of the Bad Herrenalb (Karlsruhe), CRC Press, 2001.

[31] A. M. Yaglom:*An Introduction to the Theory of Stationary Random Functions*, Dover, 2004.

[32] Y. Cao, H. Yang and L. Yin:*Finite element methods for semilinear elliptic stochastic partial differential equations*, Num. Math., 106, pp. 181-198, 2007.

[33] C. L. Farmer:*Local Geostatistics*, Paper A005 in the Proceedings of the 9th European Conference on the Mathematics of Oil Recovery, Cannes, September 2004.

[34] P. Corvi, K. Heffer, P. King, S. Tyson and G. V:*Reservoir Characterization Using Epert Kowledge, Data and Statistics*, Schlumberger Oilfield Review, 1992.

[35] P. Abrahamsen:*A Review of Gaussian Random Fields and Correlation Functions*, 1997.

[36] P. R. King, P. J. Smith:*Generation of Correlated properties on Heterogeneous Porous Media*, Mathematical Geology, Vol. 20, No. 7, 1988.

[37] R. Baker:*Modelling Soil Variability as a Random Field*, Mathematical Geology, Vol. 16, No. 5, 1984.

[38] S. Suzuki and J. Caers:*A Distance-based Prior Model Parameterization for Constraining Solutions of Spatial Inverse Problems*, Mathematical Geology, 2008.

[39] G. B. Folland:*Introduction to Partial Differential Equations*, Princenton University Press, 1995.

[40] C. Ayan and et al:*Measuring Permeability Anisotropy: The Latest Approach*, Schlumberger Oilfield Review, 1994.

[41] W. Luo:*Wiener Chaos Expansion and Numerical Solutions of Stochastic Partial Differential Equations*, California Institue of Technology, California, 2006.

[42] A. M. Elfeki:*Stochastic Models for Characterizing Variability of Hydro-Geological Parameters*, 5th International Water Technology Conference, Alexandria, Egypt, 2000.

[43] A. Keese:*A Review of Recent Developments in the Numerical Solution of Stochastic Partial Differential Equations*, Institue of Scientific Computing, Technical University Braunschweig, Germany, 2003.

[44] C. L. Farmer:*The Generation of Stochastic Fields of Reservoir Parameters with Specified Geostatistical Distributions*, Proceedings of the 1987 IMA Conference on Mathematics in Oil Production. Ed, Sir Sam Edwards and P.R. King. Published by Oxford University Press, 235-252, 1988.

[45] N. V. Krylov:*Lectures on Elliptic and Parabolic Equations in Sobolev Spaces*, American Mathematical Society, 2008.

[46] M. Shinozuka and G. Deodatis:*Simulation of Stochastic processes by Spectral Representation*, Applied Mechanics Reviews, 44, 1991.

[47] M. Hairer, A. M. Stuart, J. Voss, and P. Wiberg:*Analysis of SPDEs Arising in Path Sampling Part I: The Gaussian Case*, Communications in Mathematical Sciences, Vol 3, No 4, 2005.

[48] R. Potsepaev, C.L. Farmer and M. Aziz:*Stochastic partial dierential equations as priors in ensemble methods for solving inverse problems*, Oxford Centre for Collaborative Applied Mathematics, University of Oxford, Report Number 09/47, 2010.

[49] K. Sabelfeld:*Expansion of random boundary excitations for elliptic PDEs*, Monte Carlo Methods Appl. Vol. 13, No. 56, 2007.

[50] L. D. Pitt:*A Markov property for Gaussian processes with a multidimensional parameter*, Archive for Rational mechanics and Analysis, Springer Berlin, 1971.

[51] L. C. Evans:*Partial Differential Equations*, American Mathematical Society, 1998.

[52] R. S. Strichartz:*A Guide to Distribution Theory and Fourier Transform*, World Scientific Publishing Company, 2003.

[53] S. C. Brenner and L. Ridgeway Scott:*The Mathematical Theory of Finite Element Methods*, Springer, 1994.

[54] E. Suli:*Finite Element Methods For Partial Differential Equations*, Lecture Notes, Comlab, Oxford University, `http://web.comlab.ox.ac.uk/people/Endre.Suli/fem.ps`, 2007.

[55] M. S. Gockenbach:*Understanding and Implementing the Finite Element Method*, Siam, 2006.

[56] W. Xu:*Conditional Curvilinear Stochastic Simulation Using Pixel-based Algorithms*, Mathematical Geology, 1996.

[57] J. Taylor:*Random Fields*, Lecture Notes, Department of Statistics, Stanford University, `http://www-stat.stanford.edu/~jtaylo/courses/stats352/notes/random_fields.pdf`, 2009.

[58] A. D. Rendall:*Local and Global Existence Theorem For Einstein Equations*, Max-Planck-Gesellschaft, 2000.

[59] *Partial Differential Equation Toolbox 1 User's Guide*, Maths Works, 2009.

[60] A. Pintore and C. Holmes:*Nonstationary covariance functions via spatially adaptive spectra*, Journal of the american Statistical Association, 2004.

[61] B. *Matérn*:*Spatial Variation*, 2nd edition, Lecture Notes in Statistics, Volume 36, Springer-Verlag, 1986.

[62] L. Y. Hu and M. Le Ravalec-Dupin:*Elements for an integrated Geostatistical Modeling of Heterogeneous Reservoirs*, Oil and Gas Science and Technology, Vol 59, No 2, 2004.

[63] R. Villegas, O. Dorn, M. Moscoso and M. Kindelan:*Shape reconstruction from two-phase incompressible flow data using level sets*, Image Processing Based on Partial Differential Equations, Ed, X. Tai, K. Lie, T. Chan and S. Osher, Springer, 2006.

[64] L. Y. Hu:*Gradual Deformation and Iterative Calibration of Gaussian Related Stochastic Methods*, Mathematical Geology, Vol 32, No 1, 2000.

[65] J. R. Fanchi:*Shared Earth Modeling: Methodologies for Integrated Reservoir Simulations*, Gulf Professional Publishing, 2002.

[66] J. Wang:*Bayesian Computational Techniques For Inverse Problems in Transport Processes*, Dissertation, Cornell University, 2006.

[67] J. Caers:*Comparing the Gradual Deformation With The Probability Pertubation Method for Solving Inverse Problems*, Mathematical Geology, Vol 39, No 1, 2007.

[68] J. P. Kaipio and E. Somersalo:*Statistical Inversion Theory*, Statistical and Computational Inverse Problems, Vol 160, 2005.

[69] H. K. H. Lee, C. H. Holloman, C. A. Calder and D. M. Higdon:*Flexible Gaussian Processes Via Convolution*, Duke University, 2002.

[70] P. R. Kramer:*A Review of Some Monte Carlo Simulation Methods for Turbulent Systems*, Departments of Mathematical Sciences, Rensselaer Polytechnic Institue, 2000.

[71] D. T. Hristopulos and S. N. Elogne:*Analytic Properties and Covariance Functions for a New class of Generalized Gibbs Random Fields*, IEEE, Vol 53, Issue 12, 2007.

[72] I. Elmatzoglou:*Spatio-Temporal Geostatistical Models, With an Application in Fish Stock*, Thesis, Lancaster University, 2006.

[73] O. Schabenberger and C. A. Gotway:*Statistical Methods for Spatial Data Analysis*, Chapman and Hall, Edition 1, 2004.

[74] M. M. Hamed and P. B. Bendeit:*Reliability-Based Uncertainty Analysis of Groundwater Contaminant Transport and Remediation*, Rice University, EPA/600/R-99/028, 1999.